TECHNICAL FEASIBILITY STUDY ON BIOFUELS PRODUCTION FROM PYROLYSIS OF *Nannochloropsis oculata* AND ALGAL BIO-OIL UPGRADING

A Dissertation

by

MONET CONCEPCION CADAVILLO MAGUYON

Submitted to the Office of Graduate and Professional Studies of
Texas A&M University
in partial fulfillment of the requirements for the degree of

DOCTOR OF PHILOSOPHY

Chair of Committee,	Sergio C. Capareda
Committee Members,	Mahmoud El-Halwagi
	Ronald Lacey
	Zivko Nikolov
Head of Department,	Steve W. Searcy

December 2013

Major Subject: Biological and Agricultural Engineering

ABSTRACT

Increasing environmental concerns over greenhouse gas emissions, depleting petroleum reserves and rising oil prices has stimulated interest on biofuels production from biomass sources. This study explored on biofuels production from pyrolysis of *Nannochloropsis oculata* and subsequent bio-oil upgrading by fractional distillation and zeolite upgrading.

The extent of producing biofuels from *N. oculata* was initially investigated at various pyrolysis temperatures (400, 500 and 600^0C) at 100 psig. The distribution of the products significantly varied with temperature. Maximum char and gas yields were achieved at 400^0C (52% wt) and 600^0C (15% wt), respectively. Liquid production (aqueous and bio-oil) peaked at 500^0C (35% wt). The effect of temperature was also tested against product compositions and properties. Mass and energy conversion efficiencies were also estimated to be about 76% and 68%, respectively.

The operating condition for maximum bio-oil production from *N. oculata* pyrolysis was subsequently determined. Optimum yield was achieved at 540^0C and 0 psig where liquid yield was about 43% wt (23% wt bio-oil, 20% wt aqueous) while char and gas yields were about 32 and 12% wt, respectively. The bio-oil obtained has high carbon (72% wt) and hydrogen (10% wt) contents and high energy content (36 MJ/kg). Char and gas also contain considerable energy contents of about 20 MJ/kg and 21MJ/m^3, respectively.

Separation of the bio-oil and aqueous liquid product (ALP) components by fractional distillation was then investigated. Heavy distillates has the highest yield (75% wt), followed by light distillates (19% wt). Significant reduction in moisture contents and increase in heating values were observed in the bio-oil distillates. The ALP distillate obtained at 150-180^{0}C was found to contain considerable amounts of acids, esters, amides and lactams and has heating value of about 24 MJ/kg.

Finally, HZSM-5 upgrading was done at various temperatures and reaction times. Reaction temperature greatly affected product yields and upgraded bio-oil composition. The best operating condition was found to be 285^{0}C for 3.5 h, which can produce treated bio-oil with higher hydrocarbons (86%), lower oxygenated (3%) and lower nitrogenous (11%) components. Higher heating value (40 MJ/kg), high carbon (80% wt), and low oxygen (3% wt) contents were also achieved.

DEDICATION

To my parents, Ramon (†) and Nenita, for your infinite love and sacrifices that will never be forgotten

ACKNOWLEDGEMENTS

The author would like to thank the US Department of Energy and the National Alliance for Advanced Biofuels and Bio-products (NAABB) for funding this research project.

Education is not the filling of a pail but the lighting of a fire – William Butler Yeats.

I feel very blessed and honored to have these people who sustained the fire of learning burning within me. Thank you:

To my major advisor, **Dr. Sergio C. Capareda**, for your continuous support and patience. Thank you for the much needed encouragement and inspiration to do my best.

To the members of my advisory committee, **Dr. Ronald Lacey, Dr. Mahmoud El-Halwagi** and **Dr. Zivko Nikolov**, for your valuable comments and suggestions.

To the faculty and staff of the Biological and Agricultural Engineering Department for the generous assistance during my stay in Texas A&M University.

To the faculty and staff of the Chemical Engineering Department in the University of the Philippines Los Baños, for allowing me to pursue my PhD studies abroad. Special thanks to **Prof. Rex Demafelis** and **Dr. Jovita Movillon** for encouraging me to further my knowledge on biofuels and to **Ms. Rodora Calibo** for your valuable assistance and motherly care.

To my mentors, **Dr. Catalino Alfafara** and **Dr. Veronica Migo** for your relentless support and guidance.

To my group mates, **Jewel, Tahmina, Jinny, April, Amado, Nam, Jersson and Bjorn** for the generous help and for sharing valuable ideas during the conduct of my study.

To my Filipino friends in TAMU, **Jesselyn, Kat, Samae, Joan, Mavs, Alnald, Gally, Fred, Kristian, JC** and **Paul** for making my stay in College Station bearable and enjoyable.

To my friends, **Elezabeth, Vanica** and **Jeff**, for keeping the friendship though we are miles apart.

To my International Christian Fellowship (ICF) family especially to **Kent, Judy, Bill** and **Bel** and Discovery Bible Study group (**Si Chun, Edith, Charlotte, Silvia, Mao, Maggie, Nannan and Ying**) for the encouragement and prayers.

To my brother, **Ramon Jr**, for your love and understanding.

To my parents, **Ramon (**†) and **Nenita**, who first ignited the fire of learning. Thank you for your unconditional love and for believing in me.

To our **Almighty Father God**, who has been faithful to all His promises, I am offering this humble work of mine.

TABLE OF CONTENTS

Page

LIST OF FIGURES

Page

LIST OF TABLES

Page

1. INTRODUCTION

1.1. Research Overview

Modern human society needs tremendous amount of energy to keep up with the fast-paced evolution of technology, increasing demand for travel and housing, and growth in production of consumer goods and services. Rapid population growth also determines the increase in energy consumption though some efforts to improve energy efficiency by implementing relevant laws and standards are being made. At present, fossil fuels still serve as the main energy source. In 2011, the transportation sector consumed most of delivered energy (about 27 quadrillion Btu in the U.S.) followed by the industrial sector. The transport sector relies heavily on petroleum crude oil where typical transport fuels such as gasoline, jet fuel, and diesel are being derived. In a recent energy projection study conducted by the US Energy Information Energy (2013), crude oil production is expected to increase with average growth of about 234,000 barrels per day (bpd) until 2019, which would mainly come from onshore sources such shale and tight formations. After 2020, however, a decline in crude oil production is expected to decrease from 7.5M bpd to about 6.1M bpd in 2040 due to shift to less profitable drilling areas. As a result, oil price is expected to decrease from $111 per barrel (in 2011 dollars) to about $96 per barrel in 2015. However, after 2015 the price will tend to increase to about $163 per barrel in 2040 ($269 per barrel in nominal dollars). This will lead to an increase in diesel price to about $4.32 to $4.94 per gallon in 2040 [1]. Aside from the expected rise in fuel prices and depletion of accessible petroleum reserves, global plea

on reduction of CO_2 emissions from burning of fossil fuels which causes global warming poses another issue [1-5]. These issues stimulated renewed interest on producing sustainable and renewable biofuels from biomass. In fact, the demand for renewable fuels from biomass sources is projected to increase to about 4.2 quadrillon BTU in 2035 and 4.9 quadrillon BTU in 2040 [1]. However, studies on suitability of various biomass feedstocks and development of efficient and carbon-neutral technologies for biomass-to-biofuel conversion may be required to meet this demand.

Biomass for fuel production ranges from food and oil crops, agricultural residues, energy crops and aquatic plants such as microalgae [5]. Microalgae are a very promising feedstock for biofuel production due to its high lipid content [6], rapid growth rate [7], high photosynthetic efficiency [8] and high productivity [8, 9]. In fact, the projected yield for microalgae in a raceway pond ranges from 110 to 220 tonnes per hectare per year which is way higher than that of sugar cane (74-95 tonnes/ha-yr), switchgrass (8-20 tonnes/ha-yr) and corn (8-34 tonnes/ha-yr) [9]. Also, large-scale production of microalgae will not compete with food production since it can be cultivated on salty water [9] and does not require arable soils [6, 7]. The bio-oil produced from microalgae is also said to be more stable due to lower O/C ratio and has higher heating value as compared to wood oil [8]. Various processes can be used to convert microalgae to fuel-type components which include (1) lipid extraction followed by transesterification to produce biodiesel, (2) deoxygenation of fatty acids for green diesel production, and (3) pyrolysis of whole algal biomass [10]. Compared to the other two processes, pyrolysis is

more economically attractive since in this process the whole biomass is converted into useful products such as high-energy density bio-oil [11].

Pyrolysis is a thermochemical process that converts biomass to solid char, bio-oil and combustible gases at temperatures generally below 600^0C and with the absence of oxygen. It is said to be an energy intensive process; however, the recoverable energy from the char and combustible gases produced could possibly compensate the energy requirement of the process [12]. Pyrolysis produces energy fuels with high fuel-to-feed ratio and the process can be easily adjusted to favor char, bio-oil or gas production [8]. More interest is given to bio-oil since it is comparable to crude oil, which can be easily stored and transported, and it has low nitrogen and sulfur contents [8]. It can be used for direct combustion or can be upgraded further to liquid transport fuels and bio-chemicals [7]. Bio-oils are usually dark-brown in color with a distinctive smoky odor. It consists of a very complex mixture of oxygenated organic compounds (acids, alcohols, aldehydes, esters, ketones, phenols) with considerable fraction of water [12, 13]. Some undesirable properties of bio-oil which includes high water content, high viscosity, high ash content, low heating value (high oxygen content), high corrosiveness or acidity, and low stability limit the direct use of bio-oil as transportation fuel [12]. Hence, these properties of the bio-oil should be taken into consideration for further upgrading of the bio-oil to improve its properties as liquid fuel.

Bio-oil derived from pyrolysis of microalgae can be a potential alternative for petroleum-derived fuels if an efficient process is developed. Hence, the pyrolysis

conditions for maximum high-quality bio-oil yield should first be determined. The yield and quality of the pyrolysis products greatly depend on several factors including reactor design, reaction parameters (temperature, heating rate, residence time, pressure and catalyst) and biomass type and characteristics (particle size, shape and structure) [14, 15]. Various papers on microalgae pyrolysis focused on the decomposition characteristics of different algae species using thermogravimetric analysis [16-19]. Studies on the individual effects of process parameters such as heating rate, final temperature, and catalyst loading on pyrolysis of different microalgae species can also be found elsewhere [17-20]. Pan (2010) evaluated the effects of temperature and catalyst loading on product yields from pyrolysis of *Nannochloropsis sp* using a fixed bed reactor. Results showed that liquid and bio-oil product yields increased from 300 to 400^0C then gradually decreased from 400 to 500^0C in the direct pyrolysis process. The decrease in bio-oil yield was attributed to further cracking of the volatiles into non-condensable gases. The increase in catalyst loading, on the other hand, decreased bio-oil yield from 31.1% (0/1) to 20.7% (1/1) during catalytic pyrolysis [20]. The influence of operating pressure was investigated by Mahinpey et al (2009) using wheat straw as feedstock. Results showed that gas production was higher at lower pyrolysis pressures (10 and 20 psi) while maximum oil production (37.6%) was achieved at higher pressures of 30 and 40psi [14].

As mentioned earlier, bio-oil produced from pyrolysis must be processed further using either physical or catalytic upgrading methods to be a suitable replacement for liquid transport fuels. Bio-oils typically contain a wide variety of compounds and its

complex composition restricts its direct use as fuel or biochemical. Separation of the bio-oil to relatively simpler fractions may be done by column chromatography, solvent extraction, centrifugation and distillation [21]. Among these processes, the distillation process seems to be more attractive since no additional costs on using expensive solvents can be incurred. Also, no or minimal secondary processing steps may be required. Fractional distillation or rectification is the traditional process of separating transport fuels from the crude petroleum oil, which is usually done at atmospheric pressure. Hence, separation of bio-oil components may also be explored using this simple process.

Catalytic processes for bio-oil upgrading, on the other hand, include hydro-deoxygenation using hydro-treating catalyst, emulsification with diesel, esterification, and gasification to syngas followed by synthesis to hydrocarbons or alcohol, and zeolite upgrading [22]. Hydro-treatment processes are typically done at high temperatures. High pressure is also required for hydro-treatment to facilitate mass transport and dissociation of the poorly soluble H_2. Catalyst deactivation due to coke formation and polymerization at high temperatures are some of the problems encountered in using this process [5]. Bio-oil may also be directly combined with diesel using a surfactant in a process known as emulsification. The emulsified products have good ignition characteristics, however, the high cost of surfactant, high energy consumption, and poor quality (high acidity, low cetane, high viscosity) of the product makes this process unattractive [23, 24]. Esterification of bio-oils containing high percentage of carboxylic acids may also be done [25, 26]. Zeolite upgrading process, on the other hand, employs a relatively cheaper catalyst (HZSM-5) to improve bio-oil properties through a series of dehydration,

cracking, polymerization, deoxygenation and aromatization reactions. HZSM-5 catalyst also typically favors hydrocarbons with less than ten carbon atoms [27]. Upgrading of bio-oils using zeolite are typically done at atmospheric pressures. However, some recent studies show that HZSM-5 upgrading under H_2 pressure significantly reduce the heteroatoms (i.e. O, N and S) present in the bio-oil [27, 28].

Based on previous studies, various conversion technologies and upgrading procedures may be employed to convert different biomass materials to biofuels. In this study, biofuels production from pyrolysis of *Nannochloropsis oculata* was explored in an attempt to establish an efficient process for bio-oil production and upgrading. The first study focused on assessing the effects of reaction temperature during pressurized pyrolysis of *N. oculata.* This was followed by an optimization study to establish the combination of temperature and pressure that maximizes bio-oil yield. In the first two studies, bio-oil, char and gas yields were established at different pyrolysis conditions. Also, the composition and properties of the products were also analyzed to establish their potential applications. The third study explored on the potential of improving the quality of *N. oculata* bio-oil by fractional distillation. The recovery of water-soluble organic compounds from the aqueous liquid product was investigated as well. Lastly, the fourth study evaluated the catalytic upgrading of *N. oculata* bio-oil over HZSM-5 catalyst under moderate H_2 pressure to produce a better-quality bio-oil. From the results of these studies, technical knowledge on the operation of pyrolysis process for *N. oculata* can be derived. Also, alternative routes in upgrading the quality of the algal bio-oil can be drawn.

1.2. Research Objectives

This study generally aimed to establish an efficient method for the production of bio-oil from pyrolysis of *Nannochloropsis oculata* and evaluate various algal bio-oil upgrading processes. This study was based on the assumption that certain combination of temperature and pressure optimizes bio-oil production. Also, the bio-oil produced from *Nannochloropsis oculata* can be upgraded to alternative energy sources by separating its components through fractional distillation and by catalytic upgrading at moderate temperature and pressure using zeolite catalyst.

This project specifically aimed to:

1. Determine the effects of temperature during pyrolysis of *N. oculata* in a pressurized fixed-bed batch-type reactor based on product yields and characteristics;

2. Determine the optimum temperature and pressure for bio-oil production from pyrolysis of *N. oculata;*

3. Assess the suitability of the bio-oil obtained from pyrolysis of microalgae as an alternative for petroleum crude/transport fuels based on composition, heating value and fuel properties and evaluate the composition and energy content of pyrolysis co-products (char and gas) for potential usage;

4. Evaluate the effectiveness of upgrading the bio-oil by fractional distillation based on compositions and properties of the distillate fractions and assess the degree of separation of the bio-oil components;

5. Evaluate the potential of recovering the light organics from the aqueous liquid product (ALP) obtained from pyrolysis of *Nannochloropsis oculata,* and;

6. Assess the performance of HZSM-5 in upgrading the bio-oil obtained from *N. oculata* at moderate hydrogen pressure based on product yields and compositions and degree of heteroatoms removal.

1.3. Review of Related Literature

1.3.1. Microalgae as feedstock for biofuel production

The potential of microalgae as feedstock for biofuel production has already been studied by several researchers. Williams and Laurens (2010) provided an analysis of the biology and biochemical composition (i.e. lipids, carbohydrates, nucleic acids and protein) of microalgae based on several related articles [9]. Based on his work, microalgae as feedstock for biofuel production have several advantages, which include the following: (1) it does not compete with food production and eliminates displacement effects, (2) no or minimal amount of fresh water is required for algae cultivation since it can be grown on salty water, (3) it has high productivity and high lipid yields [9]. These advantages were also presented by Smith et al (2009) [29]. In addition, other advantages of microalgae as biofuel feedstock include less land area requirement, simpler conversion technologies, renewable, biodegradable and possible lower emission of sulfur oxides and particulates [29].

The interest in algae as biofuel feedstock was mainly based on its high lipid (or oil) content. Smith et al (2009) stated that the oil productivity of microalgae exceeds all

other oil crops [29]. A typical algae cell contains about 15-60% algal lipids, 20-60% protein, 3-5% nucleic acid and 10-50% polysaccharide [9]. Rodolfi et al (2008), on the other hand, stated that the lipid content of microalgae ranges from 70 to 85% per dry cell weight and can also be manipulated by varying the cultivating conditions [6]. The lipid content of algae was found to be inversely related to its growth rate [9]. Phospholipids and glycolipids constitute the major composition of algal lipids in actively growing cells. Furthermore, about half of the fatty acids in algae are unsaturated (and polyunsaturated) with carbon number less than C_{18}.

1.3.2. Conversion technologies for microalgae-to-biofuel production

Various biomass-to-biofuel processes can be used to convert microalgae biomass to fuel-type components. Basically, the techniques for terrestrial plant oil conversion into biofuels are also applicable to microalgae. However, some variation exists between the lipid composition of microalgae and higher plants. Some of these differences include (1) the relative proportion of polar to neutral lipids and (2) chain length or number of carbon present in fatty acids [10]. So far, there are two basic categories for the conversion of microalgae biomass which are thermochemical and biochemical conversion as shown in Figure 1 [30]. Other conversion techniques include transesterification of the extracted algal lipid to produce biodiesel and deoxygenation of fatty acids for green diesel production [10]. Gasification, anaerobic digestion and photobiological H_2 production produce gaseous products that must be immediately converted to useful energy in gas engines or gas turbines. Alcoholic fermentation, on the other hand, converts the sugar, starch or cellulose content of biomass into ethanol. In the case of starch-based

microalgae, additional processing is required before fermentation [31]. Nowadays, much attention is given to bio-oil production which can be accomplished using thermochemical liquefaction and pyrolysis. Between these two processes, pyrolysis is deemed to have the higher potential for large-scale production of biofuels that could replace petroleum-derived liquid fuel [5, 32].

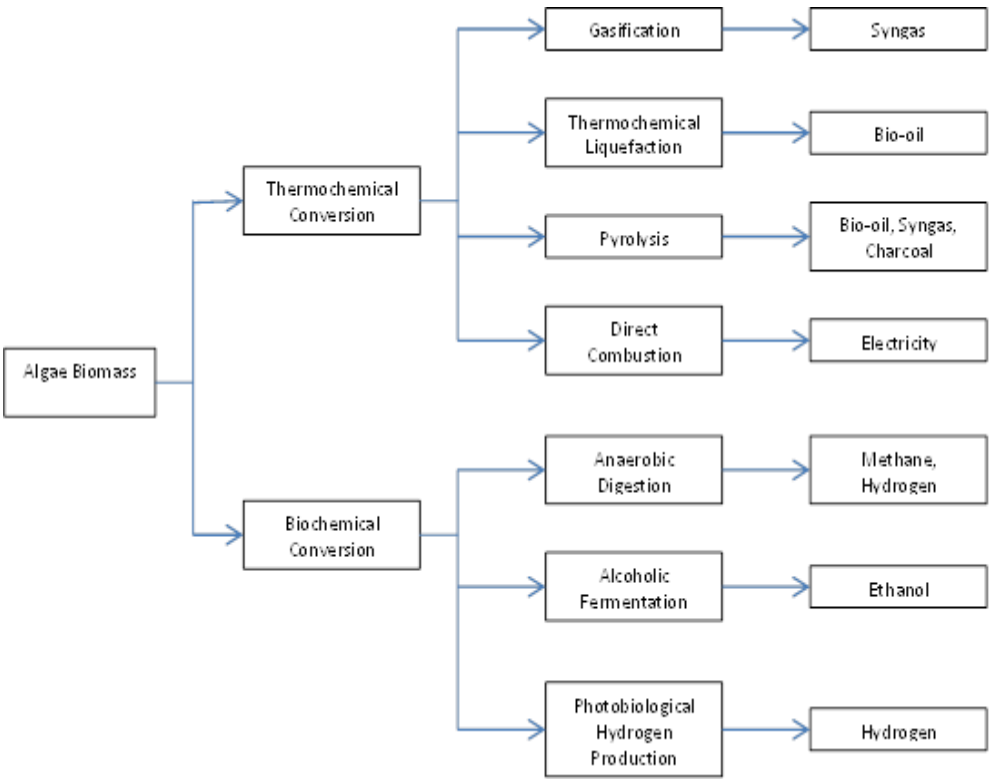

Figure 1. Potential algal biomass conversion processes (Source: Tsukuhara and Sawayama, 2005).

1.3.3. Pyrolysis

Pyrolysis produces energy fuels with high fuel-to-feed ratio and the process can be easily adjusted to favor char, liquid or gas production [8]. The bio-oil from pyrolysis of agricultural biomass is comparable to crude oil, which can be easily stored and transported, and it has low nitrogen and sulfur contents [8]. It can be used for direct combustion or can be upgraded further to liquid transport fuels and bio-chemicals [7]. Moreover, biofuels are the only sustainable source of liquid fuels nowadays [23]. The biomass-to-fuel cycle is also considered as CO_2-neutral hence it does not contribute to the greenhouse effect [23, 33]. The co-products such as char, on the other hand, could potentially be used as fertilizer due to its N, P and K content. Whereas, the recoverable heating value of the combustible gases produced could also possibly compensate the energy requirement of the pyrolysis process [7]. Various agricultural biomass such as rice husks [33], rice straw [34], bagasse [35], sawdust [36], wheat straw [14], rapeseed straw and stalk [37], corn residues [38] and switchgrass [39] were already tested for the production of bio-oil through pyrolysis.

Some studies on the pyrolytic characteristics and factors affecting the pyrolysis of microalgae are also available. According to Mahinpey et al (2009), the yield and properties of the products formed during pyrolysis are affected by several factors. These factors include reactor design, reaction parameters (temperature, heating rate, residence time, pressure and catalyst), and biomass type and characteristics (particle size, shape and structure) [14]. In the case of algae, other factors that may be considered are moisture content and species of the microalgae feedstock.

Several papers focused on the pyrolytic characteristics of different microalgae species. Peng et al (2001) compared the pyrolytic characteristics of *Spirulina platensis* (cyanobacteria) and *Chlorella protothecoides* (green algae) at different heating rates (i.e. 15, 40, 60 and 80^0C/min up to 800^0C) [19]. The study was based on the assumption that different species of algae contains varying amounts of oil [7]. The lipid content of *Chlorella protothecoides* (14.57%) was higher than *Spirulina platensis* (10.30%), while the protein content of the latter (61.44%) was higher than the former (52.64%). Both species, however, had the same volatile yield of about 71%. Also, in this study, the stages of pyrolysis were distinguished using a thermogravimetric analyzer. The three stages of pyrolysis determined were dehydration, devolatilization and solid decomposition. This observation is parallel to the results of other studies [16, 18]. The main pyrolysis reactions, which include depolymerization, decarboxylation and cracking, occurred during the devolatilization step at 150-560^0C. A linearized model was also employed in this study to determine the kinetic parameters such as activation energy (E), pre-exponential factor (A) and reaction order (n). Grierson et al (2009), on the other hand, determined the thermo-chemical properties of six (6) different algae species (*Tetraselmis chui, Chlorella like, Chlorella vulgaris, Chaetocerous muelleri, Dunaniella tertiolecta and Synechoccus)* using slow pyrolysis method (10^0C/min up to 710^0C) and Computer Aided Thermal Analysis (CATA) [7]. The highest bio-oil yield of about 43% was observed from pyrolysis of *T. chui* while the lowest was from *D. tertiolecta* (about 24%). *C. vulgaris* produced the highest amount of gas (about 25%). They also found out that microalgae tend to devolatilize at lower temperatures than lignocellulosic materials.

This may be attributed to the main components of microalgae which include protein, lipid and carbohydrate (between 60 to 80^0C). The energy requirement of the pyrolysis process (about 1MJ/kg dry algae) was also found to be lower compared to the heating value of the gas obtained at 500^0C (4.8 MJ/kg for *C. vulgaris* and 1.2 MJ/kg for *C. muelleri*). The thermo-chemical decomposition of raw *Nannochloropsis sp* as well as its lipid extract and extract residue was studied by Marcilla et al (2009) using TGA/FTIR run at a heating rate of 35^0C/min [16]. For *Nannochloropsis sp*, the thermal decomposition stages occurred at the following temperatures: (1) $<180^0$C for dehydration, (2) 180-540^0C for devolatilization, and (3) > 540^0C for solid decomposition. The hexane-soluble fraction (about 14% of the microalgae) resulted to about 82.7% weight loss during pyrolysis of the extract. It also corresponded to C-H evolution at the last decomposition stages [16].

Some operating factors for pyrolysis such as temperature, catalyst loading and heating rate were also explored. The effects of temperature and catalyst loading on product yields were studied by Pan et al (2010) using *Nannochloropsis sp* as feedstock [20]. In this study, pyrolysis was done in a fixed bed reactor (outer tube: 35mm diameter x 600mm height; inner vessel: 25 mm diameter x 120mm height) at 10^0C/min heating rate. The final temperatures tested were 300, 350, 400, 450 and 500^0C while the catalyst-to-material ratios were 0/1, 0.2/1, 0.4/1, 0.6/1, 0.8/1 and 1/1. Results showed that liquid and bio-oil product yields increased from 300^0C to 400^0C then gradually decreased from 400^0C to 500^0C in the direct pyrolysis process. Char yield decreased from 45.3% wt at 300^0C to 24.2% wt at 500^0C while gas yield increased from 18.9% wt (300^0C) to 33.5%

wt (500^0C). The decrease in bio-oil yield from 400-500^0C was attributed to the further cracking of the volatiles into non-condensable gases. The optimal temperature range was found to be 350-450^0C. The increase in catalyst loading, on the other hand, decreased bio-oil yield from 31.1% wt (0/1) to 20.7% (1/1). However, higher catalyst (1/1) resulted to more carbon and hydrogen and less oxygen in the bio-oil. Char and gas yield, on the other hand, increased from 28.01 to 34.56% wt and 24% to 29.8% wt, respectively. Li et al (2010) focused on the effects of heating rate on the pyrolytic characteristics of *Enteromorpha prolifera* (macroalga). The heating rates tested were 10, 20 and 50^0C/min up to 800^0C. Based on the results, increasing the heating rate caused an increase in (1) the initial pyrolysis temperature, (2) the temperature at which maximum weight loss occurred and (3) maximum weight loss [17].

The thermal decomposition of algal lipid was studied by Peng et al (2001). *Chlorella protothecoides s*amples with different lipid contents were used in this study [18]. The samples were (1) *Chlorella* HC- original sample, (2) *Chlorella* HC-a – residue after completely extracting the crude lipid, (3) *Chlorella*-HC-b – residue after partial extraction of the crude lipid and (4) *Chlorella*-HC-c – the crude lipid of *Chlorella* HC cells. They found out the devolatilization stage has two zones: Zone I (150-320^0C) was attributed to the decomposition of protein and carbohydrate and Zone II (340-480^0C) was accounted for the decomposition of the lipid. This observation can also be found in Marcilla et al (2009) [16].

1.3.4. Bio-oil upgrading processes

1.3.4.1. Physical upgrading

Bio-oil from pyrolysis of biomass typically contains a wide variety of compounds and its complex composition restricts its direct use as fuel or biochemical. Hence, it is necessary to separate the bio-oil to relatively simpler fractions which may have different applications depending on their characteristics. The conventional techniques in the separation of bio-oil components includes column chromatography, extraction, centrifugation and distillation [21].

Column chromatography was used by Wang et al (2011), Cao et al (2010) and Zeng et al (2011) to separate components of wood tar, and bio-oils from sewage sludge and rice husk, respectively [40-42]. Solvent extraction of valuable bio-oil components such as phenol can also be found elsewhere [43, 44]. Although these methods were found effective to a certain extent in separating specific compounds from the bio-oil, further processing is still needed to remove the solvent used in both processes. Centrifugation, on the other hand, is a simple pretreatment technique; however, the homogeneity of the bio-oil limits its applicability [45].

There are various distillation techniques which can be utilized for bio-oil separation including molecular distillation, flash distillation, steam distillation and fractional distillation [45]. Both flash and steam distillation processes are typically used as pre-separation methods only where high purity is not required [45, 46]. The separation of bio-oil components by molecular distillation can also be found elsewhere [45-48].

Wang et al (2009) used a KDL5 molecular distillation apparatus to separate sawdust bio-oil into three (3) fractions at different operating temperatures. Maximum distillate yield of about 85% wt was obtained and the degree of separation was evaluated using a separation factor, $I_{i,m}$, which is mainly the relative content of a compound in the GC-MS chromatogram [45]. Guo et al (2010), on the other hand, separated sawdust bio-oil into light, middle and heavy distillates using molecular distillation and characterized each fraction using TG-FTIR analysis. Results showed that most of the water (~70%) and acids with low boiling point were contained in the light fraction; whereas, the middle and heavy fractions contained more phenols [46]. Fractional distillation or rectification, on the other hand, is the traditional way of separating transport fuels such as gasoline and diesel from petroleum crude. Unlike molecular distillation, which is typically done under high vacuum (<0.01 torr), this process can be done at atmospheric conditions. In fractional distillation, separation takes place by repeated vaporization-condensation cycles within a packed distillation column [49]. Boucher et al (2000) studied the distillation of softwood bark residues until 140^0C using packed columns to determine the true boiling point distribution of the light fraction of the bio-oil. The distillation curve, which is a plot of cumulative distillate %wt against temperature, showed the evaporation of water at temperatures below 100^0C followed by an increase in the slope of the curve indicating the evaporation of heavier fractions [50]. Based on this data, removal of water from the bio-oil could be done by distillation to improve its combustion characteristics.

1.3.4.2. Catalytic upgrading

Some undesirable properties of bio-oil which includes high water content, high viscosity, high ash content, low heating value (high oxygen content), high corrosiveness or acidity, and low stability limit the direct use of bio-oil as transportation fuel [12]. Hence, bio-oil must be upgraded to be a suitable replacement for diesel or gasoline fuels. According to Huber et al (2006), catalytic upgrading of bio-oil may be done using various processes including: (1) hydrodeoxygenation using typical hydrotreating catalyst (sulfided CoMo or NiMo), (2) emulsification with diesel fuel, and (3) zeolite upgrading [23]. Catalytic esterification may also be done if there is high percentage of carboxylic acids in the bio-oil [25, 26, 51-53].

Hydrodeoxygenation of bio-oil typically occurs at temperatures ranging from 300 to 600^0C with high-pressure of H_2 in the presence of heterogeneous catalysts. In this process, the oxygen from bio-oil reacts with H_2 producing water and saturated C-C bonds. Industrial hydrotreating catalysts (sulfided CoMo and NiMo), Pt/SiO_2-Al_2O_3, vanadium nitride and Ruthenium can be used for this purpose [23]. Several studies on hydrodeoxygenation of crude bio-oils from mostly from lignocellulosic materials and model compounds can be found elsewhere [54-57]. Catalytic hydrotreatment of crude algal bio-oil from *Nannochloropsis sp* was also attempted by Duan et al (2011) using 5%Pd/C catalyst in supercritical water at 400^0C and 3.4MPa H_2 pressure. In his study, hydrogen and energy content increased, while oxygen and nitrogen contents decreased as compared to crude bio-oil after hydrotreatment for 4 hours at 80% catalyst intake [58]. The need for high-pressure H_2, conversion of carbon in bio-oil to gas-phase carbon,

catalyst instability and gum formation, however, are the most common problems encountered in this process [23].

Emulsification is the process of combining bio-oil with diesel directly with the aid of a surfactant. This process does not require redundant chemical transformations [24] and the bio-oil emulsions produced have promising ignition characteristics [23]. However, several factors limits the use of this process including the high cost of surfactant, high energy consumption and high acidity, low cetane number and increased viscosity of the product [23, 24].

Bio-oil esterification is mostly applicable for bio-oils containing high amounts of organic acids. Similar to biodiesel production, this process is based on acid- or base-catalyzed esterification reactions which convert the acids present in the bio-oil into useful esters at temperatures ranging from 70 to 170^0C. One major drawback in this process is the reactions involving other organic compounds present in the bio-oil. As mentioned earlier, bio-oil is a complex mixture of organic compounds, hence, other components such as aldehydes or sugars may also react during the esterification process [51, 52, 59].

Zeolite has been widely used in the petroleum refining industry due to their high activity, increased selectivity towards the gasoline fraction, and lower coke formation [60]. Zeolite upgrading employs a crystalline microporous material (zeolite) which contains active sites for the dehydration, cracking, polymerization, deoxygenation and aromatization of bio-oil components. These reactions typically occur at temperatures

ranging from 350 to 500^{0}C at atmospheric pressure. Upgrading of bio-oil from pyrolysis of beech wood [61], rice husk [62], sawdust [63], and anisole, which is a typical component of bio-oil [64] were tried using HZSM-5. Catalytic pyrolysis of *Nannochloropsis oculata* using HZSM-5 as catalyst was also studied by Pan et al (2010) [20]. Based on this study, the bio-oil from catalytic pyrolysis has lower oxygen content and higher heating value as compared to that obtained from direct pyrolysis. Carrero et al (2011), on the other hand, explored the applicability of zeolites (ZSM-5, Beta, h-ZSM-5 and h-Beta) as heterogeneous catalyst for biodiesel production from lipids exracted from *Nannochloropsis gaditana* [65]. Unlike hydrodeoxygenation, this process does not typically require H_2 supply and the operating temperatures employed are similar to bio-oil production. Zeolite catalyst can also be impregnated with metals such as gallium, nickel, platinum, palladium, etc. Thangalazhy-Gopakumar et al (2012) studied the catalytic pyrolysis of pine wood using HZSM-5 and metal-impregnated zeolites in a hydrogen environment, which was referred to as hydro-pyrolysis. At low H_2 pressures (100-300psi), HZSM-5 was found to be more active than the metal-impregnated zeolite; whereas, at higher pressures (400 psi), more hydrocarbons were produced using metal-impregnated HZSM-5. About 42.5% wt of biomass carbon was converted to hydrocarbons using hydropyrolysis with HZSM-5. Based on his study, HZSM-5 had higher activity than impregnated metals, which indicate that deoxygenation due to cracking was the major reaction occurring during catalytic pyrolysis and no or minimal hydrogenation of aromatic hydrocarbons occurred. Aromatic selectivity of major hydrocarbons such as toluene, xylene and benzene was also not affected by the

addition of metals [27]. Adjaye and Bakhshi (1995), on the other hand, compared the effectiveness of different catalyst (HZSM-5, H-Y, H-mordenite, silicalite, and silica-alumina) to increase the hydrocarbons yield in the organic distillate fraction (ODF) from fast pyrolysis maple wood bio-oil using a fixed-bed micro-reactor [66]. The highest hydrocarbons yield of about 27.9% wt was obtained from HZSM-5. Low amounts of oxygenated compounds (alcohols, ketones and phenols) were detected, which indicated the effectiveness of conversion of these compounds to hydrocarbons. Also, the presence of the catalyst reduced the formation of char during HZSM-5 treatment [66].

Typical HZSM-5 usage includes cracking of organic compounds at atmospheric pressure. However, high hydrogen pressure promotes hydrogenation of free radicals or fragments which suppresses coke formation due to condensation and polymerization reactions [27]. Aside from that, treatment with HZSM-5 at high pressure H_2 can greatly reduce the amount of heteroatoms (O, N and S) in the oil [28]. Based on Li and Savage (2013), the N/C ratio of the crude bio-oil from hydrothermal liquefaction of *Nannochloropsis sp* was reduced to about 25% of the original N/C ratio while the O/C ratio was also an order of magnitude lower than the original after HZSM-5 upgrading under 4.3MPa hydrogen pressure.

2. EVALUATING THE EFFECTS OF TEMPERATURE ON PRESSURIZED PYROLYSIS OF *Nannochloropsis oculata* BASED ON PRODUCTS YIELDS AND CHARACTERISTICS*

2.1. Introduction

The economic development of an industrial society relies heavily on the availability of energy sources. Fossil fuels still serve as the main source of energy at present. However, issues arising from the unsustainable use of fossil fuels such as increasing greenhouse gas (GHG) emissions, increasing fuel prices, and depleting petroleum fuel reserves prompted researchers to look for alternative sources of energy that are less carbon-intensive and renewable [1-4]. [1]

Biofuels are fuels that are derived from renewable feedstocks which may be in solid, liquid or gaseous forms. Biomass pyrolysis is one of the technologies that are being explored nowadays for the production of biofuels. Pyrolysis is a thermochemical conversion process that produces energy fuels with high fuel-to-feed ratio, and the process can be easily adjusted to favor char, bio-oil or gas production [8]. The bio-oil from pyrolysis of agricultural biomass is comparable to crude oil, which can be easily stored and transported, and it has low nitrogen and sulfur contents [8]. It can be used for direct combustion or can be upgraded further to liquid transport fuels and bio-chemicals

[1] *Reprinted with permission from "Evaluating the effects of temperature on pressurized pyrolysis of *Nannochloropsis oculata* based on products yields and characteristics" by MCC Maguyon and SC Capareda, 2013. *Energy Conversion and Management*, 76, 764-773, Copyright 2013 by Elsevier.

[7]. Char, on the other hand, could potentially be used as fuel or fertilizer due to its N, P and K content [8]. Whereas, the recoverable energy from the combustible gases produced could possibly compensate the energy requirement of the pyrolysis process [7]. Biofuels are the only sustainable source of energy nowadays [23]. The biomass-to-fuel cycle is also considered as CO_2-neutral hence it does not contribute to the greenhouse effect [23, 33].

Various agricultural biomass such as rice husks [33], rice straw [34], bagasse [35], sawdust [36], wheat straw [14], rapeseed straw and stalk [37], corn residues [38] and switchgrass [39] were already tested for the production of bio-oil through pyrolysis. However, the bio-oil obtained from lignocellulosic residues needs to be upgraded to be used as fuel since it has high oxygen content, high viscosity, high corrosiveness and relative instability [67, 68]. These characteristics may be attributed to the main chemical components of lignocellulosic biomass which include cellulose, hemicelluloses and lignin [37].

Microalga is another feedstock for biofuel production that is of interest to researchers nowadays. The potential of microalgae as feedstock has already been studied by several researchers [9, 29, 69, 70]. The interest in algae as biofuel feedstock was mainly based on its high lipid (or oil) content [9, 29, 71]. Moreover, compared to lignocellulosic materials, microalgae grows faster [7, 8], has high photosynthetic efficiency [8], and high productivity [8, 9]. It can be cultivated on salty water [9] and does not require arable soils [6, 7]. The bio-oil produced from microalgae is more stable

due to lower O/C ratio and has higher HHV compared to wood oil [8]. Also, microalgae, which has protein, lipid and carbohydrate as its main components, devolatilizes at lower temperatures than lignocellulosic materials [7, 19].

Several factors including reactor design, reaction parameters (temperature, heating rate, residence time, pressure and catalyst), and biomass type and characteristics (particle size, shape and structure) largely affects the yield and quality of the products formed during pyrolysis [14]. Different species of algae also contain varying amounts of oil that contains different compounds. Grierson et al (2009) studied the thermo-chemical properties of *Tetraselmis chui, Chlorella like, Chlorella vulgaris, Chaetocerous muelleri, Dunaliella tertiolecta* and *Synechococcus* using slow pyrolysis process (100C/min up to 710^0C) and Computer Aided Thermal Analysis (CATA) under unsteady state heating conditions [7]. The highest bio-oil yield (43%) was attained at 500^0C using *T. chui* as feedstock while the lowest was obtained from *D. tertiolecta* (24%). Fast pyrolysis (heating rate of 600^0C/s at 500^0C), on the other hand, was studied by Miao et al (2004) using *Chlorella protothecoides* and *Microcystis aeruginosa*. Bio-oil yields of 17.5% and 23.7% were obtained from *C. protothecoides* and *M. aeruginosa*, respectively [8]. TGA/FTIR analysis was used by Marcilla et al (2009) to examine the decomposition during pyrolysis of dry *Nannochloropsis sp*, its lipid extract and extract residue [16]. In this study, it was found out that the decomposition process has three stages, namely: (1) dehydration ($<180^0$C), (2) devolatilization ($180\text{-}540^0$C) and slow decomposition of the solid residue ($>540^0$C). Also, the decomposition of the lipid (or hexane-soluble) extract at around 450^0C resulted to 82.7% weight loss during pyrolysis. The main pyrolysis

reactions for *Spirulina platensis* and *Chlorella protothecoides*, which include depolymerization, decarboxylation and cracking, was observed at 150-560^{0}C by Peng et al (2001) using TGA at different heating rates (15, 40, 50, 80^{0}C/min up to 800^{0}C) [19]. Direct and catalytic pyrolysis of *Nannochloropsis sp* residue were compared by Pan et al (2010) using a fixed-bed reactor (outer tube: 35mm diameter x 600mm height; inner vessel: 25mm diameter x 120 mm height) at different pyrolysis temperatures (300, 350, 400, 450 and 500^{0}C) and catalyst-to-material ratios (0/1, 0.2/1, 0.4/1, 0.6/1, 0.8/1, 1/1) [20]. The highest bio-oil yield obtained in this study was 31.1% wt at 400^{0}C and 0/1 catalyst loading. This value decreased to 20.7% wt with an increase in catalyst (1/1); however, the bio-oil obtained has more carbon and hydrogen, less oxygen and has higher HHV.

Previous studies showed that the yields and qualities of pyrolysis products vary depending on microalgae species and reactor configuration. In this paper, a pressurized fixed-bed reactor was used to evaluate the effects of temperature on the yields and qualities of pyrolysis products using *Nannochloropsis oculata* as feedstock. The characteristics of *N. oculata* were also assessed to determine its suitability as feedstock for production of biofuels through pyrolysis. The heating values and composition of the char, bio-oil and gas produced at each temperature were analyzed to determine its potential as alternative energy sources. Mass and energy yields based on initial biomass input were also estimated in an attempt to establish mass and energy conversion efficiencies of the pyrolysis process.

2.2. Materials and Methods

2.2.1. Feedstock preparation and characterization

Nannochloropsis oculata samples used in this study was obtained from the Texas Agri-Life Research Algae Pond facility in Pecos, Texas. The samples were oven-dried at 105^0C until less than 10% wt moisture was obtained. Then, the dried algae samples were ground using Wiley Laboratory Mill Model #4 distributed by Arthur Thomas Company, Philadelphia, PA, USA. The average particle size diameter (PSD) of the ground algae samples was determined using USA Standard Sieve Nos. 20, 30, 40, 60 and 80 (ASTM E-11 specification, Fisher Scientific Company, USA). The HHV of the sample was determined subsequent to ASTM D 2015 using PARR isoperibol bomb calorimeter (Model 6200, Parr Instrument Company, Moline, IL). Moisture content and proximate analysis were determined in reference to ASTM standards (D 3173, D 3175 and E1755). The ultimate analysis was determined using Vario MICRO Elemental Analyzer (Elementar Analysemsysteme GmbH, Germany) in accordance with ASTM D 3176. Compositional analysis of *N. oculata* was done using NREL procedures: (1) Determination of Acid Soluble Lignin Concentration Curve by UV-Vis Spectroscopy (NREL/TP-510-42617), (2) Determination of Structural Carbohydrates and Lignin in Biomass (NREL/TP-510-42618), and (3) Determination of Extractives in Biomass (NREL/TP-510-42619). Lipid content (% wt), on the other hand, was analyzed by soxhlet extraction for 24 hours using hexane as solvent. 10 g of dry microalgae sample was used in the analysis. After the extraction process, the solvent was removed from the extracted solution by rotary evaporation (rotavap) at 40^0C and 23 mmHg vacuum

pressure. Then the amount of lipid (% wt) extracted was calculated by dividing the amount of dry oil in the flask by the initial amount of dry microalgae.

2.2.2. Pyrolysis experiment

Pyrolysis experiments were performed using a fixed-bed batch-type Parr pressure reactor (Series 4580 HP/HT, Parr Instrument Company, Moline, IL) illustrated in Figure 2. The reactor is made of AISI 316 Stainless Steel with the capacity of 1.5L. The reactor is inserted into a cylindrical ceramic fiber electrical heater with thermowell attached to a reactor controller (Series 4840, Parr Instrument Company, Moline, IL). A Type J (iron-constantan) thermocouple, also attached to the reactor controller, measures the temperature inside the reactor. Pressure gage (0-5000psi capacity) with T316 Stainless Steel Bourdon tube measures the pressure build-up inside the reactor.

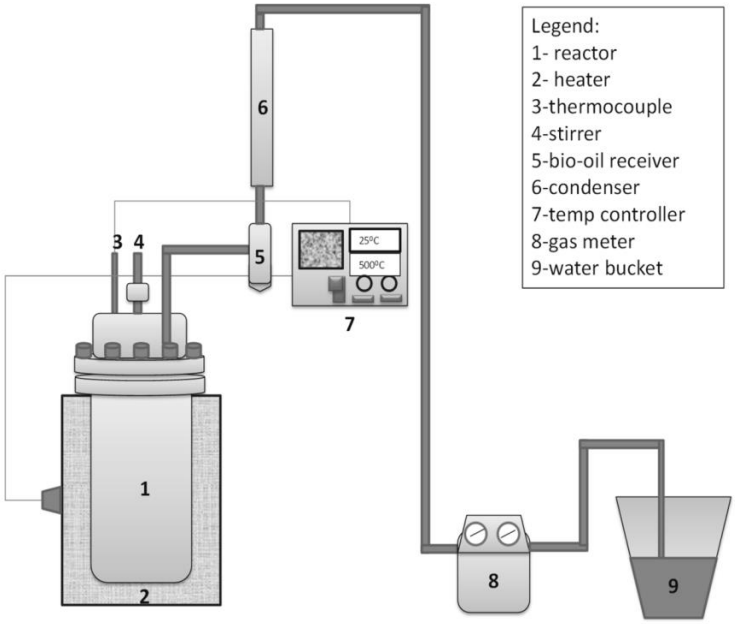

Figure 2. Pyrolysis experimental set-up.

Pyrolysis runs were carried out subsequent to a three-level, one-factorial completely randomized experimental design. The reactor temperature served as the main factor in the experiment. The temperature levels tested were 400^0C, 500^0C and 600^0C. The runs were done in triplicates for each temperature.

For each pyrolysis run, approximately 250 g of dried and ground N. oculata were loaded into the reactor. To ensure the absence of oxygen, the reactor was purged with nitrogen for 20 minutes at about 10 psi before each run. The reactor was heated at approximately 5^0C/min until the desired temperature was reached. An internal stirrer attached to a magnetic drive operated at approximately 600 rpm was used to ensure uniformity of temperature inside the reactor. The pressure build up in the reactor, due to gas production, was allowed to increase to approximately 100 psi. Then, the pressure was maintained at this level by slightly opening the gas valve attached to the condenser releasing some of the gaseous product. When the desired temperature was achieved, the reaction was allowed to proceed at the desired temperature for about 30 minutes before turning the heater off and allowing the reactor to cool down. The volume of gas produced was measured using a gas meter (METRIS® 250, Itron, Owenton, KY) with air/gas capacity of 250/195 CPH. Gas samples for analysis were also collected using 0.5L Tedlar sampling bags with combination valve. The liquid product was collected from the receiving vessel below the condenser while the char was collected from the reactor. Both were weighed using an analytical balance (Mettler Toledo, Model XP105DR, Switzerland).

2.2.3. Char and bio-oil analysis

The heating values (HHV) of the char and bio-oil samples were determined using PARR isoperibol bomb calorimeter (Model 6200, Parr Instrument Company, Moline, IL) following ASTM D2015. Proximate analysis of the char was done in reference to ASTM standards (D 3175 and E1755). The ultimate analysis of the char and bio-oil was determined using Vario MICRO Elemental Analyzer (Elementar Analysemsysteme GmbH, Germany) in accordance with ASTM D 3176. Other bio-oil analyses performed include ash content (ASTM D0482-07), moisture content (ASTM E203) using KF Titrino 701 (Metrohm, USA, Inc.), and density (ASTM D1217-93). The chemical composition of the bio-oil was also determined by GC-MS analysis using Shimadzu QP2010 Plus, with the following parameters: bio-oil dissolved in dichloromethane (10 %vol); column – DB-5ms (25m length, 0.25μm thickness and 0.25mm diameter); column temperature program: 40^0C (held for 5 minutes) then ramped to 320^0C at 5^0C/min, then held for 5 minutes at 320^0C; ion source temperature at 300^0C. The functional groups present in the bio-oil were also determined using Shimadzu IRAffinity-1 FTIR (Fourier Transform Infrared) Spectrophotometer (Shimadzu, Inc).

2.2.4. Gas analysis

The composition of the gas sample obtained from each pyrolysis run was analyzed using SRI Multiple Gas Analyzer #1 (MG#1) gas chromatograph (GC) equipped with an on-column injection system and two detectors: Helium Ionization Detector (HID) and Thermal Conductivity Detector (TCD). The columns used were 6' Molecular Sieve 13X and ShinCarbon ST 100/120 (2m, 1mm ID, 1/16OD, Silco), with

helium as the carrier gas. The calibration gas standard mixture used consisted of H_2, N_2, O_2, CO, CH_4, CO_2, C_2H_4 and C_2H_6 (Praxair Distribution, Geismar, LA) with analytical accuracy of ±2%. Initial temperature of the column was set at 65^0C for 10minutes then ramped at 16^0C/min to a final temperature of 250^0C.

2.2.5. Data analysis

Product (char, bio-oil and gas) yields (% wt) were calculated using Equation 1 shown below. Gas yield was initially calculated as volume per mass of dry algae used. The composition (% v/v) of the gas products was used to convert the volume of the gas to its mass equivalent.

$$\text{Product yield (\%wt)} = (\text{mass of product/mass of dry algae used}) \times 100 \quad (2.1)$$

Mass balance around the reactor shown in Equation 2 was then used to calculate the losses (% wt), and consequently, the mass conversion of the process.

$$\%\text{Char yield} + \%\text{ Liquid yield} + \%\text{Gas yield} + \%\text{Losses} = 100\% \quad (2.2)$$

On the other hand, energy yield (%) was estimated using Equation 3. The energy yield calculated for each product was then supplied to the energy balance of the process to determine the % energy loss.

$$\text{Energy yield (\%)} = \text{Product yield (\%wt)} \times (HV_{product}/HV_{algae}) \quad (2.3)$$

Statistical analysis of data was done by Analysis of Variance (ANOVA) at 95% confidence interval. The experimental errors were estimated as standard deviations and were represented as error bars placed in the graphs showing the results.

2.3. Results and Discussion

2.3.1. Characteristics of Nannochloropsis oculata

Table 1 shows the characteristics of *N. oculata* obtained from Texas Agri-Life Research Algae Pond Facility in Pecos, Texas. The average particle size diameter (PSD) and bulk density of the dried and ground feedstock was determined to be about 0.29 mm and 636 kg/m^3, respectively. Proximate analysis, which includes volatile matter, fixed carbon and ash, was done. Based on the results, the volatile matter (VM) present in dry *N. oculata* was relatively high (81.27% wt) similar to wood. The volatile components are the ones being liberated and transformed into gas, light hydrocarbons and tar during pyrolysis. Hence, high amounts of volatile components in the biomass could positively contribute to liquid and gas production. Fixed carbon and ash, on the other hand, remains in the residue (char) after the release of volatiles. Also, the dry N. oculata has higher combustible components (carbon, hydrogen) and lower nitrogen and oxygen content as compared to *Spirulina platensis* and *Nannochloropsis sp* residue [20, 72]. Thus, it has relatively higher HHV of about 25 MJ/kg. Compared to wood, *N. oculata* has lower oxygen content. According to Czernik and Bridgwater (2004), bio-oil tends to resemble the elemental composition of the biomass [67]. Hence, the bio-oil generated from pyrolysis of *N. oculata* may be expected to contain lesser amount of oxygenated compounds than wood bio-oil. Bio-oils with low O/C ratio is said to be more stable [8, 73].

Compositional analysis of *N. oculata* was also done using NREL procedures as stated in Section 2.2.1. Results showed that *N. oculata* contains high percentage of

extractives (47% wt), and protein (24% wt), which contributes to the nitrogen present in the biomass [74]. Water extractives (23% wt) consists of inorganic materials, nonstructural carbohydrates and nitrogenous materials among others, while ethanol extractives (24% wt) may include waxes, fats, resins, tannins, gums, starches and pigments. Table 1 also shows the acid soluble (2.89% wt) and acid insoluble (2.01% wt) components present in *N. oculata.* In the NREL procedures, the acid insoluble component after the removal of protein and ash is termed as Acid Insoluble Lignin (AIL), while the acid soluble component detected in the hydrolysis liquor is referred to as Acid Soluble Lignin (ASL). It is generally believed that microalgae do not synthesize lignin. However, recent studies show that some species of algae such as *Calliarthron cheilosporiodes (red alga), C. obicularis, C. scutata* and *C. nittellarum,* may have lignin or lignin-like polymers or oligomers produced by radical coupling of monolignols or hydroxycinnamyl alcohols [75, 76]. Further investigation may be useful to determine whether the acid soluble and acid insoluble components detected in *N. oculata* were indication of its lignin content. Nonetheless, other characteristics of the feedstock presented in Table 1 were deemed sufficient to explain the succeeding results. The carbohydrates content for microalgae typically ranges from 10-12% wt [8]. For *N. oculata,* only 7% wt was detected as structural carbohydrates or sugars. However, nonstructural carbohydrates or water-soluble sugars may also be present in the water extractives as stated earlier. The lipid content (14% wt) of *N. oculata,* on the other hand, is comparable to that of *Scenedesmus obliquus* (12-14% wt), *Chlorella vulgaris* (14-22% wt) and *Euglena gracilis* (14-20% wt) [69].

Table 1. *Nannochloropsis oculata* characteristics.

Biomass Characteristics	Nannochloropsis oculata[a] wet basis	Nannochloropsis oculata[a] dry basis	S. platensis[b]	Nannochloropsis sp residue[c]	Wood
Particle Size Diameter (mm)		0.29 ± 0.01			
Bulk Density (kg/m^3)		696.3 ± 0.20			
HHV (MJ/kg)		24.7 ± 0.49	20.52	20.7	19.5-20.5[d]
Proximate Analysis (%wt)					
Moisture	8.38 ± 0.45	---	---	7	---
VCM	74.46 ± 0.98	81.27 ± 0.98	---	63.5	82[e]
Fixed Carbon	4.74 ± 0.46	5.17 ± 0.46	---	19.6	17[e]
Ash	12.43 ± 0.65	13.57 ± 0.65	---	9.9	1[e]
Ultimate Analysis (%wt)					
C		48.31 ± 0.26	46.87	44.1	50.6-53.1[d]
H		7.66 ± 0.12	6.98	7.09	6.1-6.4[d]
N		4.80 ± 0.02	10.75	5.51	0.2-0.4[d]
S		0.81 ± 0.05	0.54	---	---
O[e]		24.85 ± 0.36	34.86	33.4	40.6-42.7[d]
Molar formula	$CH_{1.9}N_{0.08}S_{0.007}O_{0.38}$				
Compositional Analysis (%wt)					
Extractives		47.35 ± 3.79			
Water		23.26 ± 1.32			
Ethanol		24.09 ± 4.22			
Acid Solubles		2.89 ± 0.18			
Acid Insolubles		2.01 ± 0.63			
Protein		23.95 ± 2.36			
Sugars		6.87 ± 0.17			
Lipid		14.46 ± 0.91			

[a] Experimental values
[b] adapted from Jena et al (2011) [27]
[c] adapted from Pan et al (2010) [26]
[d] adapted from Demirbas (1997) [28]
[e] adapted from McKendry (2002) [38]
[f] By difference, %O = 100-C-H-N-S-Ash

2.3.2. The effect of temperature on product yields and mass conversion efficiencies

The effect of temperature on products yields during pyrolysis of *N. oculata* is shown in Figure 3. The variation in temperature had significant effects on both gaseous

product (p-value <0.0001) and char (p-value=0.0013) yields. Gas yield significantly increased from 400^{0}C (3.96 %wt) to 600^{0}C (14.85 %wt). Conversely, char production decreased significantly from 400^{0}C (51.75 %wt) to 500^{0}C (36.50 %wt). Then, it tended to level off from 500^{0}C to 600^{0}C as can be seen from the plot. These observations are similar to the results obtained by Pan et al (2010) [20]. This could indicate that the decomposition of biomass was complete at 500^{0}C and 100 psi.

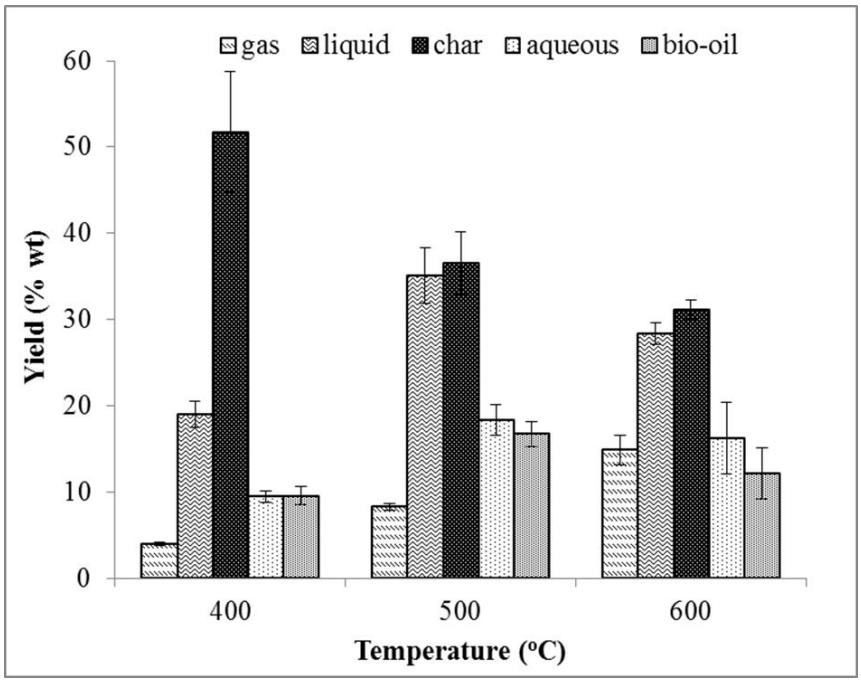

Figure 3. Products yields at different temperatures.

On the other hand, an increase in liquid product yield was observed with an increase in temperature from 19 %wt at 400^{0}C to 35.09 %wt at 500^{0}C (p-value = 0.0001). The increase in liquid product yield at 500^{0}C could possibly be attributed to the decomposition of algal lipid. The thermal decomposition of algae can be divided into three steps, namely: (1) dehydration (<180^{0}C), (2) devolatilization where the main

pyrolysis process occurs (180-540^{0}C) and (3) solid decomposition (>540^{0}C) [16, 17, 19]. According to Marcilla et al (2009), the decomposition of lipid occurs during the latter portion of the devolatilization stage (~500^{0}C) preceded by the breakdown of polysaccharides and proteins [16]. However, further heating the biomass to 600^{0}C decreased the liquid product yield (p-value=0.0092) which could be due to secondary cracking of the oil vapors forming incondensable gaseous products [20]. This observation is consistent with the further increase in gas yield from 500 to 600^{0}C as can be seen in Figure 3. Based on this result, maximum liquid yield was obtained at 500^{0}C (35% wt). Lower liquid yields were achieved for *C. protothecoides* (17.5% wt) and *M. aeruginosa* (23.7%wt) from fast pyrolysis at the same temperature (500^{0}C) at a heating rate of 600^{0}C/s. This could indicate the variation in product yields as different pyrolysis modes (slow or fast) and microalgae species are employed. A study by Liang (2013) also revealed that slow pyrolysis results to higher liquid yields at the same pyrolysis temperature of 500^{0}C than fast pyrolysis using *C. protothecoides* as feedstock [77]. According to Benemman and Oswald (1996) as cited by Carriquiry et al (2011), the price of microalgae harvested from an open pond system (218 t/ha-yr capacity) is about $193/t biomass [78]. At this rate, the price of the liquid product would be about $1.75/gallon based on maximum liquid yield. This amount is relatively lower than the suggested algal oil price ($2.86/gallon) to be competitive with petroleum-based fuels [79]. However, further processing of the liquid product to obtain fuel-type components may add to the estimated cost.

The liquid product obtained contains two immiscible fractions: (1) the yellowish aqueous fraction, and (2) the dark-brown organic fraction or bio-oil, which separated immediately. Based on Figure 3, the yield of aqueous fraction increased significantly from 9.44% wt at 400^0C to about 18.33% wt at 500^0C (p-value = 0.006) then leveled off from 500^0C to 600^0C (p-value = 0.3678). On the other hand, bio-oil yield increased from 400^0C (9.56% wt) to 500^0C (16.75% wt) (p-value = 0.0044) as shown in Figure 3. Then, it tended to decrease from 500^0C to 600^0C (12.12% wt) (p-value = 0.0287). Obviously, this trend is parallel to that of the liquid product. Hence, the decrease in the liquid product yield from 500^0C to 600^0C could be directly attributed to the decrease in the organic bio-oil fraction.

Mass conversion efficiencies at different temperatures (Figure 4) were then estimated using Equation 2.2. Based on Figure 4, most of the feedstock was converted to char at all temperature levels. On the average, the mass conversion efficiency of the process was about 76% regardless of the temperature level. The percentage loss of about 24% may be accounted to the uncondensed bio-oil that was trapped by the filter attached to the gas meter (see Figure 2). Also, some of the char and bio-oil that adhered to the sides of the reactor were not collected.

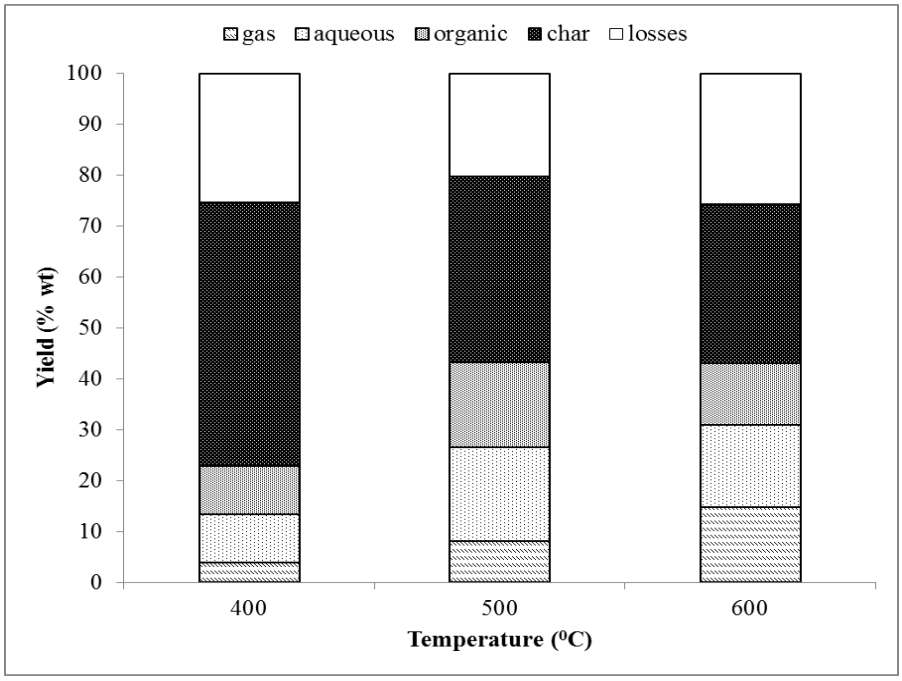

Figure 4. Mass conversion efficiencies of the pyrolysis process at different temperatures.

2.3.3. The effect of temperature on product composition and properties

2.3.3.1. Char

Proximate analysis of the char samples obtained at different pyrolysis temperatures is shown in Figure 5. Based on the plot, the volatile matter content of the biomass evidently decreased from 81% wt (Table 1) of the original *N. oculata* to 53% wt after pyrolysis at 400^0C. Further heating of the biomass to 500^0C decreased the volatile matter content to approximately 20% wt. This trend is similar to that observed by Uzun et al (2007) using olive-oil residue as feedstock [80]. The increase in temperature, therefore, allowed more volatile components to be liberated from the algal biomass forming liquid and incondensable gas components. After 500^0C, however, no significant change in volatile matter content was observed. This further explains the leveling off of

char yield from 500^0C to 600^0C (Figure 3). Evidently, the decrease in the amount of char was mainly due to the release of volatile components from the biomass. The fixed carbon and ash contents, on the other hand, both increased to 42% wt and 39% wt at 500^0C, respectively. Intuitively, the reduction in the amount of volatiles tended to increase the relative concentration of the nonvolatile fractions (i.e. fixed carbon, ash) in the char. Similar to volatile matter, no significant change in fixed carbon and ash was observed from 500^0C and 600^0C.

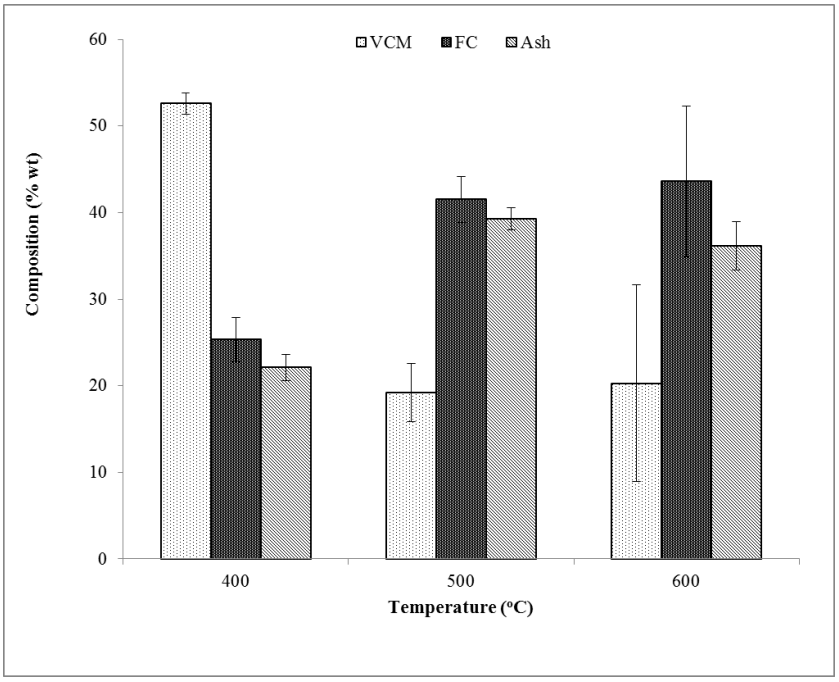

Figure 5. Proximate analysis of char from *N. oculata* at different temperatures.

Ultimate analysis (Figure 6), on the other hand, shows that the combustible elements (carbon and hydrogen) and oxygen in the char significantly decreased as pyrolysis progressed from 400^0C to 500^0C. Further heating up the process to 600^0C, however, did not significantly change the elemental composition of the char. This

observation is consistent with the proximate analysis. The volatiles that were released from the biomass during pyrolysis may contain carbon, hydrogen and oxygen forming different compounds in the liquid and gas products. The HHV of the char, on the other hand, decreased from 26.87 MJ/kg at 400^0C to 20.44 MJ/kg at 500^0C. This may still be attributed to the release of volatile combustible components from the biomass at higher temperatures.

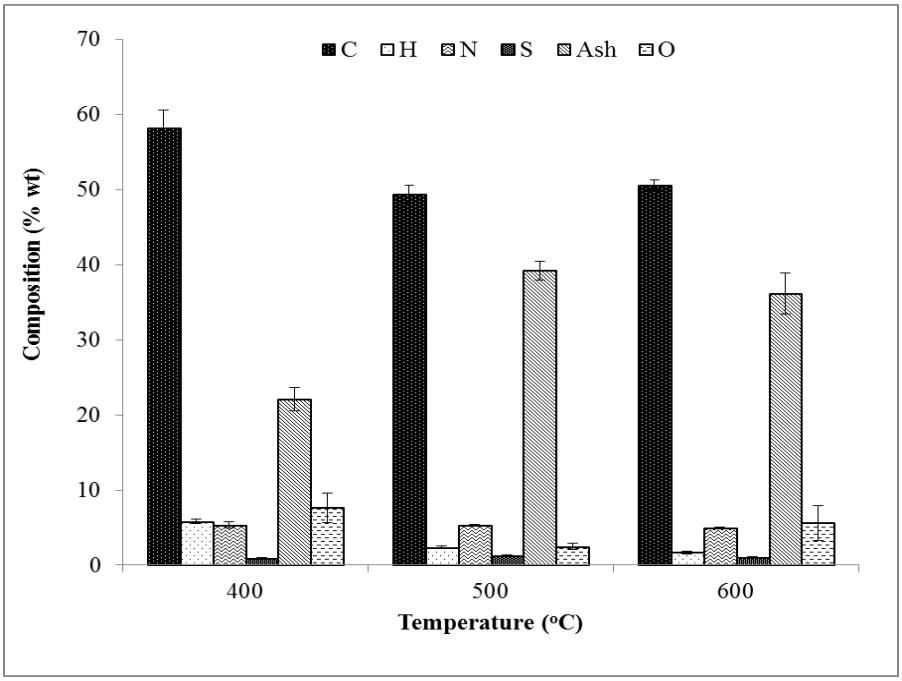

Figure 6. Ultimate analysis of char from *N. oculata* at different temperatures.

Based on the properties discussed, the high carbon content of the char makes it suitable for several applications such as fuel or activated carbon. Further investigation on the application of char as fuel was done using Van Krevelen diagram (Figure 7). According to McKendry (2002), biomass can be compared to fossil fuels using atomic O:C and H:C ratios, known as the Van Krevelen diagram [81]. Fuels with higher energy

can be found at the lower left corner (near the origin) of the Van Krevelen diagram since this region represents low H:C and O:C ratios [81]. Higher H:C and O:C ratio decrease the energy value of a fuel due to the lower energy contained in the C-H and C-O bonds compared to C-C bonds [82]. Based on Figure 7, the original feedstock (*N. oculata*) has relatively higher H:C and O:C ratio compared to coal and lignite, hence, contains lesser energy value. However, the chars produced from pyrolysis of *N. oculata* approaches the coal region as shown in the Van Krevelen diagram. It can also be seen that the H:C and O:C ratios of the char obtained at higher temperatures are much lower than that of the original feedstock (N. oculata) and char produced from low temperature pyrolysis.

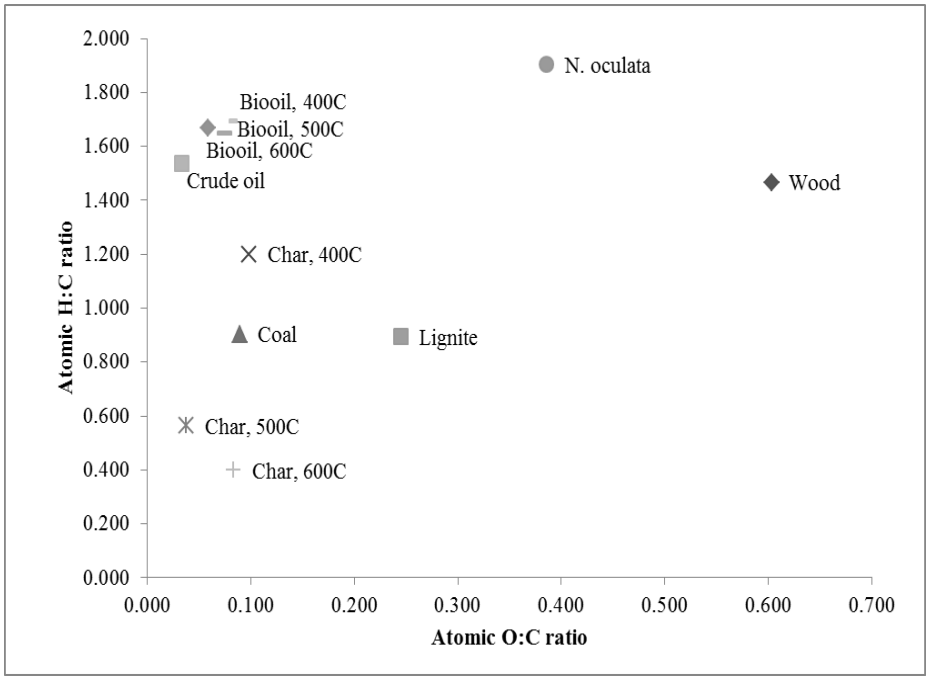

*coal, lignite and wood were adapted from McKendry (2002) [38]

Figure 7. van Krevelen diagram for char and bio-oil at different temperatures.

2.3.3.2. Bio-oil

The elemental composition of the bio-oil samples obtained at different pyrolysis temperatures are shown in Figure 8. As stated in Section 2.3.2, the bio-oil considered in this paper is the dark-brown organic fraction of the liquid product. It can be deduced from Figure 8 that varying the pyrolysis temperature does not significantly affect the elemental composition of the algal bio-oil. On the average, algal bio-oil from *N. oculata* contains 76% carbon, 11% hydrogen, 5% nitrogen, 7% oxygen, 0.56% sulfur and 0.36% ash by weight. Based on the elemental analysis, the molar formula for algal bio-oil is $CH_{1.7}N_{0.06}S_{0.003}O_{0.06}$. This result varies from the elemental composition of bio-oil resulting from pyrolysis of *C. protothecoides* which contains 62% carbon, 8.8% hydrogen, 9.7% nitrogen and 19.4% oxygen. This variation could indicate the effect on bio-oil quality as different microalgae species are used. The carbon and hydrogen contents of the bio-oil from *N. oculata* were higher than that of wood-derived bio-oil (54-58% wt carbon, 5.5-7.0% wt hydrogen) [67]. However, the carbon content of the bio-oil is still slightly lower than crude oil (82% wt). The oxygen content (7% wt) of algal bio-oil, on the other hand, was lower than wood bio-oil (35-40% wt) [67]. According to Czernik and Bridgwater (2004), the oxygen content of bio-oil depends on biomass type and process severity (i.e. temperature, residence time) [67]. Compared to wood, *N. oculata* has lower oxygen content (see Table 2.1) which resulted to bio-oil with less oxygenated compounds. Low oxygen content of the bio-oil is desirable since oxygen causes several disadvantages. These disadvantages include (1) low energy density, (2) immiscibility with hydrocarbons, and (3) instability of the bio-oil [67]. The nitrogen in

the bio-oil, on the other hand, could have been derived from the hydrolysis, decarboxylation and deamination of the protein content of *N. oculata* [20, 83]. Table 1 shows that *N. oculata* contains relatively high percentage of protein (24% wt) which is typical for microalgae [69]. Based on the Van Krevelen diagram (Figure 7), the H:C (1.6) and O:C (0.7) ratios were the same for algal bio-oils obtained at different temperatures. It can also be noted that the H:C versus O:C plots for algal bio-oils were almost near the region of crude oil.

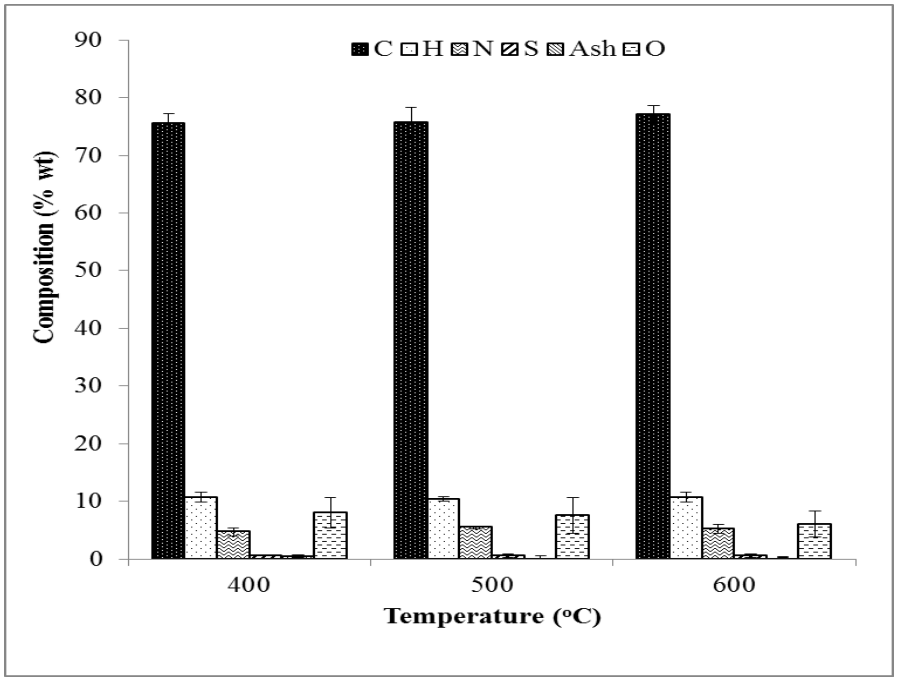

Figure 8. Ultimate analysis of bio-oil from *N. oculata* at different temperatures.

The average moisture content of algal bio-oils obtained from pyrolysis of *N. oculata* was approximately equal to 3.03% wt. This value is relatively lower than wood-derived bio-oil (15-30% wt) [67]. Water in bio-oils is typically generated by the dehydration reactions occurring during pyrolysis [16, 19, 67]. It enhances the flow

characteristics of the bio-oil by reducing its viscosity and lessens NOx emission during combustion. However, it tends to lower the HHV and decreases the combustion rate of the bio-oil [67]. The average HHV of algal bio-oil, on the other hand, was estimated to be equal to 38.35 MJ/kg. This value is relatively higher than the bio-oils produced from *C. protothecoides* (30 MJ/kg) and *M. aeruginosa* (29 MJ/kg). The high HHV of the algal bio-oil from *N. oculata* can be attributed to the high amount of combustible components (carbon and hydrogen) and low oxygen content. However, this value is still slightly lower than that of heavy fuel oil (40 MJ/kg). Hence, further processing of the algal bio-oil to improve its HHV and reduce its oxygen content may still be necessary to make the bio-oil a suitable alternative to crude oil.

Functional group compositional analysis of the aqueous liquid fraction and organic bio-oil obtained at different pyrolysis temperatures was done using FTIR spectrometry. This nondestructive technique was used for other pyrolytic oils [84-90]. Figure 9 shows that the FTIR spectra for the aqueous liquid fractions obtained at different temperatures are the same. Similarly, the FTIR spectra for bio-oils follow the same pattern. For the aqueous fraction, the dominant peak in the range of 3600-3200 cm^{-1} indicates the presence of water, phenol or alcohol. For the organic bio-oil fraction, the peaks observed at 3200-2800 cm^{-1} for C-H stretching vibration and at 1475-1350 cm^{-1} for C-H deformation suggest the presence of alkanes. The peaks in the range of 2260 – 2220 cm^{-1} suggest the presence of nitriles. C=O stretching vibrations were also identified at 1750-1650 cm^{-1}, which can be the due to ketones, aldehydes or esters present in the aqueous and bio-oil liquid fractions. C=C stretching vibrations at 1660-1630 cm^{-1}

suggests the presence of alkenes. The peak at 1650-1540 cm^{-1} is attributed to the asymmetric CO_2 stretching indicative of carboxylates. The peak absorbance detected at 820-690 cm^{-1} suggests the presence aromatic compounds in the bio-oil.

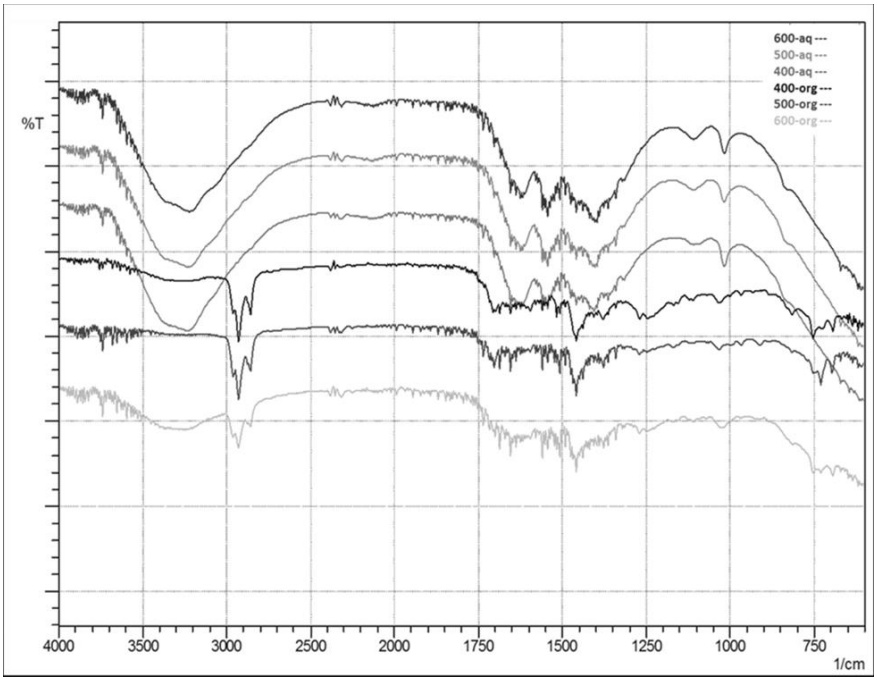

Figure 9. FTIR spectra of the aqueous liquid fractions and algal bio-oils at different temperatures.

The chemical composition of the algal bio-oil obtained at 500^0C (temperature with highest bio-oil yield) was further characterized using GC-MS. Figure 10 shows the GC-MS chromatogram for algal bio-oil while Table 2 summarizes the peaks detected as well as the relative percentage area of the chromatographic peaks. The identified compounds were grouped into the following categories: alkanes, alkenes, alcohols, esters, benzene and aromatic compounds, ketones, and nitriles. Based on Table 2, algal bio-oil consists mainly of saturated aliphatic (34.92%), unsaturated aliphatic (34.43%)

and aromatic (14.19%) hydrocarbons ranging from C_8-C_{21}, which is almost similar to diesel fuel range of C_8-C_{25}. According to Du et al (2011), high amounts of aliphatic and aromatic hydrocarbons in bio-oil from microalgae could be due to larger amount of lipids that are being cracked as hydrocarbons during pyrolysis [87]. It may also be important to note that unlike in bio-oils from lignocellulosic biomass no phenolic compounds were detected in algal bio-oil [74]. Nitrogen containing compounds such as nitriles (13.71%), on the other hand, is expected due to high amount of protein (24% wt) present in the *N. oculata* feedstock. N-containing compounds in the bio-oil may cause potential NOx emission during combustion. Hence, further upgrading of the algal bio-oil to reduce its nitrogen content may be necessary to make the bio-oil suitable as transport fuel. The presence of weak base such as pyrrole, on the other hand, made the pH of the algal bio-oil alkaline (8.5 – 8.9). This pH value is very much different from that of bio-oils obtained from lignocellulosic materials (typically 2-3) [87]. Other minor compounds identified were alcohols (0.89%), esters (0.95%) and ketones (0.91%).

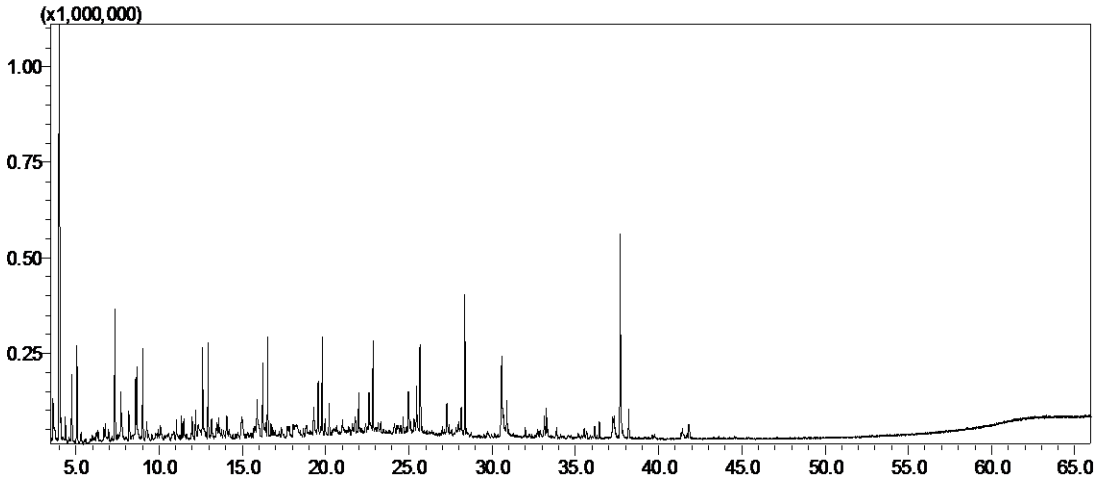

Figure 10. GC-MS chromatogram of bio-oil obtained at 500^{0}C and 100 psig.

Table 2. Chemical composition of bio-oil obtained at 500^{0}C and 100 psig.

Compound	Relative Content (%)	Compound	Relative Content (%)
Alkanes	**34.92**	**Alcohols**	**0.89**
Octane	3.2	1-Octanol, 2-butyl-	0.52
Nonane	2.72	1-Nonanol, 4,8-dimethyl-	0.37
Decane	2.73		
Octane, 3,3-dimethyl-	0.31	**Esters**	**0.95**
Undecane	2.85	Pentadecanoic acid, 14-methyl-, methyl ester	0.95
Tridecane	5.46		
Undecane, 2,6-dimethyl-	1.04	**Benzene and Aromatic Compounds**	**14.19**
Octadecane, 2-methyl-	0.6	Pyrrole	1.21
Dodecane, 2,6,11-trimethyl-	2.96	Ethylbenzene	4.2
Cyclohexane, pentyl-	0.55	Benzene, 1,3-dimethyl-	1.67
Hexadecane	7.2	p-Xylene	2.24
Octane, 2-cyclohexyl-	0.38	1H-Pyrrole, 2,4-dimethyl-	0.42
Decane, 3,7-dimethyl-	1.12	Benzene, propyl-	0.66
Eicosane	2.34	Benzene, 1-ethyl-3-methyl-	0.84
Pentadecane, 2,6,10-trimethyl-	0.38	Benzene, 1,2,3-trimethyl-	0.82
Tetradecane	0.37	Benzene, 1-ethyl-2-methyl-	0.87
Heptadecane, 2,6,10,15-tetramethyl-	0.27	1H-Pyrrole, 2,3,5-trimethyl-	0.46
Cyclopentane, 1-methyl-2-(2-propenyl)-, trans-	0.44	Benzene, 1,2,4-trimethyl-	0.8
Alkenes	**34.43**	**Ketones**	**0.91**
1-Octene	2.27	Cyclohexanone, 4-ethyl-	0.91
4-Octene, (E)-	0.44		
1-Heptene, 2,6-dimethyl-	0.52	**Nitriles**	**13.71**
1-Nonene	2.39	Pentanenitrile	0.94
cis-2-Nonene	0.21	Hexanenitrile	1.12
1-Undecene	5.66	Heptanonitrile	1
2-Undecene, (E)-	0.8	Nonanenitrile	0.36
1-Dodecene	1.78	Dodecanenitrile	0.86
3-Tetradecene, (Z)-	4.3	Oleanitrile	1.23
7-Tetradecene, (E)-	0.36	Hexadecanenitrile	7.66
7-Tetradecene, (Z)-	0.84	Pentadecanenitrile	0.54
1-Hexadecene	1.01		
5-Octadecene, (E)-	0.39		
2-Hexadecene, 3,7,11,15-tetramethyl-, [R-[R*,R*-(E)]]-	1.21		
1,3,5-Cycloheptatriene	12.11		
Cyclohexene, 1-methyl-	0.14		

In this study, pyrolysis was done under moderate pressure (100 psig) as stated in Section 2.2.2. According to Mahinpey (2009), pressure could also affect the yield and properties of pyrolysis products [14]. Hence, a control experiment (500^{0}C, atmospheric pressure) was done to evaluate the potential effect of pressure on products yields and

bio-oil quality. The control experiment was done at 500^0C since maximum bio-oil yield was obtained at this temperature based on Figure 3. Results of the control experiment showed that char yield remained at 37% wt at 500^0C under atmospheric condition. The incondensable gas yield, on the other hand, was lower (9% wt) than under pressurized conditions (12% wt). Liquid yield was higher under atmospheric conditions (37% wt) than at 100 psi (35% wt). The higher gas yield and lower liquid yield observed at 100 psi could be due to secondary cracking of the vapors forming incondensable gas components. This could have occurred when the vapor was allowed to stay in the reactor until the desired pressure was reached. However, the bio-oil produced at atmospheric pressure has lower HHV of about 35.55 MJ/kg than that obtained at 100 psi. This may be due to its lower carbon content (72% wt) and higher nitrogen and sulfur contents of about 12% wt and 1.5% wt, respectively. Based on the results, bio-oils with higher quality but at lower yields may be produced from pressurized pyrolysis. This result could be a motivation for further investigation on the effects of pressure on microalgae pyrolysis.

2.3.3.3. Gaseous product

Table 3 shows the composition of the gaseous products obtained at different pyrolysis temperatures. The combustible gases present in the syngas were H_2, CO, CH_4, C_2H_4 and C_2H_6. The concentration of hydrocarbons in the gaseous product tended to increase with further heating of the biomass, which may be due to cracking of the vapors forming incondensable gaseous compounds [67]. Among the hydrocarbon gases, the content of methane was the highest which is similar to the results obtained by Pan et al

(2010) and Uzun et al (2007) [20, 80]. The large difference between the hydrogen content of the gas obtained at 400^0C and 500^0C is consistent with that reported by Grierson et al (2009) [7]. In his study, H_2 production for green algae (*C. vulgaris and T. chui*) and *D. tertiolecta* peaked at around 430^0C and 460^0C, respectively. Also, the evolution of CH_4 was observed at around 480 to 520^0C. This could be the possible reason for the increase in CH_4 concentration from 400^0C to 600^0C. C_2H_4 and C_2H_6 evolve at 450^0C which could explain the increase in their concentrations at 400^0C to 500^0C. The concentrations of non-combustible components in the gaseous product, on the other hand, were relatively low at higher temperatures. However, the gaseous product contained large amount of CO_2 at 400^0C, which could be due to the cracking and reforming of functional carboxyl groups. According to Marcilla et al (2009), CO_2 production typically peaks around 340^0C then decreases and peaks again at 740^0C [16]. This could explain the decrease in the CO_2 concentration from 61.60 %vol at 400^0C to 6.06 %vol at 600^0C. The HHV of the gaseous product was largely dependent on the amount of combustible components present. The low HHV of the gas obtained at 400^0C (5.66 MJ/m^3) could be attributed to its high CO_2 content. On the other hand, the high HHV of the gas generated at 600^0C (27.45 MJ/m^3) was mainly due to its high hydrocarbon content particularly CH_4 (44.55 %vol).

Table 3. Gas properties at different temperatures.

	Composition (% vol)								
Temp	**H_2**	**CO**	**CH_4**	**C_2H_4**	**C_2H_6**	**O_2**	**N_2**	**CO_2**	**HV (MJ/m^3)**
400^oC	2.44	5.97	5.84	1.06	3.74	0.59	6.43	61.60	5.66
500^oC	15.27	3.58	20.96	3.40	11.58	1.41	6.01	10.28	19.93
600^oC	14.46	4.27	44.55	1.13	11.61	1.25	5.23	6.06	27.45

2.3.4. The effect of temperature on energy yield and energy conversion efficiency

Figure 11 shows the energy yield of the process based on product yields and HHV of the pyrolysis products. Energy yields (in MJ/ton dry algae) were calculated using Equation 2.3 (Section 2.2.5). The energy yield from char dramatically decreased from 13, 995 MJ/dry ton at 400^0C to 6,520 MJ/dry ton at 600^0C. This may be attributed to the significant reduction in the amount of char with lower HHV obtained at 600^0C. Char, however, still contained most of the energy from the biomass. The energy yields from algal bio-oil, on the other hand, increased as temperature is increased from 400^0C (3,422 MJ/ton) to 500^0C (6,449 MJ/ton). As discussed in Section 2.3.2, the yield of bio-oil decreased as pyrolysis temperature increased from 500^0C to 600^0C. Intuitively, the energy yield from bio-oil also decreased at 600^0C as shown in Figure 11. The energy yield from the gaseous product increased from 161 MJ/ton at 400^0C to about 5,713 MJ/ton at 600^0C. This may be due to the production of higher amounts of combustible components in the gaseous product resulting to higher HHV at higher temperatures.

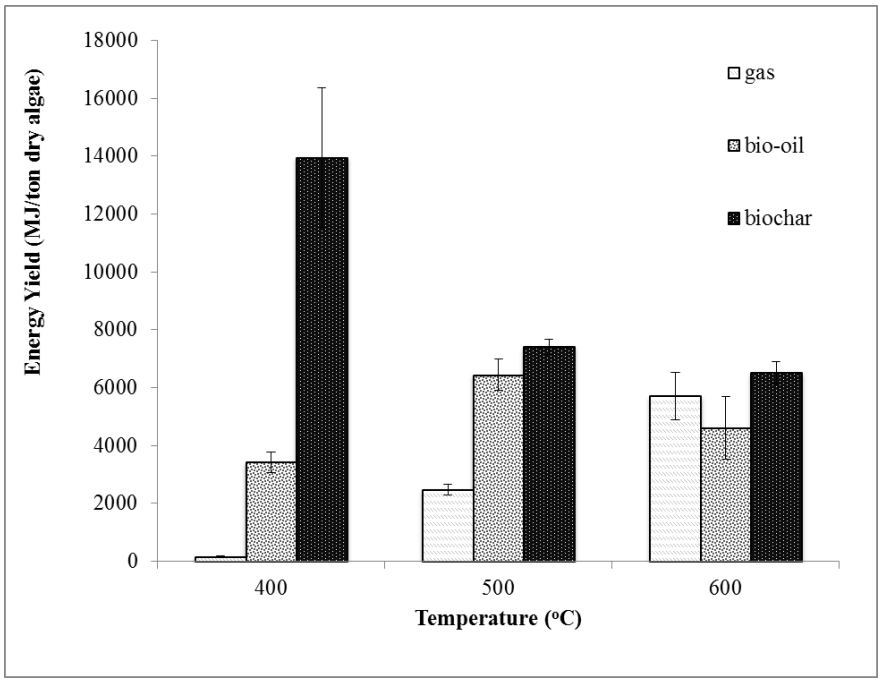

Figure 11. Energy yields at different pyrolysis temperatures.

Energy recovered (%) from the biomass at different pyrolysis temperatures shown in Figure 12 were then estimated using the energy balance of the process. On the average, the energy conversion efficiency of the process was approximately 68%. The energy losses could be due to the formation of noncombustible components (i.e. water, CO_2) in the products and energy lost in the unrecovered products as discussed in Section 2.3.2. Similar to Figure 11, the distribution of the energy recovered in the products varied with temperature.

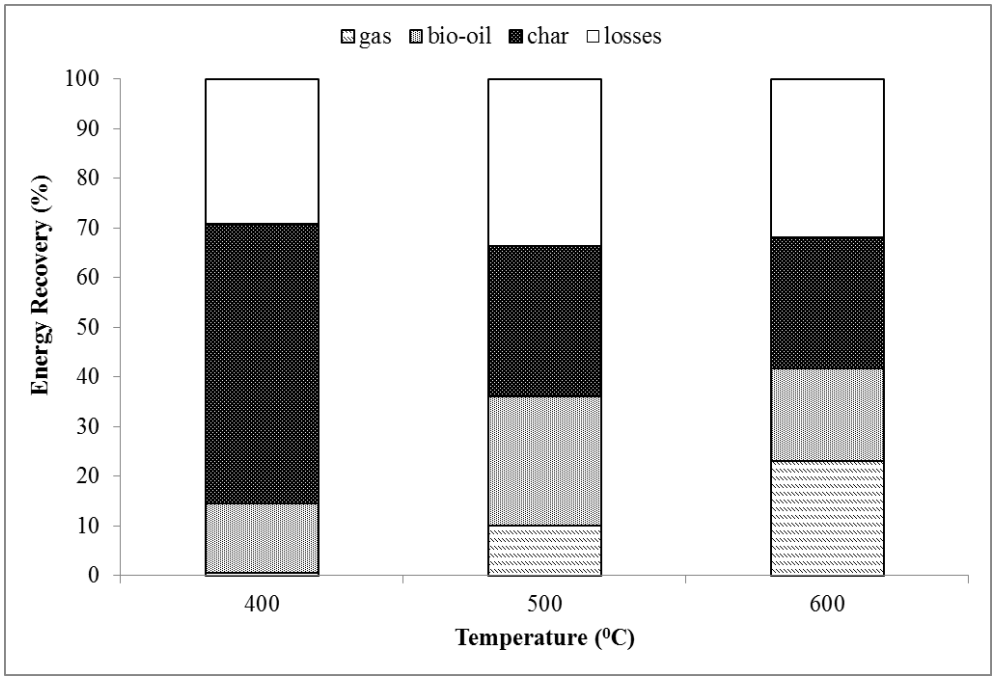

Figure 12. Energy conversion efficiencies of the pyrolysis process at different temperatures.

2.4. Conclusions

Pyrolysis of *Nannochloropsis oculata* at different temperatures (400^0C, 500^0C and 600^0C) in a fixed-bed batch reactor at 100 psi showed that the process can be manipulated to favor char, bio-oil and gas production. The yield of char decreased to a certain extent as pyrolysis temperature is increased. Therefore, peak production of char can be expected at the lowest temperature (400^0C). At 400^0C, char production was approximately equal to 52 %wt. On the other hand, liquid product yield initially increased from 400^0C to 500^0C then decreased from 500^0C to 600^0C. The increase in liquid product yield could be attributed to further dehydration and devolatilization of the algal biomass forming the aqueous and organic (bio-oil) liquid fractions. Hence, maximum liquid product yield of about 35 %wt was obtained at 500^0C. Also, the

highest amount of organic bio-oil fraction of about 17 %wt was obtained at 500^0C. The decrease in liquid product yield from 500^0C to 600^0C could be due to further cracking of the volatiles forming incondensable gases. Hence, the increase in temperature from 500^0C to 600^0C further increased the gas yield from 8 %wt to about 15 %wt, respectively. The hydrocarbon components of the gaseous product were also enriched as temperature was increased, which indicated that more energy can be generated from the gas at higher temperatures. Most of the mass and energy from the biomass were retained in the char. The variation in temperature resulted to varying char and gas properties. On the other hand, no significant variation in algal bio-oil properties and composition was observed as temperature is varied. The composition and heating values of char, bio-oil and gas indicated that these products can be used as alternative energy sources.

3. DETERMINING THE OPERATING CONDITIONS FOR MAXIMUM BIO-OIL PRODUCTION FROM PYROLYSIS OF *Nannochloropsis oculata* USING RESPONSE SURFACE ANALYSIS

3.1. Introduction

The increasing demand for energy and rapid depletion of fossil fuels leading to tremendous escalation of petroleum fuel prices dictated the need for sustainable energy sources [2-4]. Global concern for increasing greenhouse gas emission also called for the development of carbon-neutral technologies. At present, biofuels from plant biomass are the only sustainable source of liquid fuels. Moreover, the biomass-to-fuel cycle can be a carbon-neutral technology if efficient methods and sustainable feedstocks are utilized [13, 23, 33].

Microalgae are a very promising feedstock for biofuel production due to its high lipid content [6], rapid growth rate [7], high photosynthetic efficiency [8] and high productivity [8, 9]. Also, large-scale production of microalgae will not compete with food production since it can be cultivated on salty water [9] and does not require arable soils [6, 7]. The bio-oil produced from microalgae is also said to be more stable due to lower O/C ratio and has higher heating value as compared to wood oil [8]. Various processes can be used to convert microalgae to fuel-type components which include (1) lipid extraction followed by transesterification to produce biodiesel, (2) deoxygenation of fatty acids for green diesel production, and (3) pyrolysis of whole algal biomass [10]. Compared to the other two processes, pyrolysis is more economically attractive since in

this process the whole biomass is converted into useful products such as high-energy density bio-oil [91].

Pyrolysis is a thermochemical process that converts biomass to solid char, bio-oil and combustible gaseous products at temperatures generally below 600^0C and with the absence of oxygen. It is said to be an energy intensive process; however, the recoverable energy from the char and combustible gases produced could possibly compensate the energy requirement of the process [12]. Pyrolysis produces energy fuels with high fuel-to-feed ratio and the process can be easily adjusted to favor char, bio-oil or gas production [8]. More interest is given to bio-oil since it is comparable to crude oil, which can be easily stored and transported, and it has low nitrogen and sulfur contents [8]. Bio-oil can be used for direct combustion or can be upgraded further to liquid transport fuels and bio-chemicals [7]. Bio-oils are usually dark-brown in color with a distinctive smoky odor. It consists of a very complex mixture of hydrocarbons and oxygenated organic compounds (acids, alcohols, aldehydes, esters, ketones, phenols) with considerable fraction of water [12, 13]. Some undesirable properties of bio-oil which includes high water content, high viscosity, high ash content, low heating value (high oxygen content), high corrosiveness or acidity, and low stability limit the direct use of bio-oil as transportation fuel [12]. Hence, these properties of the bio-oil should be taken into consideration for further upgrading of the bio-oil to improve its properties as liquid fuel.

Bio-oil derived from pyrolysis of microalgae can be a potential alternative for petroleum-derived fuels if an efficient process is developed. Hence, the pyrolysis conditions for maximum high-quality bio-oil yield should first be determined. The yield

and quality of the pyrolysis products greatly depend on several factors including reactor design, reaction parameters (temperature, heating rate, residence time, pressure and catalyst) and biomass type and characteristics (particle size, shape and structure) [14, 15]. Various papers on microalgae pyrolysis focused on the decomposition characteristics of different algae species using thermogravimetric analysis [16-19]. Studies on the individual effects of process parameters such as heating rate, final temperature, and catalyst loading on pyrolysis of different microalgae species can also be found elsewhere [17-20]. Pan (2010) evaluated the effects of temperature and catalyst loading on product yields from pyrolysis of *Nannochloropsis sp* using a fixed bed reactor [20]. Results showed that liquid and bio-oil product yields increased from 300 to 400^0C then gradually decreased from 400 to 500^0C in the direct pyrolysis process. The decrease in bio-oil yield was attributed to further cracking of the volatiles into non-condensable gases. The increase in catalyst loading, on the other hand, decreased bio-oil yield from 31.1% (0/1) to 20.7% (1/1) during catalytic pyrolysis. The influence of operating pressure was investigated by Mahinpey et al (2009) using wheat straw as feedstock [14]. Results showed that gas production was higher at lower pyrolysis pressures (10 and 20 psi) while maximum oil production (37.6%) was achieved at higher pressures of 30 and 40psi.

Based on the studies reviewed and to our knowledge, the operating conditions for the maximum production of algal bio-oil were not yet established. Also, most of the studies on algal pyrolysis dealt with the individual effects of reaction parameters (temperature, pressure) in a stepwise manner and limited information is available on

their possible interaction. Mass conversion efficiencies and energy recoveries including possible process losses were not yet accounted. The composition and properties of pyrolysis products (bio-oil, char, gas) at optimum operating conditions were also not yet determined.

Hence, this paper generally aimed to establish the operating conditions for maximum production of high-quality bio-oil from pyrolysis of microalgae, specifically *Nannochloropsis oculata*. The extent of bio-oil production from pyrolysis of microalgae at different combinations of reaction parameters, particularly temperature and pressure, was investigated. The individual effects and interaction of the selected reaction parameters (temperature, pressure) were also evaluated based on the yield of bio-oil and its co-products (char, gas). Response surface analysis was used to determine the combination of temperature and pressure that maximizes algal bio-oil production. Comparison among the composition and properties of *N. oculata* bio-oil, wood-derived bio-oil and heavy fuel oil revealed the suitability of the bio-oil produced from microalgae as an alternative source of energy. Char and gas compositions and properties were also determined to identify their potential usages. From the results, the technical knowledge necessary for the operation of pyrolysis process and for maximum production of bio-oil from microalgae can be derived.

3.2. Materials and Method

3.2.1. Feedstock preparation and characterization

Nannochloropsis oculata samples used in this study was obtained from the Texas Agri-Life Research Algae Pond facility in Pecos, Texas. The samples were oven-dried at 105^0C until less than 10% wt moisture was obtained. Then, the dried algae samples were ground using Wiley Laboratory Mill Model #4 distributed by Arthur Thomas Company, Philadelphia, PA, USA. The heating value of the sample was determined subsequent to ASTM D 2015 using PARR isoperibol bomb calorimeter (Model 6200, Parr Instrument Company, Moline, IL). Proximate analysis was determined in reference to ASTM standards (D 3175 and E1755). The ultimate analysis was done using Vario MICRO Elemental Analyzer (Elementar Analysemsysteme GmbH, Germany) in accordance with ASTM D 3176.

3.2.2. Pyrolysis experiment

Pyrolysis experiments were performed using a fixed-bed batch-type Parr pressure reactor (Series 4580 HP/HT, Parr Instrument Company, Moline, IL) illustrated in Figure 2.1. The reactor specifications were already described in Section 2.2.2.

Pyrolysis runs were carried out subsequent to a completely randomized general factorial experimental design. The reactor temperature and pressure served as the main factors in the experiment. The temperature levels tested were 400^0C, 500^0C and 600^0C, while pressure levels were 0, 50 and 100 psig. The runs were done in replicates for each temperature and pressure combinations.

For each pyrolysis run, approximately 250 g of dried and ground *N. oculata* were loaded into the reactor. To ensure the absence of oxygen, the reactor was purged with nitrogen for 20 minutes at about 10psi before each run. The reactor was heated until the desired temperature was reached. On the other hand, the pressure build up in the reactor, due to gas production, was allowed to increase up to the desired pressure. Then, the pressure was maintained at that level by slightly opening the gas valve attached to the condenser releasing some of the gaseous product. When the desired temperature was achieved, the reaction was allowed to proceed at the desired temperature for about 30 minutes before turning the heater off and allowing the reactor to cool down. The volume of gas produced was measured using a gas meter (METRIS® 250, Itron, Owenton, KY) with air/gas capacity of 250/195 CPH. Gas samples for analysis were also collected using 0.5L Tedlar sampling bags with combination valve. The liquid product was collected from the receiving vessel below the condenser while the char was collected from the reactor. Both were weighed using an analytical balance (Mettler Toledo, Model XP105DR, Switzerland).

3.2.3. Gas analysis

The composition of the gas sample obtained from pyrolysis at optimum condition was analyzed using SRI Multiple Gas Analyzer #1 (MG#1) gas chromatograph (GC) equipped with an on-column injection system and two detectors: Helium Ionization Detector (HID) and Thermal Conductivity Detector (TCD). The columns used were 6' Molecular Sieve 13X and ShinCarbon ST 100/120 (2m, 1mm ID, 1/16OD, Silco), with helium as the carrier gas. The calibration gas standard mixture used consisted of H_2, N_2,

O_2, CO, CH_4, CO_2, C_2H_4, C_2H_6, C_3H_6 and C_3H_8 (Praxair Distribution, Geismar, LA) with analytical accuracy of ±2%. Initial temperature of the column was set at 65^0C for 10minutes, then ramped at 16^0C/min to a final temperature of 250^0C.

3.2.4. Char and bio-oil analysis

The heating value of the char and bio-oil samples was determined using PARR isoperibol bomb calorimeter (Model 6200, Parr Instrument Company, Moline, IL) following ASTM D2015. Proximate analysis of the char was done in reference to ASTM standards (D 3175 and E1755). The ultimate analysis of the char and bio-oil was determined using Vario MICRO Elemental Analyzer (Elementar Analysemsysteme GmbH, Germany) in accordance with ASTM D 3176. Other bio-oil analyses performed include moisture content (ASTM E203) using KF Titrino 701 (Metrohm, USA, Inc.), pour point (D97-12), flash point (D93-12), kinematic viscosity using Cannon-Fenske Reverse-flow viscometer subsequent to ASTM D445, density (ASTM D1217-93) and pH using Accumet model 25 pH/ion meter. The chemical composition of the bio-oil was also determined by GC-MS analysis using Shimadzu QP2010 Plus, with the following parameters: bio-oil dissolved in dichloromethane (10 %vol); column – DB-5ms (25m length, 0.25μm thickness and 0.25mm diameter); column temperature program: 40^0C (held for 5 minutes) then ramped to 320^0C at 5^0C/min, then held for 5 minutes at 320^0C; ion source temperature at 300^0C.

3.2.5. Data analysis

Product (bio-oil, char and gas) yields (% wt) were calculated using Equation 3.1 shown below. Gas yield was initially calculated as volume per mass of dry algae used. The composition (% vol) of the gas products was used to convert the volume of the gas to its mass equivalent.

$$\text{Product yield (\%wt)} = (\text{mass of product/mass of dry algae used}) \times 100 \quad (3.1)$$

Mass balance around the reactor shown in Equation 3.2 was then used to calculate the losses (% wt), and consequently, the mass conversion of the process.

$$\%\text{Char yield} + \%\text{ Liquid yield} + \%\text{Gas yield} + \%\text{Losses} = 100\% \quad (3.2)$$

On the other hand, energy recovery (%) was estimated using Equation 3.3. The energy yield calculated for each product was then supplied to the energy balance of the process to determine the % energy loss.

$$\text{Energy recovery (\%)} = \text{Product yield (\%wt)} \times (HV_{product}/HV_{algae}) \quad (3.3)$$

Statistical analysis of data was done by Analysis of Variance (ANOVA) at 95% confidence interval. The experimental errors were estimated as standard deviations and were represented as error bars placed in the graphs showing the results.

3.3. Results and Discussion

3.3.1. The effect of temperature and pressure on products yields

3.3.1.1. Model fitting

Table 4 shows the product yields at different combinations of temperatures and pressures. Char yields varied from 29 to 57% wt while gas yields ranged between 3 to 20% wt. Liquid product, on the other hand, varied from 19 to 38% wt. The liquid product obtained from pyrolysis of *N. oculata* consists of two immiscible fractions which separated immediately. The yellowish aqueous liquid fraction mainly contains water and water-soluble compounds. From Table 4, the yield of aqueous liquid fraction ranged from 9 to 20% wt. On the other hand, the dark-brown organic liquid fraction or bio-oil is a mixture of saturated and unsaturated hydrocarbons, and some oxygenated compounds which varied from 6 to 18% wt.

Table 4. Effect of temperature and pressure on process yields (% wt).

Pressure (psig)	Temperature (^{o}C)	Char Yield (%wt)	Gas Yield (%vol/wt)	Liquid Yield[a] (%wt)	Aqueous Yield (%wt)	Organic Yield (%wt)
0	400	55.01 ± 0.01	10.62 ± 1.00	24.75 ± 3.37	18.48 ± 3.37	6.28 ± 0.01
	500	37.02 ± 5.61	9.21 ± 1.00	37.67 ± 0.57	19.94 ± 2.45	17.73 ± 3.01
	600	33.03 ± 0.33	14.52 ± 0.50	36.44 ± 3.86	20.45 ± 1.21	15.99 ± 2.64
50	400	56.88 ± 4.47	8.85 ± 0.49	23.40 ± 2.59	17.29 ± 0.73	6.11 ± 1.85
	500	32.72 ± 0.01	12.75 ± 2.00	33.46 ± 0.74	20.20 ± 0.33	13.26 ± 1.07
	600	28.96 ± 0.30	17.70 ± 3.01	32.95 ± 2.07	20.43 ± 1.03	12.52 ± 1.05
100	400	55.74 ± 1.90	2.90 ± 0.09	18.72 ± 2.06	9.14 ± 0.62	9.59 ± 1.45
	500	37.31 ± 4.77	12.46 ± 0.80	34.92 ± 4.55	18.31 ± 2.53	16.61 ± 2.02
	600	30.47 ± 0.23	19.83 ± 2.00	29.05 ± 0.37	18.63 ± 0.09	10.43 ± 0.28

[a] Liquid product = bio-oil + aqueous

A second-order polynomial equation was used to investigate the effects of temperature and pressure on products yields in terms of linear, quadratic and interactive terms as follows:

$$Y = \beta_0 + \sum_{i=1}^{k} \beta_i X_i + \sum_{i=1}^{k} \beta_{ii} X_i^2 + \sum_{i=1}^{k} \sum_{i<j} \beta_{ij} X_i X_j + \epsilon \quad (3.4)$$

where Y is product yield (%wt); β_0 represents the model intercept; X_1, X_2 are the levels of temperature and pressure, respectively; and β_i, β_{ij} are the regression coefficients. According to Montgomery (2011), a polynomial of higher degree such as second-order model must be used if there is a curvature in the system [92].

The p-value of each term in Equation 3.4 was analyzed using analysis of variance (ANOVA) in the Design Expert 8.0.7.1 software. The significant terms based on their p-values (α=0.05) were included in the model for products yields. The regression models for predicting products (liquid, bio-oil, aqueous, char and gas) yields are presented in Equations 3.5 to 3.9 using actual temperature and pressure values. Table 5 shows the F- and p-values for each term in the regression models. For liquid yield, the linear terms (T, P) and quadratic term (T^2) were significant. Linear term (T), interactive (TP) and quadratic terms (T^2, P^2) were considered to be significant for bio-oil yield based on p-values while the pressure term, P, was included in the model based on hierarchy. As shown in Table 5, the p-value for pressure (p=0.2762) is higher than α = 0.05 which indicates that this term may not be significant. However, the quadratic term, P^2, was found to be significant (p=0.0278). Based on the hierarchy principle, if a model contains high-order term such as P^2, it should also contain all of the lower-order terms, which is

in this case the linear term, P [92]. The linear (T, P), interactive (TP) and quadratic (T^2) terms, on the other hand, defined aqueous yield. Only temperature terms (T, T^2) were found to significantly affect char yield as shown in Equation 3.8. Lastly, gas yield was greatly dependent on temperature term (T) and interactive (TP) effect based on their p-values. Similar to bio-oil yield, the pressure term (P) was included in the gas yield model due to hierarchy.

$$Y_{liquid}\ (\%wt) = -184.75 + 0.84\ T - 0.03\ P - 7.80 \times 10^{-4}\ T^2 \quad (3.5)$$

$$Y_{bio\text{-}oil}\ (\%wt) = -150.90 + 0.62\ T + 0.13\ P - 4.44 \times 10^{-4}\ TP - 5.71 \times 10^{-4}\ T^2 + 8.56 \times 10^{-4}\ P^2 \quad (3.6)$$

$$Y_{aqueous}\ (\%wt) = -33.88 + 0.21\ T - 0.16\ P + 3.76 \times 10^{-4}\ TP - 2.09 \times 10^{-4}\ T^2 \quad (3.7)$$

$$Y_{char}\ (\%wt) = 286.73 - 0.88\ T + 7.67 \times 10^{-4}\ T^2 \quad (3.8)$$

$$Y_{gas}\ (\%wt) = 3.52 + 0.02\ T - 0.32\ P + 6.52 \times 10^{-4}\ TP \quad (3.9)$$

It must be noted that the predictions that can be derived from Equations 3.5 to 3.9 are precise only in the specific reactor configuration and feedstock used in this study. Also, these equations may only be used for interpolation between temperature and pressure ranges of 400 to 600^0C and 0 to 100 psig, respectively. Nonetheless, the models developed in this paper are still useful in identifying the terms and interactions that are significant on products yields.

Table 5. Analysis of Variance (ANOVA) for the regression models.

Source	Sum of squares	DF	Mean square	F value	P value
Liquid yield					
Model	663.72	5	132.74	18.18	< 0.0001
T-Temperature	332.07	1	332.07	45.48	< 0.0001
P-Pressure	87.19	1	87.19	11.94	0.0048
T^2	243.12	1	243.12	33.3	< 0.0001
Residual	87.61	12	7.3		
Lack of Fit	24.49	3	8.16	1.16	0.376
Pure Error	63.12	9	7.01		
Cor Total	751.33	17			
R-Squared	0.8834				
Bio-oil yield					
Model	287.98	5	57.6	19.68	< 0.0001
T-Temperature	95.94	1	95.94	32.79	< 0.0001
P-Pressure	3.81	1	3.81	1.3	0.2762
T^2	130.53	1	130.53	44.61	< 0.0001
P^2	18.32	1	18.32	6.26	0.0278
Residual	35.11	12	2.93		
Lack of Fit	7.14	3	2.38	0.77	0.5414
Pure Error	27.97	9	3.11		
Cor Total	323.09	17			
R-Squared	0.8913				
Aqueous yield					
Model	184.42	5	36.88	10.23	0.0005
T-Temperature	71.05	1	71.05	19.7	0.0008
P-Pressure	54.53	1	54.53	15.12	0.0022
TP	28.28	1	28.28	7.84	0.016
T^2	17.39	1	17.39	4.82	0.0485
Residual	43.28	12	3.61		
Lack of Fit	15.97	3	5.32	1.75	0.2255
Pure Error	27.31	9	3.03		
Cor Total	227.7	17			
R-Squared	0.8099				

Table 5 continued…

Source	Sum of squares	DF	Mean square	F value	P value
Char yield					
Model	2139.82	5	427.96	49.31	< 0.0001
T-Temperature	1884.01	1	1884.01	217.1	< 0.0001
T^2	235.01	1	235.01	27.08	0.0002
Residual	104.14	12	8.68		
Lack of Fit	26.16	3	8.72	1.01	0.4337
Pure Error	77.98	9	8.66		
Cor Total	2243.96	17			
R-Squared	0.9536				
Gas yield					
Model	378.62	3	126.21	36.81	< 0.0001
T-Temperature	293.44	1	293.44	85.59	< 0.0001
P-Pressure	0.23	1	0.23	0.068	0.7984
TP	84.96	1	84.96	24.78	0.0002
Residual	48	14	3.43		
Lack of Fit	27.81	5	5.56	2.48	0.1119
Pure Error	20.19	9	2.24		
Cor Total	426.62	17			
R-Squared	0.8875				

3.3.1.2. Response surface analysis

The experimental data was further evaluated using response surface analysis. Response surface is a graphical representation of the response (i.e. product yield) plotted versus the levels of the factors considered (i.e. temperature, pressure). In response

surface analysis, at least two quantitative factors are required to be able to predict the response at various combinations of the design factors [92].

Figure 13 shows the contour plots of the response surfaces for liquid, bio-oil and aqueous yields. As mentioned in Section 3.3.1.1, the liquid product from the pyrolysis process contains the aqueous and bio-oil fractions. Based on Table 5, liquid product yield was affected significantly by temperature ($p<0.0001$), pressure ($p=0.0048$) and T^2 ($p<0.0001$). Figure 13 clearly illustrates these temperature and pressure effects on liquid product yield. At a constant pressure (e.g. 0 psig), increasing the temperature to a certain extent tends to increase liquid yield. Based on the figure, maximum liquid yield could be in the region between 500 and 570^0C. Increasing the temperature beyond this region tended to decrease liquid yield. According to Akhtar and Amin (2012), an increase in temperature typically increases biomass conversion due to the extra energy input, which is useful for breaking the biomass bonds [93]. Also, the increase in liquid product yield at 500^0C could be attributed to the decomposition of algal lipid. The thermal decomposition of algae can be divided into three steps, namely: (1) dehydration ($<180^0$C), (2) devolatilization where the main pyrolysis process occurs ($180\text{-}540^0$C) and (3) solid decomposition ($<540^0$C) [16, 17, 19]. According to Marcilla et al (2009), the decomposition of lipid occurs during the latter portion of the devolatilization stage ($\sim500^0$C) preceded by the breakdown of polysaccharides and proteins [16]. However, after reaching its maximum, liquid or oil yield typically goes down with further increase in temperature [93]. For the effect of pressure, on the other hand, liquid yield decreased with an increase in pressure at constant temperature (e.g. 550^0C). This may be due to

secondary cracking of the vapors forming incondensable gaseous components as the vapors were kept inside the reactor to maintain the desired pressure.

The contour plot for bio-oil yield, on the other hand, is almost similar to that of liquid yield. Based on the contour lines, bio-oil production from *N. oculata* was also favored at low pressure (0 psig) and moderate temperatures ranging from 500 to 570^{0}C. As mentioned earlier, bio-oil was obtained as a fraction of the liquid product. Hence, the variations in bio-oil production could have directly affected the trends observed in liquid production. On the other hand, circular contour lines were observed in the aqueous yield plot. Based on the plot, maximum generation of aqueous fraction could be expected around 540^{0}C and 25 psig. Water, which mainly constitutes the aqueous liquid fraction, could be derived from the initial moisture contents of the feedstock and from the dehydration reactions [93]. It may also come from the decomposition of oxygenates present in the solid-feed and water-gas shift reactions [93-95].

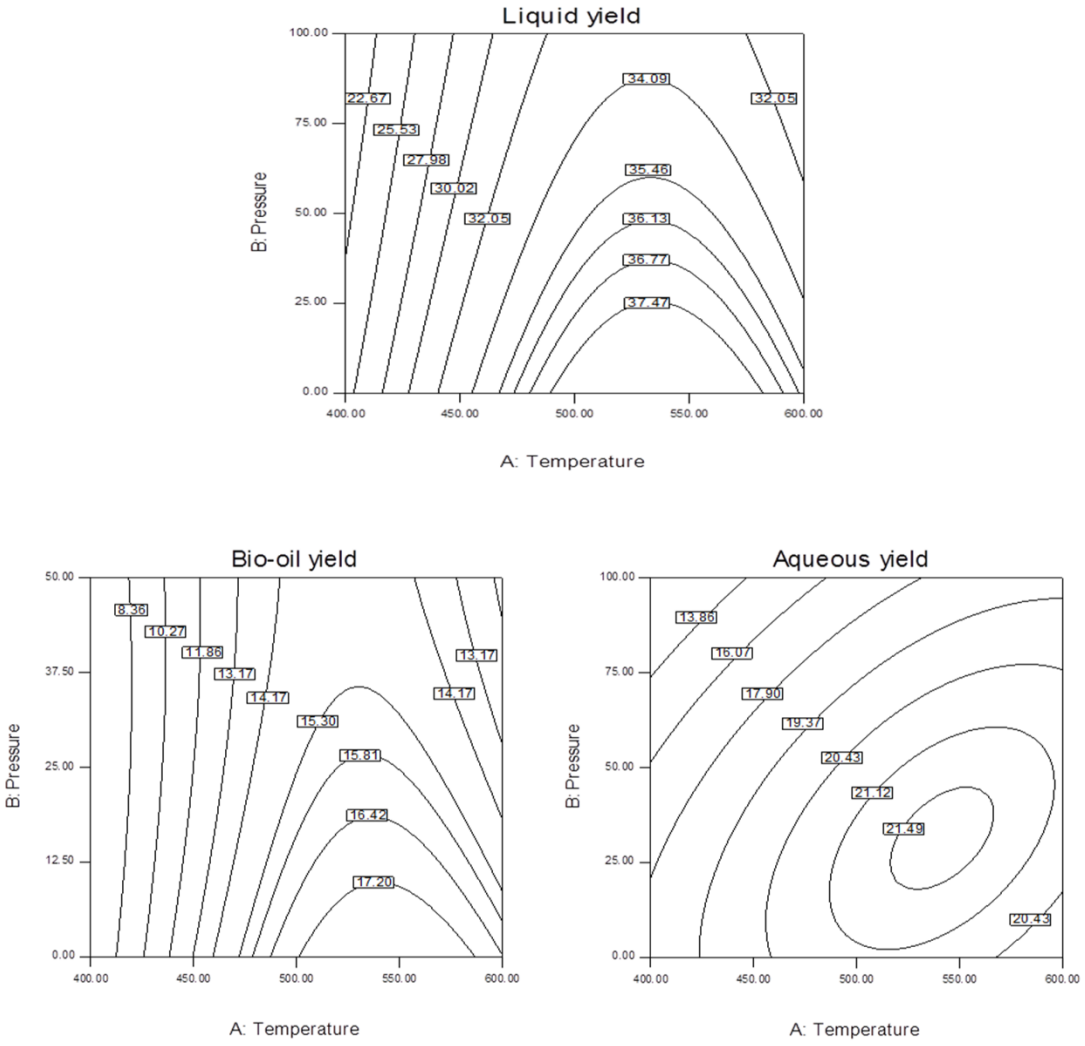

Figure 13. Contour plots for liquid, bio-oil and aqueous yields.

Based on Table 5, only the temperature terms, T and T^2, significantly affected char yield. Pressure effects, on the other hand, were found to be insignificant which was similar to that observed by Whitty et al (2008), Mahinpey et al (2009) and Melligan et al (2011) for black liquor, wheat straw and Miscanthus, respectively [14, 96, 97]. As

shown in Figure 14, for all pressure values, char yields tended to decrease as temperature was increased from 400 to 600^{0}C. These observations are similar to the results obtained by Pan et al (2010) [20]. The decrease in char, which is the residual biomass after pyrolysis, can be attributed to the release of volatile components of the biomass forming liquid products and incondensable gases. Maximum char yield of about 57% wt was observed at 400^{0}C regardless of pressure.

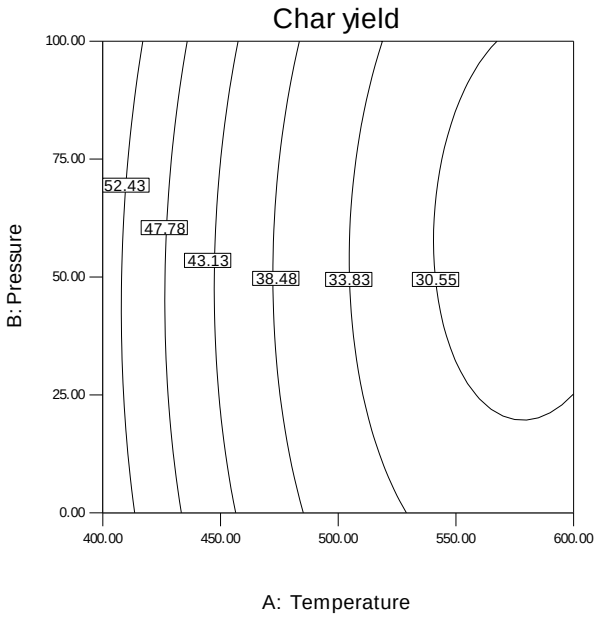

Figure 14. Contour plot for char yield.

Gaseous product yield, on the other hand, was significantly affected by temperature ($p<0.0001$) and the interaction between temperature and pressure ($p=0.0002$). The curvature in the contour lines as shown in Figure 15 indicates the interaction between temperature and pressure [92]. In general, gas yield increased as

temperature was increased from 400 to 600^{0}C. Pressure effects, on the other hand, seem to vary at different temperature regions. At low temperatures (<500^{0}C), gas yield tended to decrease as pressure is increased from 0 to 100 psi. Whereas, at high temperature regions (>500^{0}C), increasing the operating pressure tended to increase gas production. This observation further exemplifies the effects of the interaction term. During pyrolysis, the feedstock undergoes through primary and secondary reactions which involves heat and mass transfer mechanism. Primary reactions include removal of moisture and breakage of weak bonds leading to the formation of primary or intermediate products. Secondary reactions, on the other hand, may include secondary cracking or re-polymerization of the intermediates formed [93, 98]. The yields and composition of the product obtained from pyrolysis are very sensitive to operational variations and biomass type in such competitive reactions [93]. At low temperatures, the increased pressure could have prevented some volatiles from escaping the solid which could potentially decrease bio-oil and gas production. Also, the energy input at low temperatures may not be sufficient enough the break some biomass bonds. At high temperatures, on the other hand, more volatiles were apparently released based on the decrease in char yield as mentioned earlier. Under this condition, the increased pressure could have enhanced the secondary cracking of the volatiles released leading to higher gas formation. Also, according to Tamhankar et al (1984), increased gas concentration increases gas-volatiles reactions decreasing the secondary char formation reactions [99]. Based on the contour plot, maximum gas yield (20% vol/wt) was obtained at 600^{0}C and 100 psig operating conditions which indicate that high temperatures and pressures favor gas formation.

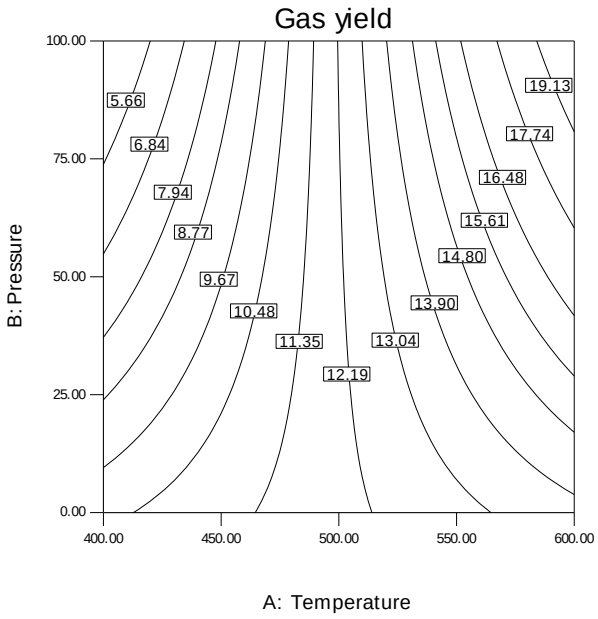

Figure 15. Contour plot for gas yield.

3.3.2. Optimization and validation

The combination of temperature and pressure that maximizes bio-oil yield was determined by numerical optimization using Design Expert Version 8.0.7.1. Result of the numerical optimization showed that maximum bio-oil yield could be obtained at 540^0C and 0 psig. At this condition, a maximum liquid yield of about 39% wt was predicted, which contains approximately 18% wt bio-oil and 21% wt aqueous fraction. Char and gas yields, on the other hand, would be about 33% wt and 13% vol/wt, respectively. A validation experiment was conducted in triplicate and averages of the products yields obtained were presented in Table 6. Result of the validation experiment shows that at 540^0C and 0 psig liquid product yield was about 43% wt, which consists of about 23% wt bio-oil and 20% wt aqueous product. Char and gas yields were about 32%

wt and 12% vol/wt, respectively, which were close to the predicted values. The result obtained from the validation experiments agrees well with prediction values. Similar to the predicted result, liquid yield was the major pyrolysis product in the actual experiment at 540^0C and 0 psig. Hence, the accuracy of the models was validated under these optimal conditions.

Table 6. Predicted and actual products yields at optimum conditions (540^0C, 0 psig).

	Product Yields	
Product	**Predicted**	**Validation**
Liquid (%wt)	39.14	43.33 ± 1.17
Bio-oil (%wt)	18.25	23.32 ± 1.14
Aqueous (%wt)	20.89	20.02 ± 0.08
Char (%wt)	33.09	31.59 ± 1.03
Gas (%vol/wt)	12.63	11.85 ± 1.40

Mass conversion efficiency at 540^0C and 0 psig was also estimated to be equal to 84.18±2.24% wt. The percentage loss of about 16% wt may be accounted to the uncondensed bio-oil that was trapped by the filter attached to the gas meter. Also, some of the char and bio-oil that adhered to the sides of the reactor were not collected. In the succeeding sections, the operating condition for maximum bio-oil production (540^0C, 0 psig) will be referred to as optimum condition to simplify the discussions.

3.3.3. Characterization of optimum N. oculata bio-oil (NBO)

The composition and properties of the bio-oil obtained from pyrolysis of *N. oculata* at optimum temperature and pressure (540^0C, 0 psig) was analyzed to determine its suitability as an alternative source of energy. Table 7 shows the elemental

composition, moisture content and fuel properties of the optimum *N. oculata* bio-oil (NBO). On the average, NBO contains 72% carbon, 10% hydrogen, 8% nitrogen, 0.15% sulfur and 10% oxygen by wt. Based on elemental analysis, the molar formula for NBO is $CH_{1.6}N_{0.09}S_{0.0008}O_{0.10.}$ Bio-oil from *C. prototheco*ides has lower carbon and hydrogen contents of about 62% and 8.8% wt, respectively as compared to that of *N. oculata.* Also, bio-oil with higher nitrogen (9.7% wt) and oxygen (19.4% wt) percentages were observed from *C. prototheco*ides [8]. This could indicate that different microalgae species may result to varying compositions of the bio-oil. The carbon and hydrogen contents of NBO were also observed to be relatively higher than wood-derived bio-oil. However, the carbon content of NBO is relatively lower than heavy fuel oil (85% wt). The bio-oil produced from *N. oculata* also contains some heteroatoms (primarily O and N). According to Czernik and Bridgwater (2004), the oxygen content of bio-oil depends on biomass type and process severity (i.e. temperature, residence time) [67]. *N. oculata* feedstock originally contains about 25% wt oxygen, which is lower than that of wood (41-43% wt). Hence, the oxygen content of algal bio-oil was lower than wood-derived bio-oil (35-40% wt) as expected. However, it is still higher than that of heavy fuel oil (1% wt). Low oxygen content of the bio-oil is desirable since oxygen causes several disadvantages. These disadvantages include (1) low energy density, (2) immiscibility with hydrocarbons, and (3) instability of the bio-oil [67]. Hence, further processing of the bio-oil to remove its oxygen content and improve its heating value is still needed to be a suitable alternative for heavy fuel oil. The nitrogen in the bio-oil, on the other hand, could have been derived from the hydrolysis, decarboxylation and deamination of the

protein content of *N. oculata* [20, 83]. Bio-oils from microalgae typically contain high nitrogen contents because of their high protein contents [87]. Nitrogen-containing compounds in the bio-oil may cause potential NOx emission during combustion. Hence, further processing of NBO to reduce its nitrogen content may be necessary.

The moisture content of bio-oil was found to be equal to about 6% wt. This value is relatively lower than wood-derived bio-oil (15-30% wt). Water in bio-oils is typically generated by the dehydration reactions occurring during pyrolysis [16, 19, 67]. It enhances the flow characteristics of the bio-oil by reducing its viscosity and lessens NOx emission during combustion. However, it tends to lower the heating value and decreases the combustion rate of the bio-oil [67]. Hence, further processing to remove the water present in NBO may be necessary to improve its combustion characteristics. Other properties of the bio-oil were also determined including heating value (36 MJ/kg), pour point (-6 ± 3^0C), flash point (40^0C), viscosity (10.29 cSt), density (840 kg/m^3) and pH (7.8) as shown in Table 7. The heating value of NBO is higher than that of wood-derived bio-oil (16-19 MJ/kg) but still lower than heavy fuel oil (40 MJ/kg). Algal bio-oil (NBO) has density that is comparable to No. 2 diesel fuel (0.83 kg/l), which is lower than lignocellulosic bio-oil (1.2 kg/l) [87]. It is also less viscous than wood-derived bio-oil. The presence of nitrogenous bases in NBO rendered its pH slightly alkaline (7.8), which is very different from that of lignocellulosic bio-oil (2-3).

Pressure may have a negative effect on bio-oil yield as discussed in Section 3.1.2. However, comparison of the properties of bio-oil obtained at optimum condition (540^0C, 0 psig) and under a pressurized environment (500^0C, 100 psig) revealed that

higher quality bio-oil can be obtained from pyrolysis at higher pressures. This could indicate that there may be competition between yield and quality of bio-oil produced with increasing pressure. As shown in Table 4, the carbon content and heating value of the bio-oil obtained at 500^0C and 100 psig are higher than that of NBO, which was produced at 540^0C and 0 psig. This may be due to the secondary reactions that possibly occurred at high pressures, which could have removed greater amounts of heteroatoms (O and N) from the bio-oil. This observation could be a motivation for further investigation on the effects of pressure on bio-oil quality.

Table 7. Comparison among NBO, heavy fuel oil and other bio-oils.

Characteristics	Optimum *N. oculata* bio-oil (NBO)	Algal bio-oil (500^oC and 100psig)	Wood-derived bio-oil[a]	Heavy fuel oil[a]
Moisture (%wt)	5.92 ± 1.18	2.02 ± 0.57	15-30	0.1
Ultimate analysis (%wt)				
C	72.32 ± 0.20	75.77 ± 2.57	54-58	85
H	9.64 ± 0.10	10.41 ± 0.39	5.5-7.0	11
N	7.75 ± 0.57	5.49 ± 0.24	0-0.2	0.3
S	0.15 ± 0.04	0.54± 0.25	-	-
O	10.14 ± 0.90	7.55 ± 3.09	35-40	1
H/C	0.13	0.14	-	0.13
Heating Value (MJ/kg)	35.87 ± 0.40	38.5 ± 0.44	16-19	40
Pour pt (^{o}C)	-6 ± 3			
Flash pt (^{o}C)	40			
Viscosity (cSt)	10.29 ± 0.87		25-1000[b]	
Density (kg/l)	0.84 @25^0C		1.2[b]	
pH	7.8		2-3[b]	

[a] adapted from reference Czernik and Bridgwater (2004)
[b] adapted from reference Du et al (2011)

The chemical composition of NBO was further characterized using GC-MS. Table 8 summarizes the peaks detected as well as the relative percentage areas of the compounds present in the algal bio-oil. The identified compounds were grouped as follows: alkanes, alkenes, alkynes, annulenes, alcohols, acids, benzene and aromatic compounds, esters, amides and nitriles. Based on Table 8, the optimum algal bio-oil (NBO) mostly contains saturated aliphatics (35.22%), unsaturated aliphatics as alkenes (27.19%), and annulenes (10.98%) ranging from C_8 to $C_{20,}$ which is within the range of diesel fuel (C_8 to C_{25}). NBO also contains some aromatic compounds (6.01%) including pyrrole, which is a colorless heterocyclic aromatic compound that darkens readily upon exposure to air. The high amounts of aliphatic and aromatic compounds present in algal bio-oil could be attributed to the pyrolytic decomposition of the lipid content of microalgae [87]. On the other hand, the amides (0.35%) and nitriles (9.68%) present in the algal bio-oil could be derived from the protein content (24% wt) of *N. oculata.* Some other minor components of NBO are alcohols (4.47%) and esters (5.49%). It may also be important to note that unlike in bio-oils from lignocellulosic sources, the algal bio-oil from *N. oculata* does not contain phenolic compounds based on GC-MS analysis [74].

Table 8. Chemical composition of optimum algal bio-oil (NBO).

Compound	Relative Content (%)	Compound	Relative Content (%)
Alkanes	**35.22**	**Annulenes**	**10.98**
Cyclohexane, (4-methylpentyl)-	0.63	1,3,5,7-Cyclooctatetraene	1.83
Decane	2.22	1,3,5-Cycloheptatriene	9.15
Dodecane, 2,6,11-trimethyl-	3.33		
Eicosane	1.16	**Alcohols**	**4.47**
Hexadecane	7.54	1-Pentanol, 4-methyl-2-propyl-	0.59
Nonadecane, 2-methyl-	1.19	1-Octanol, 3,7-dimethyl-, (S)-	0.74
Nonane	2.14	1-Dodecanol, 3,7,11-trimethyl-	1.24
Octane	2.68	2-Methyl-Z,Z-3,13-octadecadienol	1.9
Pentadecane, 2,6,10-trimethyl-	0.48		
Tetradecane	1.76	**Benzene and Aromatic Compounds**	**6.01**
Tridecane	8.65	Pyrrole	1.31
Undecane	2.45	Ethylbenzene	2.29
Undecane, 3,6-dimethyl-	0.99	o-Xylene	0.92
		Benzene, propyl-	0.46
Alkenes	**27.19**	Benzene, 1-ethyl-3-methyl-	0.41
1-Decene	3.65	Benzene, 1,2,4-trimethyl-	0.62
1-Dodecene	2.4		
1-Heptene, 2,6-dimethyl-	0.48	**Esters**	**5.49**
1-Hexadecene	1.65	Methyl tetradecanoate	0.56
1-Nonene	2.48	Hexadecanoic acid, 15-methyl-, methyl ester	4.27
1-Octene	2.53	9-Octadecenoic acid (Z)-, methyl ester	0.66
1-Undecene	3.11		
2-Hexadecene, 3,7,11,15-tetramethyl-, [R-[R*,R*-(E)]]-	1.15	**Amides**	**0.35**
2-Undecene, (E)-	0.59	N,N-Dimethyldodecanamide	0.35
3-Tetradecene, (Z)-	6.02		
4-Octene, (E)-	0.36	**Nitriles**	**9.68**
7-Hexadecene, (Z)-	0.39	Pentanenitrile, 4-methyl-	0.72
7-Tetradecene, (E)-	1.64	Hexanenitrile	0.57
8-Heptadecene	0.52	Benzene, 1-ethyl-4-methyl-	0.53
cis-2-Nonene	0.22	Heptanonitrile	0.75
		Dodecanenitrile	0.83
Alkynes	**0.61**	Pentadecanenitrile	5.56
1-Octadecyne	0.61	Oleanitrile	0.72

The suitability of NBO as a source of liquid transport fuel was further evaluated using the van Krevelen diagram as shown in Figure 16. The plot of O:C vs H:C, known as the van Krevelen diagram, is typically used for comparing biofuels to fossil fuels [81, 82]. Fuels with higher energy can be found at the lower left corner (near the origin) of the van Krevelen diagram since this region represents low H:C and O:C ratios [81]. Higher H:C and O:C ratios decrease the energy value of a fuel since C-H and C-O bonds contain lesser energies compared to C-C bonds [82]. Based on Figure 16, NBO has lower H:C ratio and almost the same O:C ratio as fatty acid methyl ester (FAME), which indicates its higher energy value. To approach crude oil and diesel region, on the other hand, deoxygenation of the bio-oil may be necessary.

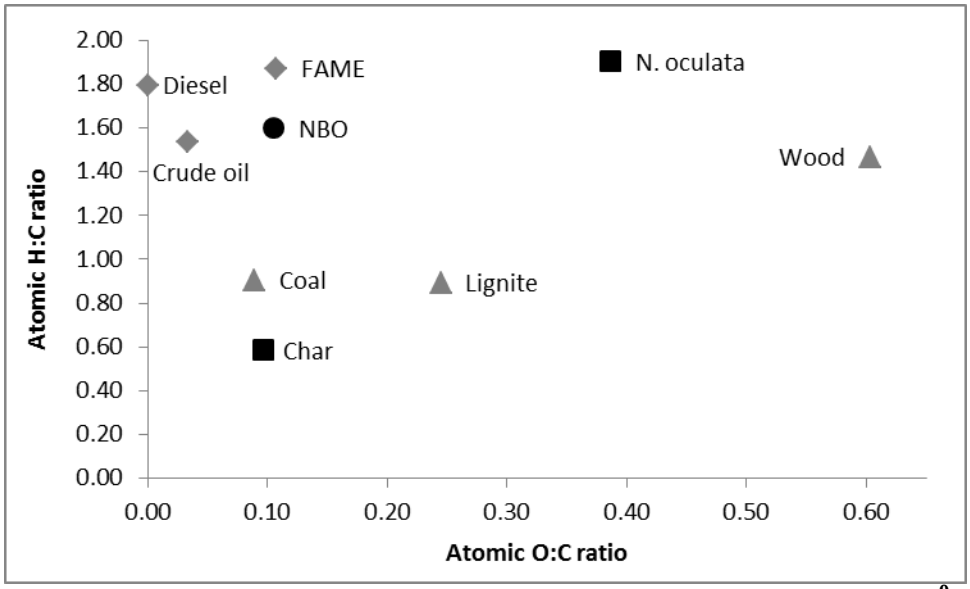

Figure 16. van Krevelen diagram for char and bio-oil from pyrolysis at 540^{0}C and 0 psig.

3.3.4. Characteristics of the pyrolysis co-products

3.3.4.1. Char

The composition and heating value of the char obtained from pyrolysis of *N. oculata* at optimum conditions was analyzed to assess its suitability as a solid fuel. Table 9 compares the proximate and elemental compositions and heating values of the feedstock, *N. oculata*, and char obtained at optimum conditions. The volatile matter (VM) content of the biomass evidently decreased from 81% wt of the original *N. oculata* to about 22% wt after pyrolysis at 540^0C and 0 psig. This could be attributed to the release of volatile components from the biomass to form liquid and incondensable gas components. Intuitively, the reduction in the amount of volatiles tended to increase the relative concentration of the nonvolatile fractions (i.e. fixed carbon, ash) in the char. Fixed carbon (FC) increased from 5% wt to about 44% wt while ash content increased from 14% wt to approximately 31% wt. High ash content is not desirable since it reduces the heating value of the fuel [82]. Ultimate analysis, on the other hand, shows that the hydrogen and oxygen in the biomass significantly decreased after pyrolysis. The volatiles that were released from the biomass during pyrolysis may contain oxygen and hydrogen that formed different compounds in the bio-oil or gas produced. The removal of hydrogen and oxygen resulted to an increase in carbon content, which is consistent with the increase in fixed carbon content as mentioned earlier. The heating value of the original biomass (25 MJ/kg) decreased to about 20 MJ/kg, which could be attributed to VM reduction and increase in ash content.

The high carbon content of the char, however, makes it suitable for several applications such as solid fuel or activated carbon. Further evaluation on the applicability of char as fuel was done using van Krevelen diagram as shown in Figure 16. As can be seen from Figure 16, the original feedstock, *N. oculata,* has higher H:C and O:C ratio compared to coal and lignite, hence, contains lesser energy value. Reduction in hydrogen and oxygen contents was observed after pyrolysis at 540^0C and 0 psig as discussed earlier. Consequently, the O:C and H:C values of the char were also reduced approaching the coal region.

Table 9. Composition of char from pyrolysis of *N. oculata* at 540^0C, 0 psig.

Sample	Ultimate analysis (% wt)					Proximate analysis (% wt)			HV (MJ/kg)
	C	H	N	S	O	VM	FC	Ash	
N. oculata	48.31	7.66	4.8	0.81	24.85	81.26	5.17	13.57	24.69
Biochar	50.25	2.45	7.75	2.45	6.45	22.12	44.01	30.65	20.05

3.3.4.2. Gaseous product

The incondensable gaseous product obtained from pyrolysis could also be a potential source of energy. To assess the recoverable energy from the gas produced, the composition (in %vol) of the gas sample obtained from pyrolysis at optimum conditions (540^0C, 0 psig) was analyzed using gas chromatography. The heating value of the gaseous product, on the other hand, was estimated by using the volume fraction and heating value of each gas components as shown in Equation 3.10.

$$HV_{gas} = \sum_{i=1}^{n} HV_i \, f_i \qquad (3.10)$$

where HV_{gas} is the heating value of the gaseous product (MJ/m^3); HV_i represents the heating value of component gas (MJ/m^3); and f_i represents the volume fraction of component gas.

Combustible gases are present in the gaseous product including H_2 (4%), CH_4 (15%), CO (6%), C_2H_4 (3%), C_2H_6 (9%), C_3H_6 (3%) and C_3H_8 (4%). Noncombustible components, on the other hand, include oxygen (2%), nitrogen (11%) and carbon dioxide (37%). Among the hydrocarbon gases, methane content was the highest, which is similar to that observed by Pan et al (2010) and Uzun et al (2007) [20, 80]. Methane production typically peaks around 480 to 520^0C, which is close to the operating temperature (540^0C) [7]. The evolution of hydrogen from microalgae, on the other hand, usually happens at around 430 and 460^0C [7]. Hence, hydrogen produced at lower temperatures could have undergone secondary reactions at 540^0C. Carbon dioxide, which has the highest % volume among the gases present, could have been derived from the decarboxylation of the biomass. The heating value of the gas produced is largely dependent on the amount of combustible gas components. Using Equation 3.10, the heating value of the gas was estimated to be equal to 20.80 ± 0.75 MJ/m^3.

3.3.5. Energy yield and recovery

Energy recovery efficiencies for each product at optimum process conditions (540^0C, 0 psig) were then estimated using product yields and heating values of the product and feedstock as shown in Equation 3.3. Based on the results of the calculation, most of the energy from *N. oculata* was transferred to the bio-oil (34%). About 26% of

the energy from the feedstock was recovered in the char while 8% was converted to energy in the form of combustible gases. On the average, the energy conversion efficiency was about 68%. The energy losses could be attributed to the formation of noncombustible products such as water and CO_2. Also, some energy could be possibly lost in the unrecovered products as discussed in Section 3.3.2.

By multiplying the product yield by the heating value of the product, the energy yield (in MJ/ton dry algae) of each product was also calculated. Corresponding to energy recovery discussed above, the highest energy yield of about 8,400 MJ/dry ton was estimated for the bio-oil produced at optimum conditions. This may be attributed to the high yield and heating value of bio-oil produced at 540^0C and 0 psig. The energy yield for char, on the other hand, would be about 6,300 MJ/dry ton while for gaseous product it was estimated to be around 1,900 MJ/dry ton.

3.4. Conclusions

Pyrolysis of *Nannochloropsis oculata* at different temperatures (400^0C, 500^0C and 600^0C) and pressures (0, 50 and 100 psig) in a fixed-bed batch reactor showed that the process can be manipulated to favor bio-oil, char and syngas production. Peak production of char can be expected at the lowest temperature (400^0C) at all pressure values. At 400^0C, char production was approximately equal to 57% wt. Gas production, on the other hand, was greatly affected by temperature and the interaction of temperature and pressure. Maximum gas yield (20% w/v) was observed at 600^0C and 100 psig. Liquid product yield was critically dependent on temperature and pressure. Hence,

optimization using response surface analysis was done to determine the temperature and pressure combination that maximizes bio-oil yield. Optimum temperature and pressure for bio-oil production were found to be equal to 540^0C and 0 psig based on numerical optimization and actual validation experiments. At 540^0C and 0 psig, maximum liquid product yield was attained at 43% wt (20% wt aqueous; 23% wt bio-oil). Char and gas yields were approximately equal to 32 and 12% by wt, respectively. The composition and heating values of the products (biochar, bio-oil and syngas) were also evaluated. Results indicate that these products can be used as alternative energy sources.

4. SEPARATION OF BIO-OIL AND AQUEOUS LIQUID PRODUCT COMPONENTS BY FRACTIONAL DISTILLATION

4.1. Introduction

Biomass is an abundant renewable and sustainable source of various kinds of bio-chemicals and transport fuel components. It refers to a wide variety of organic materials such as agricultural wastes, livestock manure, sewage sludge and aquatic organisms such as microalgae. Various routes, which are generally categorized to biochemical and thermochemical processes, can be used to convert biomass to useful products. Fermentation can be used to convert cellulosic biomass into ethanol. Biogas production, on the other hand, can be done by gasification [30]. Nowadays, pyrolysis is gaining more importance as a thermochemical conversion route due to its ability to convert biomass into biofuels and variety of chemicals [100]. Pyrolysis converts biomass to solid char, liquid and gaseous products at temperatures generally below 600^0C and with the absence of oxygen. More interest is given to the liquid product since it could be a potential source of liquid transport fuels and value-added products. Production of transport fuel components through the carbon-neutral biomass-to-fuel cycle is a more attractive option considering the increasing concern for global climate change due to increasing greenhouse gas emissions [7, 8, 12, 67].

Based on the previous papers (Sections 2 and 3), the liquid product from pyrolysis of biomass such as microalgae contains two immiscible fractions, namely: (1) the dark-brown organic layer or bio-oil, and (2) yellowish aqueous liquid product (ALP).

Bio-oil from pyrolysis of biomass typically contains a wide variety of compounds and its complex composition restricts its direct use as fuel or biochemical. Hence, it is necessary to separate the bio-oil to relatively simpler fractions which may have different applications depending on their characteristics. The conventional techniques in the separation of bio-oil components includes column chromatography, extraction, centrifugation and distillation [21]. Column chromatography was used by Wang et al (2011), Cao et al (2010) and Zeng et al (2011) to separate components of wood tar, and bio-oils from sewage sludge and rice husk, respectively [40-42]. Solvent extraction of valuable bio-oil components such as phenol can also be found elsewhere [43, 44]. Although these methods were found effective to a certain extent in separating specific compounds from the bio-oil, further processing is still needed to remove the solvent used in both processes. Centrifugation, on the other hand, is a simple pretreatment technique; however, the homogeneity of the bio-oil limits its applicability [45]. There are various distillation techniques which can be utilized for bio-oil separation including molecular distillation, flash distillation, steam distillation and fractional distillation [45]. Both flash and steam distillation processes are typically used as pre-separation methods only where high purity is not required [45, 46]. The separation of bio-oil components by molecular distillation can also be found elsewhere [45-48]. Wang et al (2009) used a KDL5 molecular distillation apparatus to separate sawdust bio-oil into three (3) fractions at different operating temperatures. Maximum distillate yield of about 85% wt was obtained and the degree of separation was evaluated using a separation factor, $I_{i,m}$, which is mainly the relative content of a compound in the GC-MS chromatogram [45]. Guo et

al (2010), on the other hand, separated sawdust bio-oil into light, middle and heavy distillates using molecular distillation and characterized each fraction using TG-FTIR analysis. Results showed that most of the water (~70%) and acids with low boiling point were contained in the light fraction; whereas, the middle and heavy fractions contained more phenols [46]. Fractional distillation or rectification, on the other hand, is the traditional way of separating transport fuels such as gasoline and diesel from petroleum crude. Unlike molecular distillation, which is typically done under high vacuum (<0.01 torr), this process can be done at atmospheric conditions. In fractional distillation, separation takes place by repeated vaporization-condensation cycles within a packed distillation column [49]. Boucher et al (2000) studied the distillation of softwood bark residues until 140^0C using packed columns to determine the true boiling point distribution of the light fraction of the bio-oil. The distillation curve, which is a plot of cumulative distillate %wt against temperature, showed the evaporation of water at temperatures below 100^0C followed by an increase in the slope of the curve indicating the evaporation of heavier fractions [50]. Based on this data, removal of water from the bio-oil could be done by distillation to improve its combustion characteristics.

On the other hand, there is limited information on the fate of the aqueous fraction of the liquid product, which will be referred in this study as ALP. A typical aqueous fraction of bio-oil from lignocellulosic biomass contains sugars, organic acids, hydroxyacetone, hydroxyacetaldehyde, furfural, and small amounts of guiacols, which may be further processed into hydrogen, alkanes, aromatics, or olefins [21, 101, 102]. Separation of valuable by-products such as organic acids from ALP may be important

since these compounds can also be used as intermediates in the production of fuels and bio-chemicals. Separation of acetic acid from a model aqueous fraction of bio-oil was studied by Teella et al (2011) [21]. In his study, nanofiltration and reverse osmosis (RO) membranes were used to separate acetic acid from a model aqueous solution containing water, glucose, acetic acid, hydroxyacetone, formic acid, furfural, guaiacol, and catechol [21]. Although this method was found to be feasible based on the retention factors (above 90% for glucose, negative values for acetic acid), the drawbacks for this process are (1) the need for high trans-membrane pressures and (2) the membrane used cannot be reused due to the damage caused by guaiacols and phenols present in the aqueous fraction of bio-oil.

In this study separation of the bio-oil and ALP components obtained from pyrolysis of *N. oculata* was done by fractional distillation. The distillate yields for each distillate fractions at various boiling point ranges were determined. Distillation curves for both bio-oil and ALP layers of the liquid product were also plotted. Also, the composition and properties of the distillate fractions from bio-oil and ALP were analyzed and compared to traditional fossil-derived transport fuels to determine their potential applications.

4.2. Materials and Method

4.2.1. Production of bio-oil and aqueous liquid product (ALP)

The bio-oil and aqueous liquid product (ALP) used in this study was produced from pyrolysis of ground and dried *Nannochloropsis oculata* in a fixed-bed batch-type

Parr pressure reactor at 540^0C and atmospheric pressure (0 psig) as described in Chapter 3. Separation of the two liquid layers was done using a separatory funnel where the aqueous liquid layer at the bottom was first collected in a glass container followed by the organic dark-brown bio-oil layer.

4.2.2. Distillation experiment

The distillation set-up used in this study consisted of a 50-ml distillation flask, Vigreux distilling column, distillation head, thermometer, condenser, cowhead adapter and 15-ml receiving flasks as illustrated in Figure 17. For each distillation run, approximately 25 g of sample was placed inside the pre-weighed distillation flask with boiling chips to promote even boiling of the liquid. A heating mantle with a controller was used to heat the sample inside the distillation flask. The temperature inside the column was measured using a laboratory thermometer (maximum reading 400^0C) with the bulb slightly below the arm of the distillation head. The distillation head was used to connect the distilling column to the condenser and thermometer. During distillation, the heater is first turned on and cooling water is allowed to flow through the annulus of the condenser. The temperature after the first drop is recorded then the distillate fractions were collected at various boiling point ranges as summarized in Table 10. The end of the condenser was attached to a cowhead adapter, which directs the condensate from the condenser to a pre-weighed receiving flask. Each fraction was weighed using an analytical balance (Mettler Toledo, Model XP105DR, Switzerland). The yield for each fraction was calculated by dividing the weight of the distillate fraction obtained by the weight of the sample (aqueous, bio-oil) used. Distillation experiments for both the

aqueous and bio-oil liquid products were done in triplicates and average values were reported together with the standard deviation placed as error bars in the graphs.

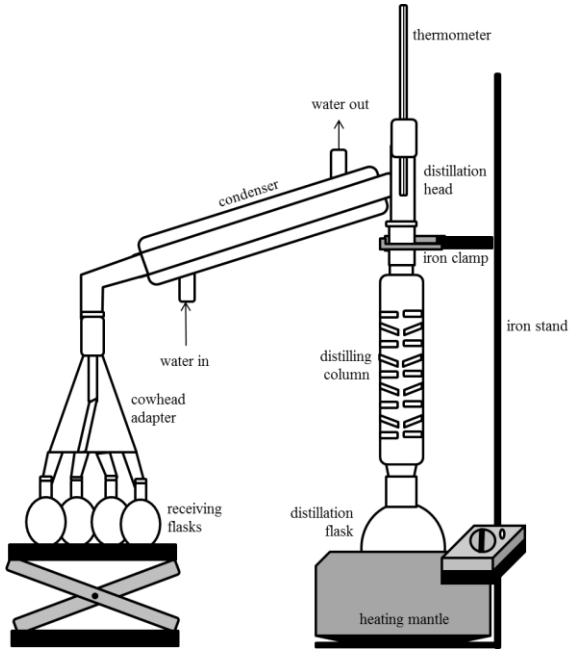

Figure 17. Distillation set-up.

Table 10. Temperature ranges for distillate fractions.

Sample	Distillate fraction	Vapor temperature (^{o}C)
Bio-oil	Fraction 1 (BF1)	<140
	Fraction 2 (BF2)	140-160
	Fraction 3 (BF3)	160-200
	Fraction 4 (BF4)	200-250
	Fraction 5 (BF5)	250-287
	Residue (BF6)	>287
Aqueous	Fraction 1 (AF1)	<90
	Fraction 2 (AF2)	90-100
	Fraction 3 (AF3)	100-110
	Fraction 4 (AF4)	110-150
	Fraction 5 (AF5)	150-180
	Residue	>180

4.2.3. Analysis of the distillate fractions

The distillates obtained from the fractional distillation experiments were collected in small glass vials and analyzed immediately for their chemical composition and properties. Heating values of the distillate samples was determined using PARR isoperibol bomb calorimeter (Model 6200, Parr Instrument Company, Moline, IL) following ASTM D2015. Ultimate analysis was determined using Vario MICRO Elemental Analyzer (Elementar Analysemsysteme GmbH, Germany) in accordance with ASTM D 3176. Moisture content was analyzed by following ASTM E203 using KF Titrino 701 (Metrohm, USA, Inc). The chemical composition of the bio-oil was also determined by GC-MS analysis using Shimadzu QP2010 Plus, with the following parameters: bio-oil dissolved in dichloromethane (10 %vol); column – DB-5ms (25m length, 0.25μm thickness and 0.25mm diameter); column temperature program: 40^0C (held for 5 minutes) then ramped to 320^0C at 5^0C/min, then held for 5 minutes at 320^0C; ion source temperature at 300^0C. The functional groups present in the bio-oil were also determined using Shimadzu IRAffinity-1 FTIR (Fourier Transform Infrared) Spectrophotometer (Shimadzu, Inc).

4.3. Results and Discussion

4.3.1. Characteristics of the liquid product from pyrolysis of N. oculata

The liquid product from pyrolysis of *N. oculata* at optimum operating conditions (540^0C, 0 psig), which consists of two immiscible layers as mentioned in Section 3, was used in this study. Liquid product yield from pyrolysis of *N. oculata* was about 43% wt (23% wt bio-oil; 20% wt aqueous). The top organic dark-brown layer was referred in

this study as the bio-oil. It consists of about 72% carbon, 10% hydrogen, 8% nitrogen, 0.15% sulfur and 10% oxygen by weight. Based on the van Krevelen diagram (Figure 16), this product could be a potential alternative to crude oil after further processing to improve its quality. The algal bio-oil has carbon content that is still below than that of heavy fuel oil (85% wt) while its nitrogen and oxygen contents are higher relative to 0.3% and 1% wt of heavy fuel oil, respectively [67]. Also, the algal bio-oil contains about 6% wt moisture. The relatively high moisture and oxygen contents of the algal bio-oil render its heating value of about 36 MJ/kg lower than that of heavy fuel oil (40 MJ/kg) [67]. On the other hand, the yellowish aqueous liquid product (ALP), which settles at the bottom layer of the liquid product, consists of about 65% wt moisture. The remaining 35% wt may consist of water-soluble organic compounds as indicated by the FTIR results shown in Figure 2.8 (Section 2.3.3.2). Based on the peak absorbances in the FTIR spectra in Figure 2.8, phenols and alcohols (3600-3200 cm^{-1}), ketones, aldehydes, carboxylic acids, and esters (1750-1650 cm^{-1}) and aromatic (820-690 cm^{-1}) compounds may be present in the aqueous liquid fraction.

4.3.2. Distillate yields

Figure 18 shows the distribution of the distillate fractions from algal bio-oil at different boiling point ranges after fractional distillation at atmospheric condition. The six (6) distillate fractions of the bio-oil were referred in this paper as BF1 to BF6. The first two fractions (BF1 and BF2) consist of two immiscible aqueous and organic layers. BF1 has about 3% wt organic layer and 2% wt aqueous layer while BF2 contains about 7% wt organic and 6% wt aqueous fractions. The presence of aqueous layers in BF1 and

BF2 may be attributed to the moisture present in the bio-oil. The first fractions typically contain most of the water from the bio-oil. In the separation of sawdust bio-oil components using molecular distillation, the Fraction I also contains about 50-70% water content while the middle fraction has only about 1-2% moisture content. [45]. The boiling point range ($<160^0$C) where the aqueous layers appeared is near the boiling point of water (100^0C) and close to the range of boiling points for aqueous liquid product distillation, which will be discussed later in this section. Based on the yields, BF5 (51% wt) was the major product of the fractional distillation of bio-oil followed by BF6 (23% wt). BF5 has almost the same color as the algal bio-oil while BF6 is darker in color and more viscous than BF5. On the other hand, lower yields were observed from the middle fractions, BF3 (1% wt) and BF4 (6% wt).

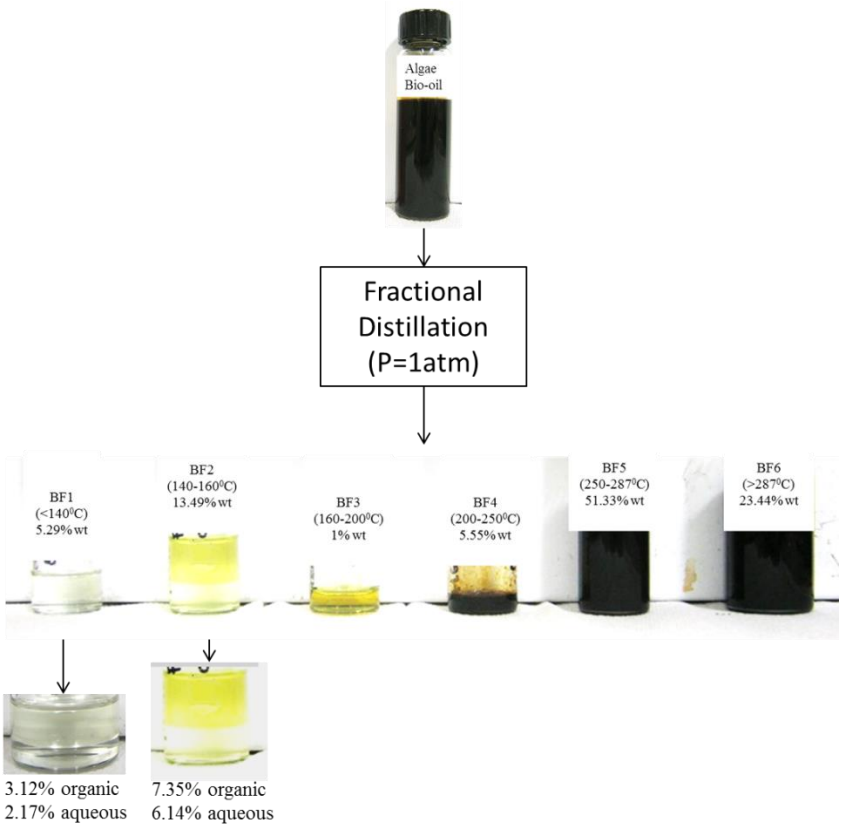

Figure 18. Distribution of distillate fractions of algal bio-oil.

The boiling point ranges and distillate yields for ALP, on the other hand, are shown in Figure 19. Lower boiling points close to the boiling point of water were employed for ALP since it consists mostly of water (65% wt). The five (5) ALP distillate fractions were referred in this paper as AF1 to AF5. Based on Figure 19, about 49% wt were distilled below 100^0C and an additional 30% wt was condensed just above the boiling point of water ($100\text{-}110^0$). Based on the total amount of distillates (which is greater than 65% wt) and the color of the distillates (AF1, AF2 and AF3), there may be other organic components with similar or lower boiling points than water that was

removed from ALP at this condition. A light yellow distillate fraction, AF4 (4% wt), was distilled at around 110-150^{0}C while a darker yellow transparent distillate fraction, AF5 (13% wt), was obtained at about 150-180^{0}C.

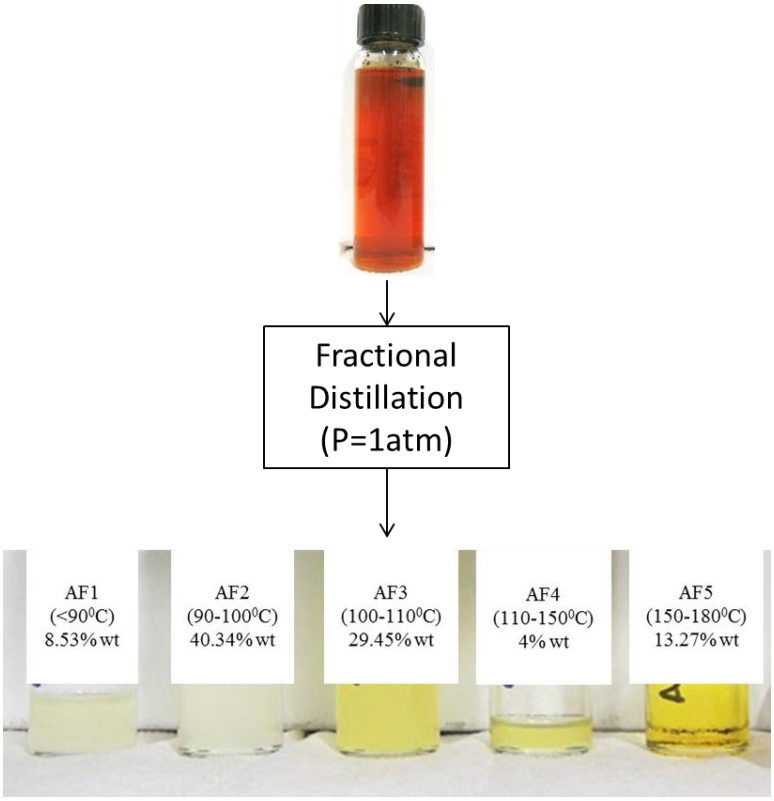

Figure 19. Distribution of distillate fractions of the aqueous liquid product (ALP).

4.3.3. Distillation curves

The distillation curves, which represent the temperature of the distilling vapor as a function of cumulative mass percentage of the distillate, for bio-oil and ALP are shown in Figure 20. The same plot was used by Agblevor et al (2012) to compare the distillation characteristics of HZSM-5 biocrude oil and 4350 gas oil in a high temperature simulated distillation (HTSD) set-up [103]. Boucher et al (2000) also

plotted the distillation curve for the light fraction of the bio-oil from softwood bark [50]. Figure 20 clearly shows that bio-oil fractions boil at higher temperatures than that of ALP. In an ideal distillation curve, the lower boiling components distill completely (indicated by a straight horizontal line at a lower temperature) followed by distillation of the higher boiling components (indicated by a ramp from the lower temperature to a straight horizontal line at a higher temperature) as illustrated in Figure 20. Bio-oil and ALP distillation curves slightly varied from an ideal distillation plot since both plots are empirical and a wide variety of compounds are present in the bio-oil and ALP. Nonetheless, both plots show distinct boiling point ranges for the lower and higher boiling components. For empirical plots such as Figure 20, the distillate at the beginning of the distillation is enriched with lower boiling components while the distillate at the later stages of the distillation is enriched with higher boiling components. For bio-oil, lower boiling components condensed at temperatures ranging from 50 to 160^0C while higher boiling components were obtained at temperatures higher than or equal to 250^0C. The lower boiling components for ALP, on the other hand, were collected at temperatures below 100^0C while the higher boiling components were obtained at temperatures higher than or equal to 150^0C. For ALP, a black solid residue amounting to about 4% wt adhered to the surface of the distillation flask after fractional distillation. This ALP residue was not considered in the later characterization of distillation products. The non-distillation fraction or residue (BF6) obtained from bio-oil distillation, on the other hand, was more viscous and has darker color than the original algal bio-oil but can still be recovered from the distillation flask. This non-distillation residue that looks like

black coke is similar to that decribed by Xu et al (1999) as cited by Wang et al (2009) for the separation of bio-oil by rectification at normal and reduced pressures [45, 104]. BF6 was further characterized in the succeeding sections since was about 23% wt of the original bio-oil and may have potential uses based on its composition and properties.

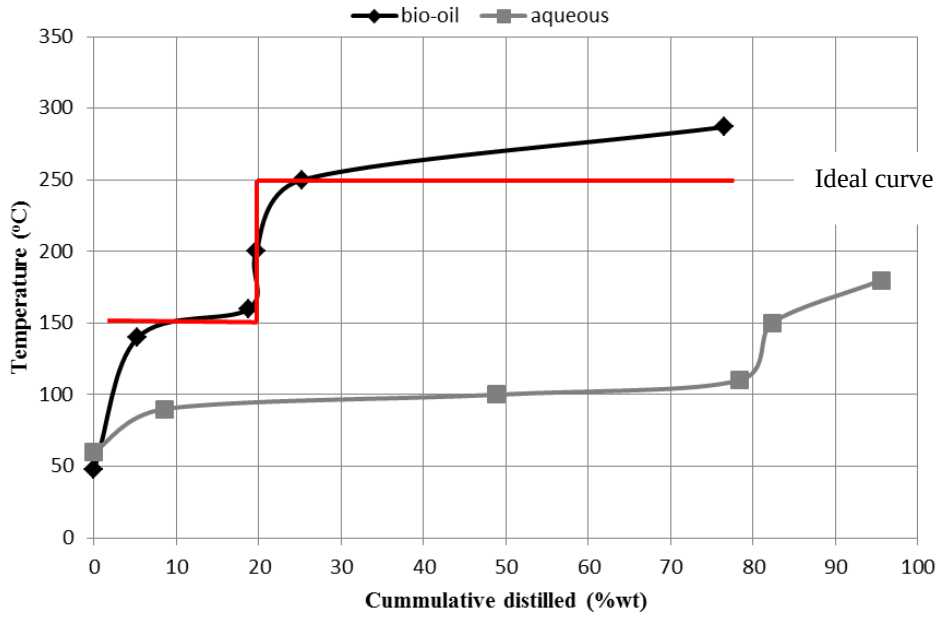

Figure 20. Distillation curves for algal bio-oil and aqueous liquid product.

4.3.4. Characteristics of distillate fractions

One of the main goals in further processing bio-oil either by chemical or physical means is to improve the quality of the bio-oil or its components. This section shows the variation of the bio-oil and ALP fractions from their corresponding original material (i.e. bio-oil, ALP).

4.3.4.1. Moisture content and heating value

The original bio-oil contains about 6% moisture. Water present in the bio-oil obtained from pyrolysis is typically generated by the dehydration reactions occurring during pyrolysis [16, 19, 67]. It has positive effect on the flow characteristics of the bio-oil by reducing its viscosity and NOx emission during combustion. However, water also tends to lower the heating value and decreases the combustion rate of the bio-oil [67]. Due to this, the removal of water from the bio-oil may be necessary to improve its heating value and combustion characteristics. ALP, on the other hand, is expected to be mainly composed of water. As mentioned earlier, the ALP obtained from this study only has 65% wt water and the remaining 35% could potentially be water-soluble organics. Hence, ALP cannot be directly reused as water source or disposed in waterways without treatment since the organics present in ALP could potentially pollute the receiving environment. Also, the organics that can be recovered from ALP may have other potential uses.

As discussed in Section 4.3.2, the first two fractions of the bio-oil (BF1 and BF2) formed aqueous layers, which contain most of the water from the original bio-oil. The moisture contents of the top portion of BF1 and BF2 were also analyzed and compared to other bio-oil fractions as shown in Figure 21-a. As can be seen from Figure 21-a, there is a considerable decrease in the moisture contents of the bio-oil fractions as compared to the original bio-oil (p-value <0.0001). Figure 21-b, on the other hand, shows that most of the water from ALP was present in the distillates that were condensed near the boiling point of water (AF2 and AF3). However, the moisture content of AF2 and AF3 (89% wt)

reveal that these fractions are not yet pure water. Nonetheless, the percentage of potential organic compounds in AF2 and AF3 are lower compared to the original ALP and further water treatment to remove the remaining organics may render the water reusable or safe for disposal. Lower moisture contents were detected for AF1 and AF4, which was condensed at >90^{0}C and 110-150^{0}C, respectively. AF5, on the other hand, has minimal moisture content of about 7% wt, which could indicate that most of the organic water-soluble compounds in ALP were condensed at 150-180^{0}C. AF5 was further characterized and compared with bio-oil fractions for its potential usage.

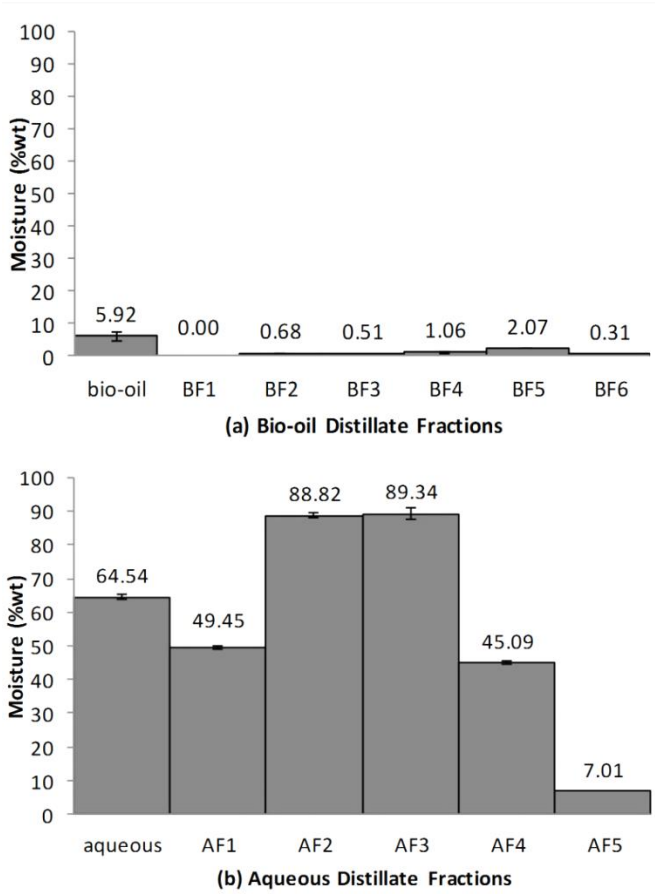

Figure 21. Moisture contents of algal bio-oil and aqueous liquid product distillate fractions.

Figure 22, on the other hand, compares the heating values (HHV) of the original bio-oil, bio-oil distillate fractions and AF5. The original bio-oil has HHV of about 36 MJ/kg, which is still lower than that of heavy fuel oil (40 MJ/kg), FAME (40.5 MJ/kg), diesel (45.7 MJ/kg) and gasoline (46.4 MJ/kg) [105]. Based on the figure, the HHVs of the distillate fractions increased significantly as compared to the original bio-oil (p-value < 0.0001). BF1 has HHV of about 42 MJ/kg, which is higher than heavy fuel oil and FAME. Whereas, the HHV of BF2 (40 MJ/kg) is almost equal to that of heavy fuel oil and FAME. The four (4) remaining bio-oil fractions (BF3, BF4, BF5 and BF6) have HHV that is still slightly lower than petroleum-derived fuels but slightly higher than the original bio-oil. AF5, which is an ALP distillate, has an HHV of about 24 MJ/kg. Although lower in value as compared to bio-oil fractions, the HHV of AL5 is higher than that of a typical wood-derived bio-oil (16-19 MJ/kg) [67]. It is even slightly higher than the energy content of methanol (22.8 MJ/kg) [105].

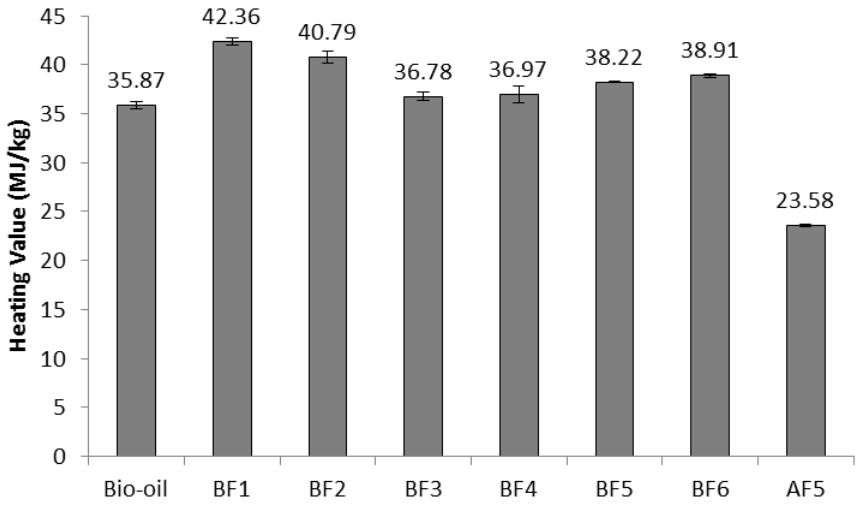

Figure 22. Comparison of the heating values of algal bio-oil, bio-oil distillates and AF5.

4.3.4.2. Elemental composition

The elemental composition in terms of C, H, O, N and S % by weight of the bio-oil distillate fractions and AF5 were analyzed to further assess their suitability as alternative energy sources. The results were also compared with the elemental composition of the original bio-oil as shown in Figure 23. BF1 has the highest carbon (82% wt) and hydrogen (11% wt) contents compared to the original bio-oil and other distillate fractions followed by BF6 (residue) and BF2. This result agrees well with the HHV results discussed previously in Section 4.3.4.1. Higher amounts of combustible carbon and hydrogen components in the distillate fractions increases their energy content. Hence, the increase in the HHV of BF1, BF2 and BF6 compared to the algal bio-oil may be attributed to the enrichment of carbon and hydrogen in the distillates. Aside from that, reduction in oxygen content was also observed in BF1, BF2 and BF6. Low oxygen content is desirable since oxygen causes several disadvantages including low energy density, immiscibility with hydrocarbons, and instability [67]. BF5, on the other hand, has almost similar elemental composition as the original bio-oil as can be seen in Figure 23. However, the HHV of BF5 was higher than the bio-oil though they have similar elemental composition. This variation in the HHV may be attributed to the difference in the amount of moisture present in BF5 and bio-oil as discussed in Section 4.3.4.1. In general, the heating value of a substance is negatively correlated to moisture content [68]. The original algal bio-oil has higher moisture content than BF5 (see Figure 21); hence, it has lower HHV. Based on Figure 23, a decrease in % carbon and hydrogen and increase in % oxygen were observed in BF3 and BF4 relative to the bio-oil.

However, these distillate fractions (BF3 and BF4) have higher HHV as compared to the algal bio-oil as mentioned in Section 4.3.4.1. Similar to BF5, this may also be attributed to lower moisture contents of BF3 and BF4 distillates relative to the bio-oil. AF5, on the other hand, contains about 48% carbon, 8% hydrogen, 10% nitrogen, 0.05% sulfur and 34% oxygen, which is very much different from the bio-oil distillates. Its carbon content is lower than lignocellulosic bio-oils (54-58% wt). However, AF5 has higher hydrogen and lower oxygen contents than wood-derived bio-oils (5.5-7% hydrogen, 35-40% oxygen).

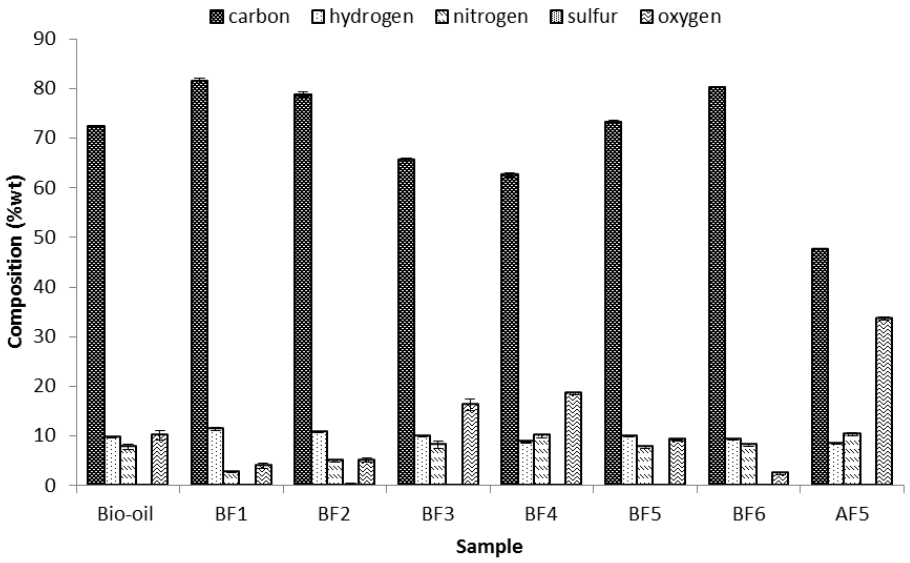

Figure 23. Comparison of the elemental composition of algal bio-oil, bio-oil distillates and AF5.

Based on the properties discussed, bio-oil distillates and AF5 could be potentially used as fuel. Further investigation on their application as fuel was done by comparing them to traditional petroleum-derived fuels and wood derived-bio-oils using the van Krevelen diagram (Figure 24). According to McKendry (2002), biofuels can be

compared to fossil fuels using the plot of atomic H:C and O:C ratios, known as the van Krevelen diagram [81, 82]. Based on Figure 4.8, the original bio-oil, which is comparable to BF5, has similar O:C ratio but lower H:C ratio compared to FAME. BF1 and BF2 is approaching the diesel region while BF6 is quite near the heavy fuel oil (HFO) region. BF3 and BF4 plots, on the other hand, were positioned farther from the liquid fossil fuels region than the bio-oil due to their higher O:C ratios, which also indicates the enrichment of oxygenated compounds in these fractions. Figure 24 also illustrates the large difference between AF5 and the bio-oil distillates. Based on the van Krevelen diagram, AF5 is near the wood-derived bio-oil region while the bio-oil distillates are near the petroleum-derived fuels.

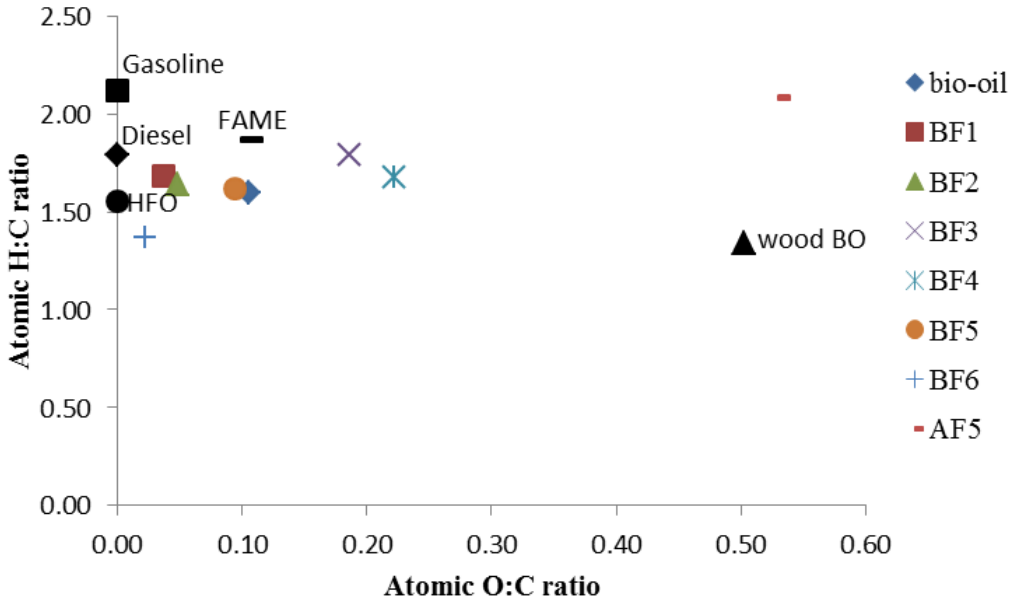

Figure 24. van Krevelen diagram for bio-oil and ALP distillates.

4.3.4.3. Functional groups

Functional group compositional analysis of the bio-oil and ALP distillates was done using FTIR spectrometry. This nondestructive technique was also used to determine the groups of compounds present in pyrolytic oils [84-87, 89, 90]. Figure 25 shows the FTIR spectra for the bio-oil and ALP distillate fractions while Table 11 summarizes the functional groups and their corresponding band position (in cm^{-1}) in the FTIR spectra. Based on Figure 25-a, AF1 and AF4 follow similar pattern while AF2 and AF3 are also the same. This result coincides with the moisture content analysis in Section 4.3.4.1. Also, ALP distillates except AF5 have distinct peaks in the 3600-3200 cm^{-1} frequency range, which indicates the presence of water. Based on Figure 25-a and Table 11, other organic compounds such as alkanes, ketones, aldehydes, carboxylic acids, esters and aromatic compounds may still be present in the AF2 and AF3 although the major component is water. For AF1 and AF4, however, alkanes, ketones, aldehydes, alcohols, carboxylic acids, esters, phenols and aromatic compounds may be present aside from water based on the band position of the peaks detected. AF5, on the other hand, mainly consists of organic compounds which may include carboxylic acids, esters, ketones, aldehydes (1750-1650 cm^{-1}), alkenes or amides (1660-1630 cm^{-1}), alkanes (1470-1350 cm^{-1}), alcohols and phenols (1300-950 cm^{-1}), and aromatic compounds (975-525 cm^{-1}) with minimal amount of water consistent with Section 4.3.4.1.

Bio-oil distillate fractions, on the other hand, have almost similar functional groups (except BF3) based on the band positions of the peaks detected as shown in Figure 25-b. BF3 may contain more oxygenated compounds such as alcohols and

phenols based on the absorbance peaks. The peak detected at 3200-2800 cm^{-1} and 1475-1350 cm^{-1} for C-H stretching and C-H deformation, respectively, indicate the presence of alkanes. C=C stretching vibrations at 1660-1630 cm^{-1} suggests the presence of alkenes or amides. Esters may also be present based on the peaks observed at 1310-1250 cm^{-1}. Lastly, the peak absorbances at 975-525 cm^{-1} could indicate the presence of aromatic compounds in the bio-oil distillates.

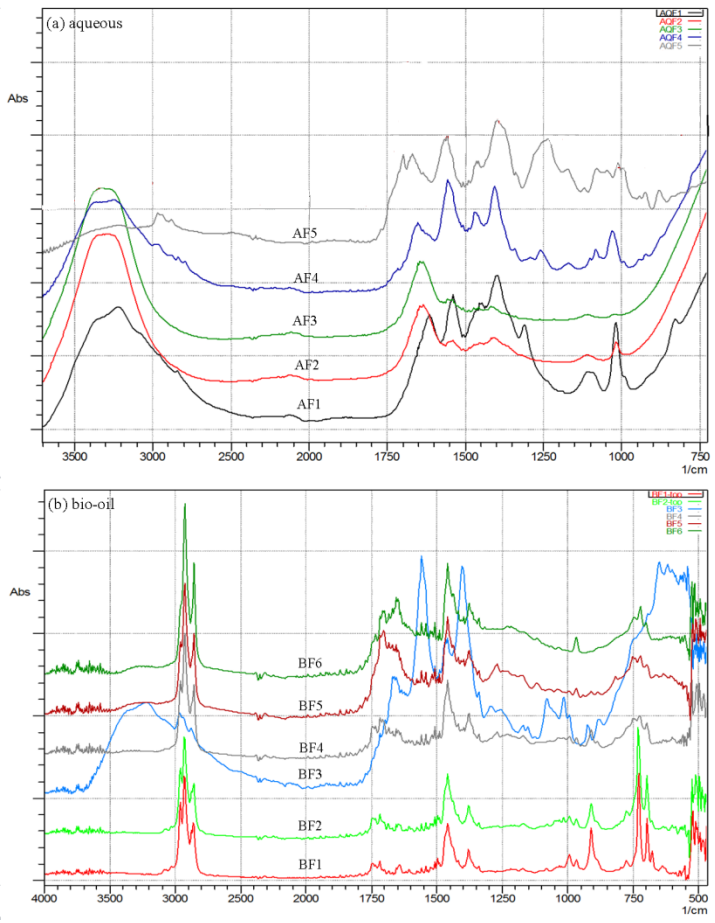

Figure 25. FTIR spectra of aqueous and bio-oil distillate fractions.

Table 11. Band position for different functional groups.

Band position (cm^{-1})	Vibration	Functional group
3600-3200	O-H stretching	Phenols, polymeric O-H, water impurities
3370-3170	NH_2 stretching	Amides
3200-2800	C-H stretching	Alkanes
2250-2000	C≡C, C≡N	Alkynes, Nitriles
1750-1650	C=O stretching	Ketones, aldehydes, carboxylic acids, esters
1660-1630	C=C stretching	Alkenes
	NH_2 scissors	Amides
1470-1350	C-H deformation	Alkanes
1310-1250	C-C-O stretching	Esters
1300-950	C-O stretching	Primary, secondary, tertiary alcohols, phenols
975-525	O-H bending C=C stretching	Mono-, polycyclic, substituted aromatic rings

4.3.4.4. Chemical composition

The chemical compositions of the bio-oil distillates and AF5 were identified using gas chromatography coupled with mass spectrometry (GC-MS). The quantity of each component was expressed in terms of relative percentage area of the chromatographic peaks. This kind of method was also used by Wang et al (2009) to directly assess the separation level of bio-oil components by molecular distillation [45].

Table 12 summarizes the compounds detected from the ALP distillate, AF5. Based on the table, AF5 consists mostly of oxygenated compounds such as carboxylic acids (21.06%) and carboxylate esters (53.85%), N-containing amides (9.89%), lactams (11.59%) and some acetates (3.61%). Typically, smaller carboxylic acids with 1 to 5 carbon atoms are water-soluble but have higher boiling points than water; hence, can be separated by distillation. Carboxylic acids are useful in the production of polymers, pharmaceuticals, food additives and solvents. The carboxylate esters present in AF5, on

the other hand, are esters of fatty acids which could be derived from the lipid content of microalgae while the nitrogen present in these compounds could be attributed to proteins. Ethyl lactate (Propanoic acid, 2-hydroxy-, ethyl ester, (S)-), after further separation, can be used as a solvent [106, 107]. According to Schlten and Leinweber (1993) as cited by Cao et al (2010), acetamide usually comes from pyrolysis of microbial cells walls and chitin, and from other precursors such as proteins and amino sugars [41, 108]. On the other hand, the decarboxylation and cyclization of γ- and δ-amino acids during pyrolysis typically produces five- and six-membered cyclic lactams, respectively [41]. Further processing to remove or reduce the nitrogen-containing species may be necessary for AF5 to be a suitable fuel replacement since these nitrogen species can be converted to NOx and N_2O during combustion causing adverse environmental effects (i.e. acid rain, photochemical smog). Recovery of these nitrogen-containing compounds, however, may also be a more favorable alternative since these compounds may be further processed into value-added products as mentioned earlier.

Table 12. Chemical composition of AF5 distillate from the aqueous liquid product.

Compound	Relative Content (%)
Carboxylic Acids	
Propanoic acid, 2-methyl-	1.16
Butanoic acid	16.06
Butanoic acid, 3-methyl-	2.43
Butanoic acid, 2-methyl-	1.41
Esters	
Propanoic acid, 2-hydroxy-, ethyl ester, (S)-	0.46
Acetic acid, 2-(dimethylamino)ethyl ester	38.06
2-Propenoic acid, 2-(dimethylamino)ethyl ester	10.31
2-Propenoic acid, 2-methyl-, 2-(dimethylamino)ethyl ester	3.36
Fumaric acid, 2-dimethylaminoethyl heptyl ester	0.84
Butyrolactone	0.82
Amides	
Acetamide, N,N-dimethyl-	8.04
Propanamide, N,N-dimethyl-	0.85
N,N-Dimethylbutyramide	1.00
Lactams	
2-Piperidinone	1.01
2-Pyrrolidinone	2.53
2,5-Pyrrolidinedione, 1-methyl-	5.95
2,5-Pyrrolidinedione, 1-ethyl-	1.49
N-Acetylpyrrolidone	0.61
Acetates	
1,2-Ethanediol, monoacetate	1.95
Ethyl Acetate	1.66

The chemical compositions of bio-oil distillates, on the other hand, are shown in Figure 26 and Table 13. The identified compounds were grouped into the following categories: paraffins, naphthenes, olefins, cycloolefins, alkynes, alcohols, benzene and

heterocyclic compounds (B&HC), esters, acids, ketones, phenolics, amines, nitriles and others. The groups of compounds identified for algal bio-oil distillates were very much different from that of bio-oil derived from lignocellulosic material such as sawdust, which mostly contains oxygenated compounds (i.e. phenols, acids) [46, 87]. Based on Figure 26, all bio-oil distillate fractions contain considerable amounts of saturated paraffins and unsaturated olefins. BF4 has the highest amount of paraffins (43.92%) while BF3 contains the highest amount of olefins (31.96%). Most of the annulenes in the form of cycloheptatriene and cyclooctatetraene are present in BF1 (20.86%) and BF2 (21.96%). BF1, BF2, BF3 and BF4 contain benzene and heterocyclic compounds while BF5 and BF6 contain most of the esters. Most of the oxygen-containing compounds such as carboxylic acids, ketones and phenols are present in BF4, which is consistent with the elemental analysis presented in Figure 23 (Section 4.3.4.2). Nitriles concentration was enriched in BF6, which contains about 80.40% nitriles. The other compound detected in BF1 was levoglucosan, which is typically used as a chemical tracer in thermal treatment of biomass at atmospheric pressure. Wang et al (2009) also detected levoglucosan in the heavy fraction produced from molecular distillation of sawdust bio-oil [45].

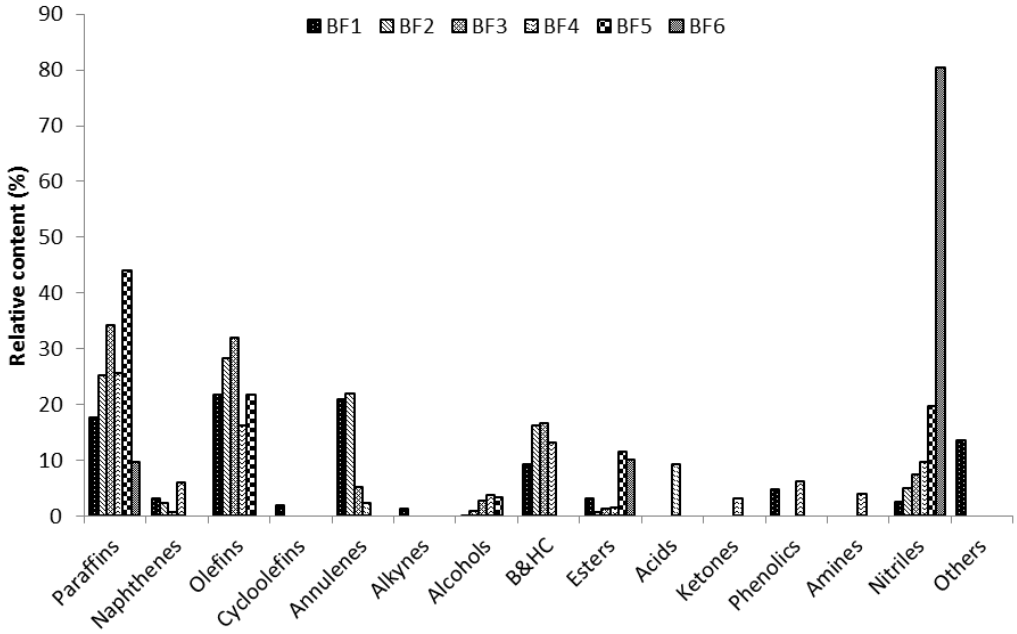

Figure 26. The chemical distribution of algal bio-oil distillates.

The degree of separation of bio-oil components was assessed in terms of separation factor, β. The separation factor was first defined by Guo et al (2010) to define the separation characteristics of typical sawdust bio-oil compounds [48]. In his study, β was calculated as follows:

$$\beta_{m\text{-}n} = M_{m\text{-}n,DF} / (M_{m\text{-}n,DF} + M_{m\text{-}n,RF}) \quad (4.1)$$

where m represents the two distillation processes, n represents the compound in the bio-oil, DF is the distillate fraction, RF is the residual fraction and $M_{m\text{-}n,DF}$ is the weight of the compound in DF calculated using the formula:

$$M_{m\text{-}n,DF} = Y_{m,DF} \times R_n \quad (4.2)$$

where $Y_{m,DF}$ is the yield of DF and R_n is the proportion of the compound n corresponding to the relative content (%). There were only two fractions obtained by Guo et al (2010)

from molecular distillation of sawdust bio-oil. Hence, Equation 4.1 was modified to include all six (6) fractions obtained from the algal bio-oil. The modified equation for separation factor, β, of algal bio-oil distillate fractions is shown in Equation 4.3.

$$\beta = M_{DF} / \sum M_{BFi} \quad (4.3)$$

where M_{DF} is the amount of the component in the boiling point range to which it should be collected, and M_{BFi} is the amount of the component in each distillate fraction where i ranges from 1 to 6.

Based on Guo et al (2010), a separation factor of 1 (β=1) means that the compound has been completely separated in the boiling range where it should be [48]. Additionally, since there are six (6) bio-oil distillates in this study, $\beta > 0.16$ means that the compound is enriched in the distillate fraction where it should belong. β=0, on the other hand, indicate that the compound did not condense in the distillate fraction where it should be. The calculated separation factor, β, for each compound is summarized in Table 13 together with the relative compositions of the each bio-oil distillate fractions. Based on Table 13, most of the higher molecular weight olefins (i.e. tetradecene, hexadecane) and naphthenes were completely separated while phenolic compounds were not condensed in the boiling point range where it should belong. According to Guo et al (2010), phenols and aldehydes are hard to distill [48]. Moreover, most alcohols, nitriles and annulenes were enriched in the distillate fraction where each compound should be. Although it appears that acids, amides and ketones were completely separated based on Figure 26, the distillate fraction where they were condensed does not correspond to the boiling point range where they should be grouped; hence, their separation factors were

either low or zero. This may be attributed to the complexity of the bio-oil. Also, other factors such as heating rate may have a potential effect on the separation of components [47].

Table 13. Chemical compositions and separation factors of bio-oil distillate fractions.

Compound	Relative content (%)						β
	BF1	BF2	BF3	BF4	BF5	BF6	
Paraffins							
Pentane, 2,3-dimethyl-	0	0.28	0	0	0	0	0
Octane	9.09	5.7	0	0	0	0	0.4
Heptane, 2,3-dimethyl-	0.71	0	0	0	0	0	1
Heptane, 2,6-dimethyl-	0.48	0	0	0	0	0	1
Hexane, 2,3,5-trimethyl-	0	0.37	0	0	0	0	0
Nonane	4.47	6.56	2.86	0.74	0	0	0.7
Nonane, 3-methyl-	0.34	0	0	0	0	0	0
Heptane, 3-ethyl-2-methyl-	0	0.22	0	0	0	0	0
Decane	1.44	4.97	6.39	2.52	1.06	0	0.06
Octane, 3,3-dimethyl-	0.37	0	0	0	0	0	0
Decane, 4-methyl-	0	0.58	0.96	0	0	0	0.18
Decane, 2-methyl-	0	0.17	0.73	0	0	0	0.37
Undecane	0.66	2.76	6.51	3.69	0	0	0.13
1-Iodo-2-methylnonane	0	0.11	0.52	0.94	0	0	0.08
Tridecane	0.14	2.25	7.16	6.35	15.38	0	0.04
Undecane, 3-methyl-	0	0	0.43	0	0	0	1
Undecane, 2,6-dimethyl-	0	0.43	1.48	1.67	1.35	0	0.02
Undecane, 2,10-dimethyl-	0	0	0.49	0	0	0	/
Octadecane, 2-methyl-	0	0	0	1.04	0	0	/
Octane, 2,3,7-trimethyl-	0	0.34	0	1.72	0	0	0.79
Dodecane, 2,6,10-trimethyl-	0	0	0	0.58	4.14	0	0.01
Dodecane, 2,6,11-trimethyl-	0	0.17	2.28	0	2.4	0	0.97
Dodecane, 2,7,10-trimethyl-	0	0	0.41	0	0	0	0
Heptadecane, 4-methyl-	0	0	0	0.52	0	0	0
Decane, 2,3,5,8-tetramethyl-	0	0	0	0.66	0	0	1
Octane, 2,6-dimethyl-	0	0	0	0.41	0	0	0
Dodecane, 2,6,11-trimethyl-	0	0	0	1.06	0	0	0
Hexadecane	0	0.24	3.46	3.39	17.1	9.53	0.2
Dodecane	0	0	0	0.26	0	0	1
Dodecane, 4,6-dimethyl-	0	0	0.53	0	0	0	0
Eicosane	0	0	0	0	2.49	0	0

Table 13 continued…

Compound	Relative content (%)						β
	BF1	BF2	BF3	BF4	BF5	BF6	
Naphthenes							
Bicyclo[2.2.1]heptane, 2-methyl-, exo-	0.51	0	0	0	0	0	1
Cyclopentane, 1-methyl-2-(2-propenyl)-, trans-	0.73	0	0	0	0	0	/
Cyclopentane, ethylidene-	1.46	1.55	0	0	0	0	0.29
Cyclopentane, 1-ethyl-2-methyl-	0	0.4	0	0	0	0	0
Cyclopentane, hexyl-	0	0	0.66	0	0	0	/
Cyclopentane, pentyl-	0	0.25	0	0.64	0	0	0
Cyclopropane, 1-heptyl-2-methyl-	0.41	0	0	0	0	0	1
Cyclopropane, 1-methyl-2-octyl-	0	0	0	4.64	0	0	/
Cyclohexane, pentyl-	0	0	0	0.66	0	0	1
Olefins							
1,7-Octadiene	0.13	0	0	0	0	0	0
1-Hexene, 5-methyl-	0.49	0	0	0	0	0	1
1-Octene	8.09	5.32	0	0	0	0	0.39
2-Octene, (E)-	1.53	0.62	0	0	0	0	0.51
2-Octene, (Z)-	0.46	0.28	0	0	0	0	0.41
cis-4-Nonene	0.63	0	0	0	0	0	0
1-Heptene, 2,6-dimethyl-	1.44	1.15	0	0	0	0	0.35
1,8-Nonadiene	0.32	0	0	0	0	0	0
1-Nonene	4.33	6.33	3.1	0	0	0	0.74
3-Nonene, (E)-	0.39	0	0	0	0	0	0
cis-2-Nonene	1.62	2.13	0.58	0	0	0	0.73
4-Dodecene, (E)-	0.55	0	0	0	0	0	0
3,4-Octadiene, 7-methyl-	0	0.4	0.76	0	0	0	/
6-Cyano-1-hexene-	0	0.33	0.84	1.46	0	0	0.07
1-Decene	1.41	5.55	7.75	4.19	0	0	0.1
trans-3-Decene	0	0.29	0.86	0	0	0	0.29
2-Decene, (E)-	0.22	0.89	0	0	0	0	0
2-Decene, (Z)-	0	0	2.61	0	0	0	1
1-Undecene	0.11	2.19	5.51	2.93	0	0	0.14
3-Undecene, (Z)-	0	0.21	0.82	0	0	0	0.35
2-Undecene, (E)-	0	0.51	1.29	1.5	0	0	0.1
2-Undecene, (Z)-	0	0	0.73	0.84	0	0	0.14
2-Tridecene, (Z)-	0	0.77	0	0	0	0	0
3-Tridecene	0	0	0.74	0	0	0	0
5-Tridecene, (E)-	0	0	0	0.83	0	0	1
5-Tridecene, (Z)-	0	0.53	0	0	0	0	0
2-Dodecene, (E)-	0	0	2.83	0	0	0	0
4-Dodecene, (Z)-	0	0.13	0.57	0	0	0	0
5-Dodecene, (Z)-	0	0	0.33	1.01	0	0	0.94

Table 13 continued…

Compound	Relative content (%)						β
	BF1	BF2	BF3	BF4	BF5	BF6	
3-Tetradecene, (Z)-	0	0.54	2.64	3.05	10.59	0	0.03
7-Tetradecene, (E)-	0	0	0	0.21	0	0	0
7-Tetradecene, (Z)-	0	0	0	0.25	4.02	0	0.99
7-Hexadecene, (Z)-	0	0	0	0	0.63	0	1
1-Pentadecene	0	0	0	0	1.42	0	1
3-Hexadecene, (Z)-	0	0	0	0	0.96	0	1
2-Hexadecene, 3,7,11,15-tetramethyl-, [R-[R*,R*-(E)]]-	0	0	0	0	4.04	0	1
Cycloolefins							
Cyclopentene, 1-butyl-	0.49	0	0	0	0	0	0
Cyclohexene, 1-methyl-	1.36	0	0	0	0	0	1
Annulenes							
1,3,5-Cycloheptatriene	18.72	18.05	1.03	0.31	0	0	0.3
1,3,5,7-Cyclooctatetraene	2.14	3.91	4.1	1.86	0	0	0.58
Alkynes							
2-Hexyne, 4-methyl-	1.26	0	0	0	0	0	1
Alcohols							
2-Furanmethanol	0	0	0	2.67	0	0	0
1-Octyn-3-ol, 4-ethyl-	0.52	0	0	0	0	0	1
1-Octanol,2-butyl-	0	0.86	1.69	0.61	0	0	0.55
E-11,13-Tetradecadien-1-ol	0	0	0.97	0	0	0	/
1-Dodecanol	0	0	0	0.51	3.24	0	0.98
Benzene and Heterocyclic Compounds (B&HC)							
Pyrrole	0	1.81	1.39	1.03	0	0	0
1H-Pyrrole, 3-methyl-	0	0	0	0.85	0	0	0
1H-Pyrrole, 1-ethyl-	0.25	0.3	0	0	0	0	/
1H-Pyrrole, 2,4-dimethyl-	0	0	0.77	0	0	0	1
1H-Pyrrole, 2,5-dimethyl-	0	0	0	1.14	0	0	0
1H-Pyrrole, 2,3,5-trimethyl-	0	0	0	0.93	0	0	/
Toluene	0	0	1.23	0	0	0	0
o-Xylene	1.38	2.91	2.54	0	0	0	0.76
Ethylbenzene	3.39	5.24	3.54	1.95	0	0	0.17
Benzene, propyl-	0.44	0.9	1.64	1.75	0	0	0.34
Benzene, 1-ethyl-2-methyl-	0.42	1.41	2.37	0	0	0	0.17
Benzene, 1,2,4-trimethyl-	0	0.63	1.84	1.4	0	0	0.13
Benzene, butyl-	0	0.32	0.86	0	0	0	0.27
Pyridine, 2-methyl-	0	0.12	0	0.49	0	0	0
Pyridine, 3-methyl-	0	0	0.5	0	0	0	0
Pyridine, 2-ethyl-	0	0.05	0	1.32	0	0	0.05

Table 13 continued…

Compound	Relative content (%)						β
	BF1	BF2	BF3	BF4	BF5	BF6	
Pyridine, 2,4-dimethyl-	0	0	0	0.44	0	0	/
Pyridine, 2-ethyl-6-methyl-	0	0	0	1.13	0	0	/
Benzofuran, 2,3-dihydro-	2.32	0	0	0	0	0	0
Indene	0	0	0	0.58	0	0	0
2-Pyrazoline, 1-methyl-4-propyl-	1.06	1.77	0	0	0	0	0.8
1H-Pyrazole, 4,5-dihydro-4,5-dimethyl-	0	0.77	0	0	0	0	/
Esters							
Acetic acid, 2-(dimethylamino)ethyl ester	0	0	0	1.14	0	0	/
Ethyl tridecanoate	1.21	0	0	0	1.98	6.22	0.02
Decanoic acid, methyl ester	0	0	0	0	0	3.85	0
Tridecanoic acid, methyl ester	0	0	0	0	1.31	0	0
Pentadecanoic acid, 14-methyl-, methyl ester	0	0	0	0	8.22	0	0
Hexadecanoic acid, ethyl ester	0	0.41	0.57	0.32	0	0	0.11
(E)-9-Octadecenoic acid ethyl ester	0.81	0.18	0	0	0	0	0
Docosanoic acid, ethyl ester	1.09	0	0	0	0	0	0
Pentafluoropropionic acid, tridecyl ester	0	0	0.74	0	0	0	/
Acids							
Propanoic acid, 2-methyl-	0	0	0	0.38	0	0	0
Hexanoic acid	0	0	0	6.94	0	0	1
Butanoic acid, 3-methyl-	0	0	0	1.91	0	0	0
Ketones							
Ethanone, 1-(2-furanyl)-	0	0	0	0.65	0	0	0
Butyrolactone	0	0	0	1.16	0	0	1
2-Cyclopenten-1-one, 2,3-dimethyl-	0	0	0	1.25	0	0	0
Phenolics							
Phenol	0	0	0	3.72	0	0	0
Phenol, 3-methyl-	0	0	0	2.36	0	0	1
Phenol, 3-ethyl-	0.4	0	0	0	0	0	0
Phenol, 2-ethyl-	0.55	0	0	0	0	0	0
2-Methoxy-4-vinylphenol	1.32	0	0	0	0	0	0
Phenol, 2-methoxy-4-(2-propenyl)-, acetate	2.45	0	0	0	0	0	0
Amines							
Acetamide, N,N-dimethyl-	0	0	0	2.61	0	0	0
6-Amino-6-methylfulvene	0	0	0	1.25	0	0	0
Nitriles							
Pentanenitrile	1.37	1.04	0.28	0.19	0	0	0.58
4,4-Dimethyl-3-oxopentanenitrile	0	0	0.94	0.55	0	0	/

Table 13 continued…

Compound	Relative content (%)						β
	BF1	BF2	BF3	BF4	BF5	BF6	
Pentanenitrile, 4-methyl-	0	1.84	2.02	1.44	0	0	/
Hexanenitrile	0.87	1.22	2.16	2.39	0	0	0.08
Heptanonitrile	0.13	0.74	1.99	2.22	0	0	0.1
Octanenitrile	0	0	0	2.79	1.83	0	0
Tridecanenitrile	0	0	0	0	0	2.87	1
Dodecanenitrile	0	0	0	0	1.69	0	1
Oleanitrile	0	0	0	0	4.02	21.02	0.7
Pentadecanenitrile	0	0	0	0	12.13	51.47	0.66
Heptadecanenitrile	0	0	0	0	0	5.04	0
Others							
Levoglucosan	13.5	0	0	0	0	0	0

4.4. Conclusions

Separation of bio-oil components by fractional distillation was explored in this study to improve the quality of bio-oil distillate fractions and assess their suitability as potential fuel substitutes. The recovery of organic compounds from the aqueous liquid product (ALP) was also done by fractional distillation. Six (6) fractions including the non-distillation residue was obtained from the fractional distillation of bio-oil. Most of the water from the original bio-oil was separated in the bottom layer of the first two fractions (BF1 and BF2) of the bio-oil. Significant reduction in the moisture contents and increase in the heating values of the bio-oil distillates were observed. The heating values of top layer of light fractions (BF1 and BF2) were found to be equal or even higher than that of petroleum-derived heavy fuel oil and fatty acid methyl ester (FAME); additionally, the heating values of other distillates (BF3 – BF6) were higher than the original bio-oil. This was attributed to their low moisture contents, high combustible

components such as carbon and hydrogen and low oxygen contents. GC-MS and FTIR analysis showed that the light fractions (BF1 and BF2) are mainly composed of paraffins, olefins, annulenes, benzene and heterocyclic compounds. Middle fractions (BF3 and BF4), on the other hand, consists mainly of paraffins, olefins, alcohols, benzene and heterocyclic compounds. Most of the oxygenated compounds such as acids, ketones, phenols and amines were condensed in BF4. BF5 was found to have similar properties as the original bio-oil based on its elemental analysis; whereas, BF6 consists mainly of nitriles, esters and paraffins. On the other hand, AF5, a distillate fraction of ALP, was found to have a heating value of about 24 MJ/kg which is higher than wood-derived bio-oil. Aside from its considerable energy content, AF5 contains various components based on GC-MS analysis which could be further processed to produce value-added chemicals. The degree of separation of bio-oil components was evaluated using a separation factor, β. Based on the result, complete separation can be achieved for some compounds such as high molecular weight olefins and naphthenes.

5. UPGRADING OF PYROLYTIC BIO-OIL FROM *Nannochloropsis oculata* OVER HZSM-5 CATALYST

5.1. Introduction

Increasing concerns on the detrimental effects of global warming brought about by greenhouse gas emissions, escalating fuel prices and depleting petroleum reserves stimulated the renewed interest on the use of biomass for fuel production [1-4]. Bio-oil produced from pyrolysis of biomass is a potential feedstock for production of liquid transport fuel components as well as valuable industrial chemicals [28]. There are several limitations, however, on the application of pyrolysis bio-oil as fuel which include its low heating value, high water content, high viscosity, low stability and the presence of heteroatoms such as oxygen and nitrogen [12, 28, 67]. Bio-oil from microalgae, for example, has superior quality compared to wood bio-oils based on heating value and chemical composition; however, its heating value is still lower than traditional transport fuels and the nitrogen content is found to be relatively higher than crude oil [109]. Hence, appropriate upgrading procedure must be done to render the bio-oil suitable for fuel applications.

There are several processes which can be used for the upgrading of bio-oil to transport fuels. Hydrodeoxygenation of bio-oil may be done using typical heterogeneous catalyst (i.e. CoMo, NiMo) at temperatures ranging from 300 to 600^0C with high H_2 pressure. In this process, the oxygen from the bio-oil reacts with H_2 forming water and saturated C-C bonds. Studies on bio-oil upgrading using this method can be found

elsewhere [54-57]. Bio-oil may also be combined with diesel directly with the aid of a surfactant using a process known as emulsification. This process does not require redundant chemical transformations and the bio-oil emulsions have promising ignition characteristics [23, 24]. However, the high cost of surfactant, high energy consumption, and high acidity, low cetane and increased viscosity of the emulsified product limits its application [23, 24]. Moreover, catalytic esterification of bio-oil that contains high amounts of carboxylic acids may be done using various combinations of acid catalysts and alcohols [25, 26, 51-53, 110].

Zeolite upgrading, on the other hand, utilizes a crystalline microporous material (zeolite), which contains active sites for the dehydration, cracking, polymerization, deoxygenation and aromatization of bio-oil components. This shape-selective catalyst with intermediate pore size of about 5.5×10^{-10} m largely favors hydrocarbons with less than ten carbon atoms [27]. Upgrading using zeolite such as HZSM-5 as catalyst typically occurs at temperatures ranging from 350 to 500^0C at atmospheric pressure. This process was already tried to lignocellulosic bio-oils from beech wood [61], rice husk [62], sawdust [63] and anisole, which is a typical component of bio-oil [64]. Catalytic pyrolysis of *Nannochloropsis oculate* over HZSM-5 catalyst was also explored by Pan et al (2010). Bio-oil with lower oxygen content and higher heating value was obtained from HZSM-5 catalyzed pyrolysis compared to direct pyrolysis without catalyst [20]. Carrero et al (2011), on the other hand, explored the applicability of various zeolites (ZSM-5, Beta, h-ZSM-5 and h-Beta) as heterogeneous catalyst for biodiesel production from lipids extracted from *Nannochloropsis gaditana* [65]. Zeolite

catalyst can also be impregnated with metals such as gallium, nickel, platinum, palladium, etc. Thangalazhy-Gopakumar et al (2012) studied the catalytic pyrolysis of pine wood using HZSM-5 and metal-impregnated zeolites in a hydrogen environment, which was referred to as hydro-pyrolysis. At low H_2 pressures (100-300psi), HZSM-5 was found to be more active than the metal-impregnated zeolite; whereas, at higher pressures (400 psi), more hydrocarbons were produced using metal-impregnated HZSM-5. About 42.5% wt of biomass carbon was converted to hydrocarbons using hydropyrolysis with HZSM-5. Based on his study, HZSM-5 had higher activity than impregnated metals, which indicate that deoxygenation due to cracking was the major reaction occurring during catalytic pyrolysis and no or minimal hydrogenation of aromatic hydrocarbons occurred. Aromatic selectivity of major hydrocarbons such as toluene, xylene and benzene was also not affected by the addition of metals [27]. Adjaye and Bakhshi (1995), on the other hand, compared the effectiveness of different catalyst (HZSM-5, H-Y, H-mordenite, silicalite, and silica-alumina) to increase the hydrocarbons yield in the organic distillate fraction (ODF) from fast pyrolysis maple wood bio-oil using a fixed-bed micro-reactor [66]. The highest hydrocarbons yield of about 27.9% wt was obtained from HZSM-5. Low amounts of oxygenated compounds (alcohols, ketones and phenols) were detected, which indicated the effectiveness of conversion of these compounds to hydrocarbons. Also, the presence of the catalyst reduced the formation of char during HZSM-5 treatment [66].

Typical HZSM-5 usage includes cracking of organic compounds at atmospheric pressure. However, high hydrogen pressure promotes hydrogenation of free radicals or

fragments which suppresses coke formation due to condensation and polymerization reactions [27]. Aside from that, treatment with HZSM-5 at high pressure H_2 can greatly reduce the amount of heteroatoms (O, N and S) in the oil [28]. Based on Li and Savage (2013), the N/C ratio of the crude bio-oil from hydrothermal liquefaction of *Nannochloropsis sp* was reduced to about 25% of the original N/C ratio while the O/C ratio was also an order of magnitude lower than the original after HZSM-5 upgrading under 4.3MPa hydrogen pressure.

Based on previous studies, upgrading of bio-oil using HZSM-5 catalyst under H_2 pressure can be employed to reduce the heteroatoms present in the bio-oil while improving its heating value. Hence, in this study, HZSM-5 was used as catalyst for upgrading of bio-oil derived from pyrolysis of *Nannochloropsis oculata.* The effectiveness of HZSM-5 upgrading at various combinations of temperature and reaction time in hydrogen environment was evaluated based on product yield, characteristics of the upgraded bio-oil, degree of deoxygenation, turnover frequency and hydrogen consumption. Also, the products formed and the compositions of the original and upgraded bio-oils were used to identify the potential mechanism of reaction over HZSM-5 as catalyst.

5.2. Materials and Method

5.2.1. Materials

The bio-oil used in this study was obtained from pyrolysis of *Nannochloropsis oculata*, which was obtained from the Texas Agri-Life Research Algae Pond Facility in

Pecos, Texas. The *N. oculata* samples were oven-dried to less than 10% wt moisture and ground (0.28mm) before pyrolysis. Pyrolysis was done using a pressurized fixed-bed batch-type reactor at 540^0C and 0psig (atmospheric pressure) as described in previous papers [109]. The zeolite ZSM-5 catalyst in 1/16 trilobe extrudate form was obtained from Tricat Industries Inc. It has a surface area of about 335 m^2/g and pore volume of about 0.37 cm^3/g. The catalyst was calcined in air at 550^0C for 4h to convert it to the hydrogen form HZSM-5 prior to use. The hydrogen gas used (UHP grade) was obtained from Airgas Distribution Inc.

5.2.2. Upgrading experiment

Figure 27 illustrates the set-up for the upgrading experiments. A 50-mL Micro Robinson-Mahoney catalytic reactor from Autoclave Engineers was used. Maximum pressure for the reactor was about 5000 psi at 650^oF (343^oC). Gases flow into and from the reactor through 1/8 in o.d. stainless steel tubing. An internal stirrer attached to a motor drive operated at approximately 500rpm was used to ensure the uniformity of the temperature inside the reactor. The temperatures inside the reactor and at the interface of reactor and heater were measured by thermocouples attached to a temperature controller. Pressure gauge with maximum reading of 5000 psi measures the pressure inside the reactor.

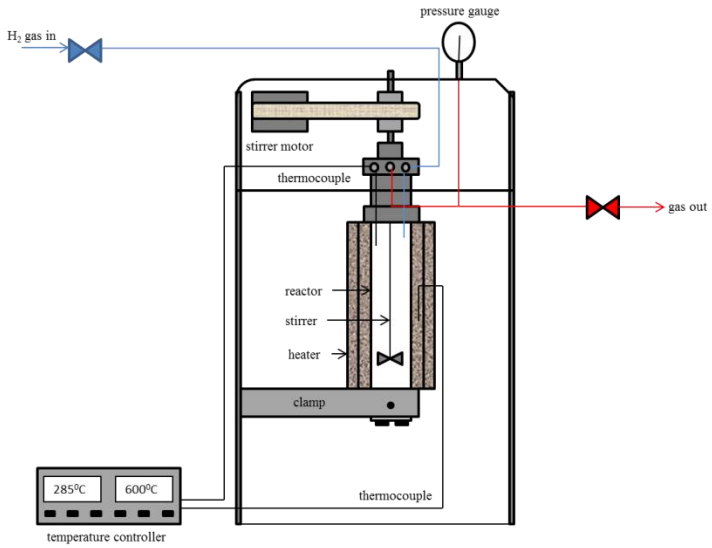

Figure 27. Experimental set-up for catalytic upgrading.

Upgrading runs were carried out subsequent to a response surface method (RSM) central composite experimental design (CCD) as shown in Table 14. Reaction temperature (200-300^{0}C) and reaction time (1-4h) served as the main factors.

Table 14. Summary of experimental runs for catalytic upgrading.

Run	Temp (^{0}C)	Time (h)
1	250	4
2	250	1
3	215	3.5
4	285	1.5
5	250	2.5
6	250	2.5
7	285	3.5
8	250	2.5
9	300	2.5
10	250	2.5
11	200	2.5
12	215	1.5
13	250	2.5

For a typical experiment, about 10 g of bio-oil was charged into the reactor together with approximately 1 g HZSM-5 (10% wt). The reactor was tightly closed and flushed with H_2 gas at 200 psi for 10 mins to ensure the removal of air inside the reactor. Then, about 600 psi H_2 gas was charged into the reactor at room temperature. The reactor was then heated to the desired temperature and allowed to proceed at that temperature for the corresponding reaction time as specified in Table 1. After the reaction time elapsed, the reactor was allowed to cool down to room temperature. The pressure inside the reactor at room temperature was recorded and used to calculate the amount of H_2 used and the yield of gas components. Gas samples were collected using 0.5L Tedlar sampling bags with combination valve. The liquid product was collected from the reactor using a pipette then the HZSM-5 was collected from the basket. The inner surface of the reactor and stirrer were washed with acetone then the washings were filtered using a pre-weighed filter paper. The residue remaining on the filter paper was defined as char while the acetone-soluble filtrate was defined as tar. The amount of coke was determined by calculating the difference between the initial and final mass of the HZSM-5 catalyst.

5.2.3. Product analysis

The liquid product obtained from the upgrading experiments were collected in small glass vials and analyzed immediately for their chemical composition and properties. Heating values of the distillate samples was determined using PARR isoperibol bomb calorimeter (Model 6200, Parr Instrument Company, Moline, IL) following ASTM D2015. Ultimate analysis was determined using Vario MICRO

Elemental Analyzer (Elementar Analysemsysteme GmbH, Germany) in accordance with ASTM D 3176. Moisture content was analyzed by following ASTM E203 using KF Titrino 701 (Metrohm, USA, Inc). The chemical composition of the upgraded bio-oil was also determined by GC-MS analysis using Shimadzu QP2010 Plus, with the following parameters: bio-oil dissolved in dichloromethane (10 %vol); column – ZB-5ms (30m length, 0.25μm thickness and 0.25mm diameter); column temperature program: 40^0C (held for 5 minutes) then ramped to 260^0C at 5^0C/min, then held for 5 minutes at 260^0C; ion source temperature at 220^0C. The functional groups present in the bio-oil were also determined using Shimadzu IRAffinity-1 FTIR (Fourier Transform Infrared) Spectrophotometer (Shimadzu, Inc).

5.2.4. Data analysis

The effectiveness of the upgrading process was evaluated using the degree of deoxygenation (DOD), which was calculated using Equation 5.1.

$$\%DOD = (O_{feed} - O_{product}) \times 100 / O_{feed} \quad (5.1)$$

where O_{feed} represents the % wt of oxygen in the bio-oil feed, and $O_{product}$ is the % wt of oxygen in the liquid product obtained. The percent by weight of oxygen was calculated by difference from the elemental composition.

Hydrogen consumption, on the other hand, was calculated using Equation 5.2 as shown below:

$$H_2 \text{ consumption} = (n_{H2,\ initial} - n_{H2,final}) \times (22.4Nl/mole)/ \text{ wt bio-oil} \quad (5.2)$$

Where

$$n_{H2,\ initial} = (V_{gas\ cap} \times P_{initial})/\ (R \times T_{initial}) \quad (5.3)$$

$$n_{H2,\ final} = (X_{H2,final} \times V_{gas\ cap} \times P_{final})/\ (R \times T_{final}) \quad (5.4)$$

$n_{H_2,initial}$ = initial amount of hydrogen (in moles) in the reactor
$V_{gas\ cap}$ = volume of the reactor that is not occupied by the liquid
$P_{initial}$ = initial pressure in the reactor
R = gas constant
$T_{initial}$ = initial temperature in the reactor
$n_{H_2,final}$ = amount of hydrogen (in moles) in the reactor after the reaction
$X_{H_2,final}$ = mole fraction of the hydrogen in the gas cap after reaction
P_{final} = pressure in the reactor after the reaction
T_{final} = final temperature in the reactor

Lastly, the turn over frequency (TOF), which represents the moles of hydrogen consumption per gram of catalyst used per time, were estimated using Equation 5.5.

$$\text{TOF (in moles/g catalyst-hr)} = (n_{H2,initial} - n_{H2,final})/(\text{wt catalyst} \times \text{reaction time}) \quad (5.5)$$

5.3. Results and Discussion

5.3.1. Product yields

Similar to the original bio-oil, the liquid product from HZSM-5 upgrading consisted of two immiscible layers, namely, the aqueous fraction and the dark-brown organic fraction. The aqueous layer, which settled at the bottom of the container, was separated using a microsyringe. The upgraded bio-oil (UPBO) considered in this study is the dark-brown fraction produced from the catalytic reaction of bio-oil with HZSM-5 as the catalyst. Figure 28 shows the response surface of UPBO yield at different combinations of reaction temperature and time. Based on statistical analysis using

ANOVA at 95% confidence level (α=0.05), the reaction temperature significantly affects the yield of UPBO (p-value = 0.0005) while reaction time is not significant (p-value = 0.0624). As can be seen from Figure 28, the yield of UPBO decreased as temperature was increased. This trend is similar to that observed by Savage et al (2013) for the upgrading of bio-oil from hydrothermal liquefaction [28]. Maximum yield was about 86% wt at 215^{0}C and 1.5 h while the lowest yield was approximately 44.5% wt at 300^{0}C and 2.5 h. The decrease in UPBO yield could be attributed to the increased conversion of bio-oil into other by-products such as char, coke, tar and gas at higher temperatures.

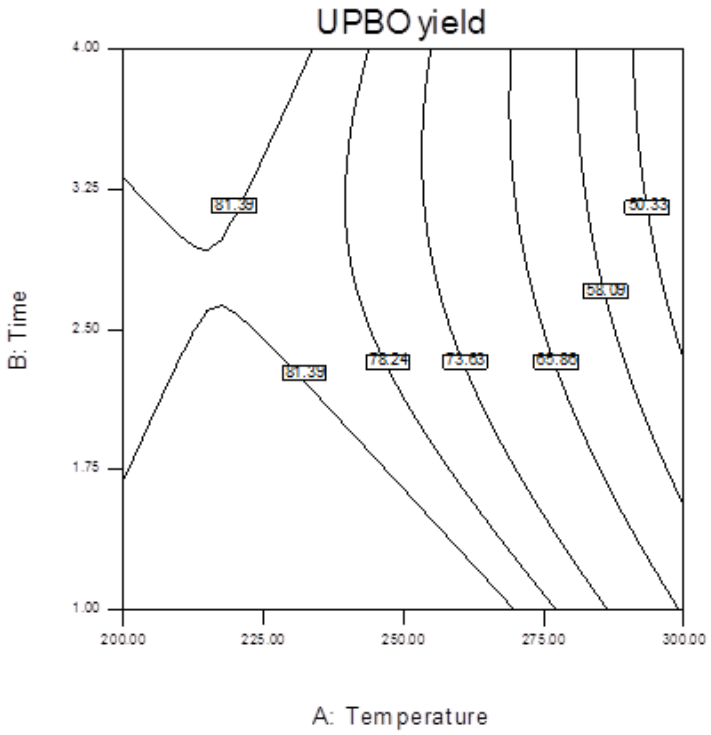

Figure 28. UPBO yield at different temperatures and reaction time.

The by-products considered in this paper include the aqueous liquid layer, tar, coke, char, and gaseous product. The response surface graphs for these by-products are shown in Figure 29. The characteristics of these by-products (except gas) were not considered in this paper and only the main product, UPBO, was further analyzed. However, knowledge on the conversion of bio-oil to other products may also be useful. As mentioned earlier, the aqueous product was a fraction of the liquid product from the upgrading process. Similar to UPBO, temperature also significantly affected the yield of the aqueous fraction (p-value = 0.0005). Based on Figure 29, aqueous yield significantly increased to a certain extent as temperature was increased indicating higher degree of dehydration of the bio-oil at higher temperatures. No aqueous liquid layer was formed at 200^0C and 215^0C while highest yield could be obtained around 275^0C. The yield of the gaseous products that evolved during the reaction was also estimated using the ideal gas law, the composition of the gas and densities of gas components. Figure 29 shows that gaseous product yield tended to increase as temperature was increased similar to that observed by Savage et al (2013) and Vitolo et al (1999) [28, 111]. This could indicate that the rates of HZSM-5 catalyzed and thermal cracking reactions increased with temperature [28]. Higher temperatures favored the catalysis of cracking reactions thus increasing gas production. Also, according to Vitolo et al (1999), the increase in temperature may have favored gasification of the tar that had been formed [111]. Hence, the maximum gas yield (4.75% wt) was recorded at the highest reaction temperature (300^0C, 2.5 h). Coke, on the other hand, was the substance that deposited on the surface of the catalyst. Maximum yield of about 12.7% wt was obtained at 300^0C and 2.5 h. As

can be seen from Figure 29, coke yield tended to increase as temperature was increased. This may be due to aromatization/polymerization reactions at higher temperatures resulting in an increasing yield of coke [111]. However, the model was found to be insignificant (p-value = 0.1076). Char is the solid fraction obtained from the catalytic reaction of the bio-oil, which was measured by filtering the acetone-washings as mentioned in Section 5.2.2. Temperature significantly affected char yield (p-value = 0.0047) and the highest yield of about 2.5% wt was obtained at 285^0C and 3.5 h. Char yield tended to increase as temperature was increased. The formation of char indicates the unstable nature of pyrolysis bio-oil and higher oxygen content in the bio-oil feed tends to produce higher amounts of char. Compared to ligno-cellulosic bio-oils, the bio-oil from *N. oculata* has lower oxygen content; hence, has lesser tendency to form char. Also, the presence of catalyst (HZSM-5) may reduce the amount of char [66]. According to Vitolo et al (1999), lower residence times also produce less char [111]. Lastly, the tar considered in this study is the acetone-soluble portion of the washings from the reactor after collecting other products. Since almost all of the remaining substances in the reactor were observed to be acetone-soluble, tar was then calculated by difference. Based on statistical data, both temperature (p-value = 0.0002) and reaction time (p-value = 0.0089) significantly affect tar production. The highest yield (27% wt) was observed at 285^0C and 3.5 h while the lowest yield (5.6% wt) was obtained at 215^0C and 1.5 h. Among other by-products, tar has the highest percentage yields; thus, it can be considered as the secondary product next to the main product, UPBO. Unlike UPBO, tar increased as temperature and reaction time were increased. In Vitolo et al (1999),

however, tar decreased with temperature, which was attributed to its conversion to gas at higher temperatures [111].

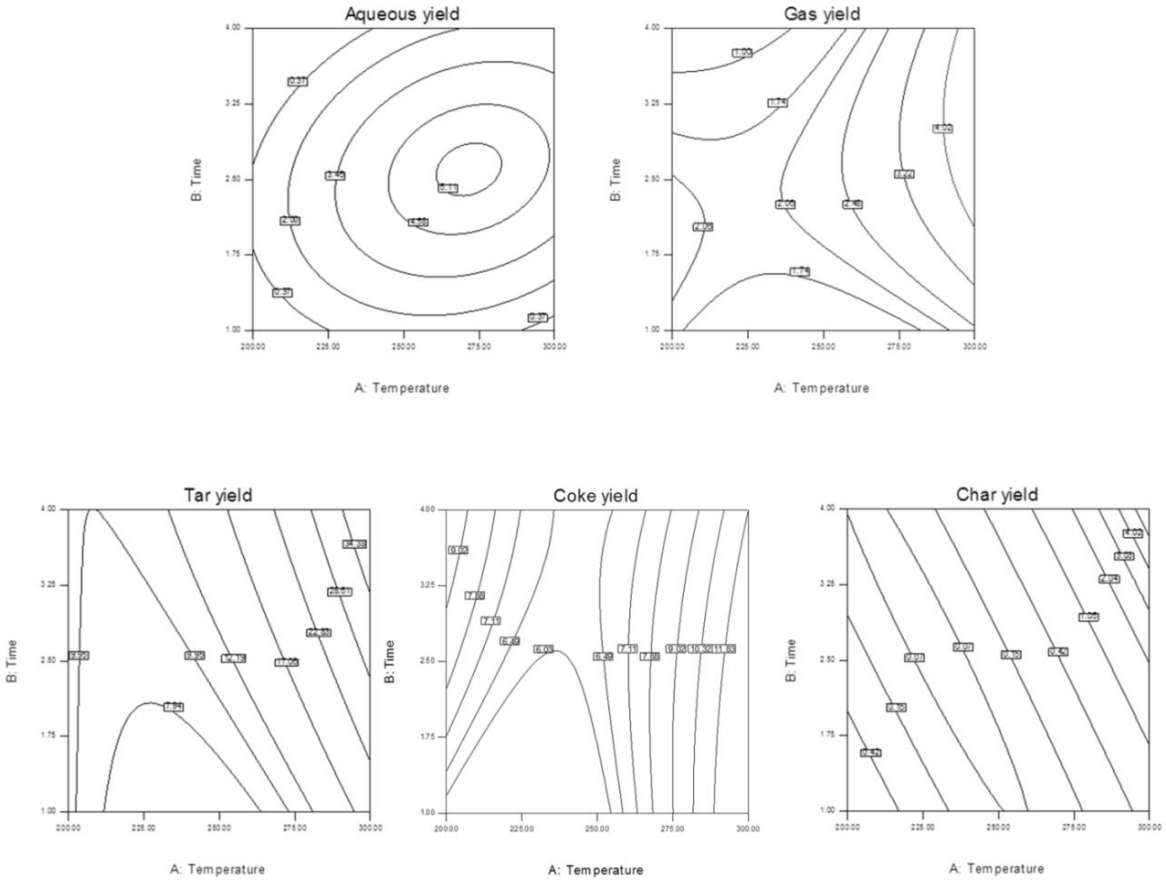

Figure 29. By-products yields at different temperatures and reaction time.

Further inspection of the products yields revealed that UPBO yield could be linearly related to tar yield as shown in Figure 30. In Vitolo (1999), oil yield was related linearly to char yield [111]. The negative slope in this plot indicates the negative correlation between UPBO and tar yields, which means that UPBO yield was higher at lower tar yields and vice versa. This may be attributed to the polymerization of bio-oil

components leading to the tar conversion rather than hydrocarbons production in the UPBO.

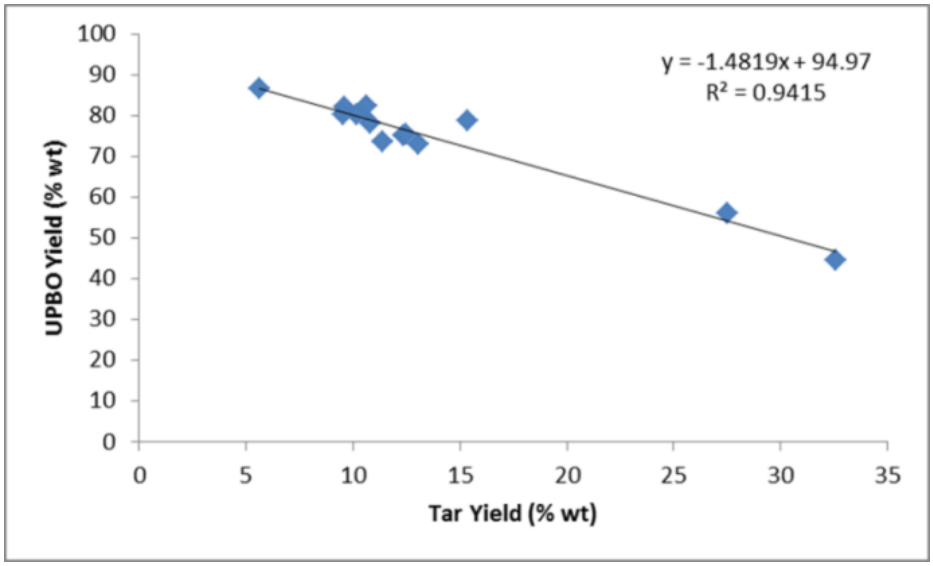

Figure 30. UPBO versus tar yield.

The yield of UPBO was also plotted against gas yield as shown in Figure 31. Similar to tar, gas production has a negative correlation with UPBO yield, which means that UPBO yield was higher at lower gas yields and vice versa. This may be attributed to further cracking of bio-oil forming incondensable gaseous products during the upgrading process. The composition of the gas product will be discussed in a later section to further explore on the conversion of bio-oil into gaseous product.

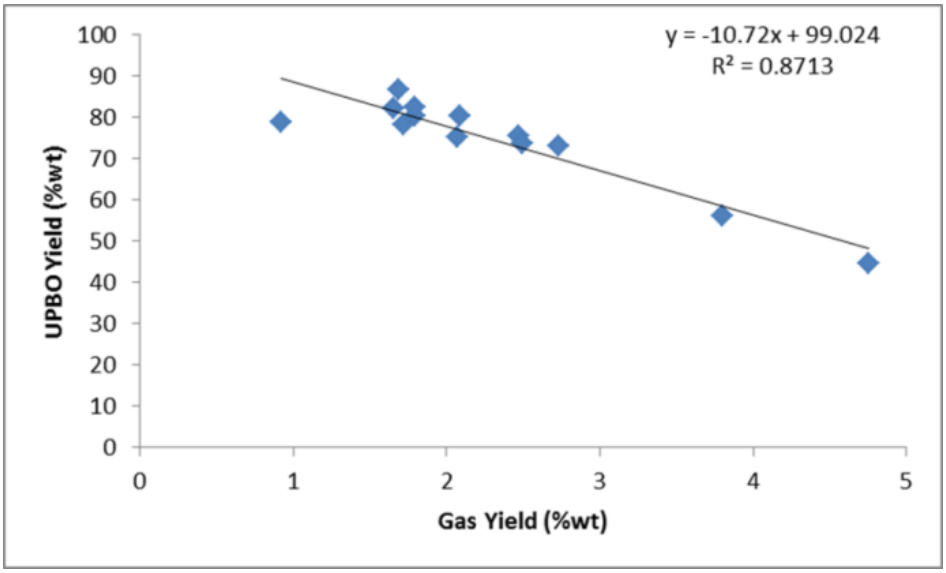

Figure 31. UPBO versus gas yield.

5.3.2. Characteristics of upgraded bio-oils

The composition and properties of the upgraded bio-oils were analyzed and compared to the original bio-oil and conventional fuels to evaluate the potential use of the upgraded product.

5.3.2.1. Moisture content and pH

Table 15 summarizes the moisture contents and pH values of the UPBOs obtained from different reaction conditions in the order of increasing temperatures. The moisture content of the upgraded bio-oils generally decreased with temperature. From moisture content of about 5.92% wt of the original algal bio-oil, complete dehydration was achieved after treatment at 250^0C for 4 h, and at 285^0C for 1 h and 3.5 h. The pH of the bio-oil, on the other hand, generally increased as temperature is increased. This may be due to significant reduction in oxygen-containing compounds such as acids, which

balances the basic nature of nitrogenous compounds in the bio-oil such as nitriles and amides. The original bio-oil is slightly basic in nature due to the presence of nitrogenous compounds such as pyrrole, which is a weak base. It may also be important to note that the pH values of the original algal bio-oil and upgraded bio-oils were very much different from that of lignocellulosic bio-oils (pH 2-3) [87].

Table 15. Moisture contents and pH values of the algal bio-oil and upgraded bio-oils.

Sample	No.	Temp (^{0}C)	Time (hrs)	Moisture (%wt)	pH
Algae bio-oil		---	---	5.92	7.8
	1	200.00	2.50	3.86	7.7
	2	215.00	1.50	3.25	7.9
	3	215.00	3.50	1.84	7.6
	4	250.00	1.00	2.76	7.9
Upgraded bio-oil	5	250.00	2.50	2.15	8.6
	6	250.00	4.00	nd	7.9
	7	285.00	1.50	nd	8.4
	8	285.00	3.50	nd	8.8
	9	300.00	2.50	2.62	8.9

5.3.2.2. Elemental composition and heating value

The elemental composition and heating values of algal bio-oil, UPBOs and conventional transport fuels are summarized in Table 16. Based on the table, generally, the carbon content of the UPBOs increased with temperature (p-value = 0.0085). The initial carbon content of the algal bio-oil was about 72% wt. This increased to about 80% wt at 285^{0}C after 3.5 h reaction time. This value is higher than biodiesel and only slightly lower than crude oil but still lower than gasoline and diesel fuel. The hydrogen content, on the other hand, slightly increased with temperature (p-value = 0.0014). A

moderate increase in hydrogen content was also observed by Li and Savage (2013) for HZSM-5 treatment of hydrothermal liquefaction bio-oil under H_2 pressure. One of the heteroatoms that need to be removed from the bio-oil is nitrogen since it can be converted to NOx and N_2O during combustion causing adverse environmental effects (i.e. acid rain, photochemical smog). The original bio-oil contains about 7.75% wt of nitrogen, which can be attributed to the high protein content (24% wt) of *N. oculata.* Based on Table 16, removal of nitrogen by HZSM-5 upgrading ranged from 13-25%, however, the final nitrogen content is still relatively higher than crude oil. Hence a secondary process to further remove the nitrogen present in the bio-oil may be necessary. Desulfurization, on the other hand, was maximum (87%) at 250^0C and 1 h reaction time. However, no trend was observed with regards to sulfur removal. The original bio-oil contains about 10.14% wt oxygen. Although this value is very much lower than typical bio-oils from lignocellulosic materials (35-40% wt), further reduction in oxygen content may still be required to improve the quality of the bio-oil. Low oxygen content of the bio-oil is desirable since oxygen causes several disadvantages. These disadvantages include (1) low energy density, (2) immiscibility with hydrocarbons, and (3) instability of the bio-oil [67]. Based on Table 16, highest deoxygenation of about 65% was achieved at 285^0C and 3.5 h. At this condition, the oxygen content of the UPBO was only about 3.42% wt, which is almost equivalent to that of crude oil (3.59% wt). This value is also very much lower than conventional biodiesel, which contains about 11% wt oxygen. However, complete deoxygenation should be done by further processing of the UPBO to achieve gasoline and diesel fuel

quality. Due to the significant reduction in oxygen content and increase in carbon content, the heating value of the bio-oil was improved from 36 MJ/kg to about 40 MJ/kg after upgrading at 285^{0}C for 3.5 h. This value is comparable to crude oil and biodiesel but still slightly lower than gasoline and diesel fuel.

Table 16. Comparison on elemental compositions and heating values of algae bio-oil, upgraded bio-oils and petroleum-derived fuels.

Sample	No.	Temp (^{0}C)	Time (hrs)	C (%wt)	H (%wt)	N (%wt)	S (%wt)	O (%wt)	HV (MJ/kg)
Algae bio-oil	---	---	---	72.32	9.64	7.75	0.15	10.14	35.87
Upgraded bio-oil	1	200	2.5	75.26	10.21	6.14	0.14	8.25	37.47
	2	215	1.5	76.28	10.33	6.23	0.12	7.04	37.94
	3	215	3.5	74.07	10.26	6.19	0.17	9.31	38.28
	4	250	1.0	77.09	10.14	6.55	0.02	6.19	38.31
	5	250	2.5	78.00	10.09	5.86	0.07	5.98	39.47
	6	250	4.0	76.64	10.23	6.17	0.06	6.91	38.48
	7	285	1.5	78.19	10.10	6.26	0.12	5.34	39.58
	8	285	3.5	80.48	9.76	6.27	0.06	3.42	39.89
	9	300	2.5	77.09	9.30	6.71	0.13	6.76	39.57
Crude oil	---	---	---	81.96	10.49	2.62	1.34	3.59	40.00
Gasoline[a]	---	---	---	88.00	12.00	0.00	0.00	0.00	46[c]
Diesel fuel[b]	---	---	---	87.00	13.00	0.00	0.00	0.00	45[c]
Biodiesel[b]	---	---	---	77.00	12.00	0.00	0.00	11.00	40[c]

[a] adapted from API Publication No. 4261[112].

[b] adapted from J. Tuttle and T. von Kuegelgen [113].

[c] adapted from GREET Model, Argonne National Laboratory [114].

Major source: American Petroleum Institute (API), Alcohols and Ethers, Publication No. 4261, 3rd ed. Washington DC, June 2001, Table B-1 [105].

The UPBOs were further compared to traditional transport fuels, crude oil and original algal bio-oil using the van Krevelen diagram as shown in Figure 32. According to McKendry (2002), biofuels can be compared to fossil fuels using atomic O:C and H:C ratios, known as the Van Krevelen diagram [81, 82]. Higher energy content fuels can be found near the y-axis since this region represents low O:C ratio. Higher O:C ratio

decreases the energy value of a fuel due to the lower energy contained in the C-O bonds compared to C-C and C-H bonds. Based on Figure 32, the bio-oil obtained from algae is comparable to biodiesel based on the H:C vs O:C plot. Different treatments in bio-oil upgrading using HZSM-5 as catalyst tended to approach the crude oil region. The upgraded bio-oil obtained at 285^{0}C after 3.5 h reaction was found to be almost similar to crude oil based on the van Krevelen diagram. However, this bio-oil is still not comparable to traditional transport fuels such as gasoline and diesel. Nonetheless, fractional distillation (similar to crude oil refining) may be done to obtain fractions of the upgraded bio-oil, which may be similar to gasoline and diesel. Co-processing of UPBO with crude oil may also be explored.

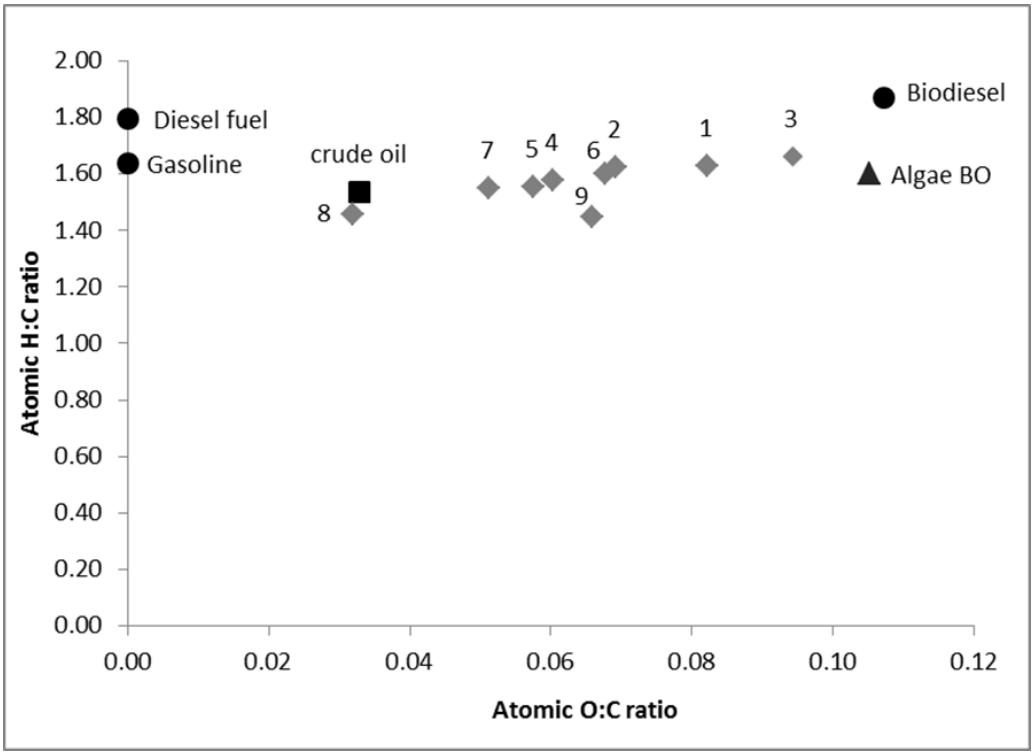

Figure 32. van Krevelen diagram for upgraded bio-oils.

5.3.2.3. FTIR analysis

Fourier Transform Infrared (FTIR) spectrophotometer was used to identify the functional group compositional analysis of the UPBOs and algal bio-oil. This non-destructive technique was also used to determine the groups of compounds present in pyrolytic oils [84-87, 89, 90]. Figure 33 shows the FTIR spectra of the UPBOs and algal bio-oil. Based on the figure, the FTIR spectra for the algal bio-oil and UPBOs (except Run 7 or 285^0C for 3.5 h) follow the same pattern but their magnitudes of peak absorbances vary. Table 17 shows the band positions (in cm^{-1}) of functional groups. For the algal bio-oil and most of the UPBOs, the distinct peak absorbances in 3200-2800cm^{-1} and 1470-1350 cm^{-1} indicate the presence of alkanes. Some phenols, alcohols and amides may also be present based on the wide peak in the 3600-3170 cm^{-1} range. Ketones, aldehydes, carboxylic acids and esters may also be present based on the peaks detected at 1750-1650 cm^{-1}. The peak absorbance in 1660-1630 cm^{-1}, on the other hand, suggests the presence of unsaturated aliphatics or alkenes while the presence of aromatic compounds may be deduced from the peak absorbances in the 975-525 cm^{-1} region. Compared to the original algae bio-oil and other UPBOs, the upgraded bio-oil obtained at 285^0C for 3.5 h (UPG Run 7) may contain higher amounts of aromatics (975-525cm^{-1}), alkanes (1470-1350 cm^{-1}) and phenols (3600-3200 cm^{-1}) based on their peak absorbances.

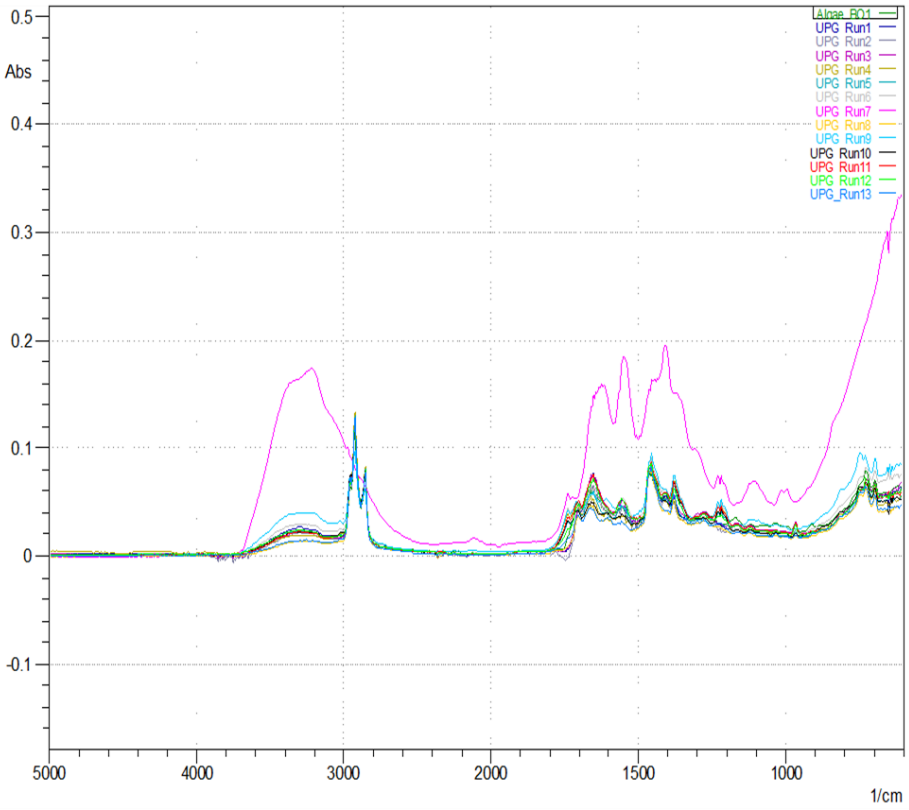

Figure 33. FTIR spectra for algae bio-oil and upgraded bio-oils.

Table 17. Band position for different functional groups in UPBO.

Band position (cm^{-1})	Vibration	Functional group
3600-3200	O-H stretching	Phenols, polymeric O-H, water impurities
3370-3170	NH_2 stretching	Amides
3200-2800	C-H stretching	Alkanes
2250-2000	C≡C, C≡N	Alkynes, Nitriles
1750-1650	C=O stretching	Ketones, aldehydes, carboxylic acids, esters
1660-1630	C=C stretching	Alkenes
	NH_2 scissors	Amides
1470-1350	C-H deformation	Alkanes
1310-1250	C-C-O stretching	Esters
1300-950	C-O stretching	Primary, secondary, tertiary alcohols, phenols
975-525	O-H bending	Mono-, polycyclic, substituted aromatic rings
	C=C stretching	

5.3.2.4. Chemical composition

The chemical composition of the algal bio-oil and UPBO obtained at 285^0C and 3.5 h were analyzed using gas chromatography coupled with mass spectrometry (GC-MS) to identify the potential mechanism of reaction. Only the UPBO obtained at the best operating condition (285^0C, 3.5 h) based on the properties discussed earlier was analyzed and compared to the original bio-oil feedstock. Figure 34 compares the groups of chemical compounds present in the algal bio-oil and UPBO. It clearly shows that saturated aliphatics (i.e. paraffins, naphthenes) significantly increased after HZSM-5 upgrading at 285^0C for 3.5 h; whereas, olefins content decreased. Benzenes and aromatic compounds also increased considerably. On the other hand, the amount of oxygenated compounds such as alcohols, acids, esters, aldehydes and ketones significantly decreased after upgrading. The phenol contents of algal bio-oil and UPBO were almost at the same level (2%). The reduction in oxygenated compounds in the bio-oil was also evident in the ultimate analysis discussed in Section 5.3.2.2. Nitrogenous compounds, which include nitriles and amides, were reduced after catalytic reaction with HZSM-5. This is consistent with the results of the ultimate analysis wherein significant reduction in nitrogen content (20%) was observed.

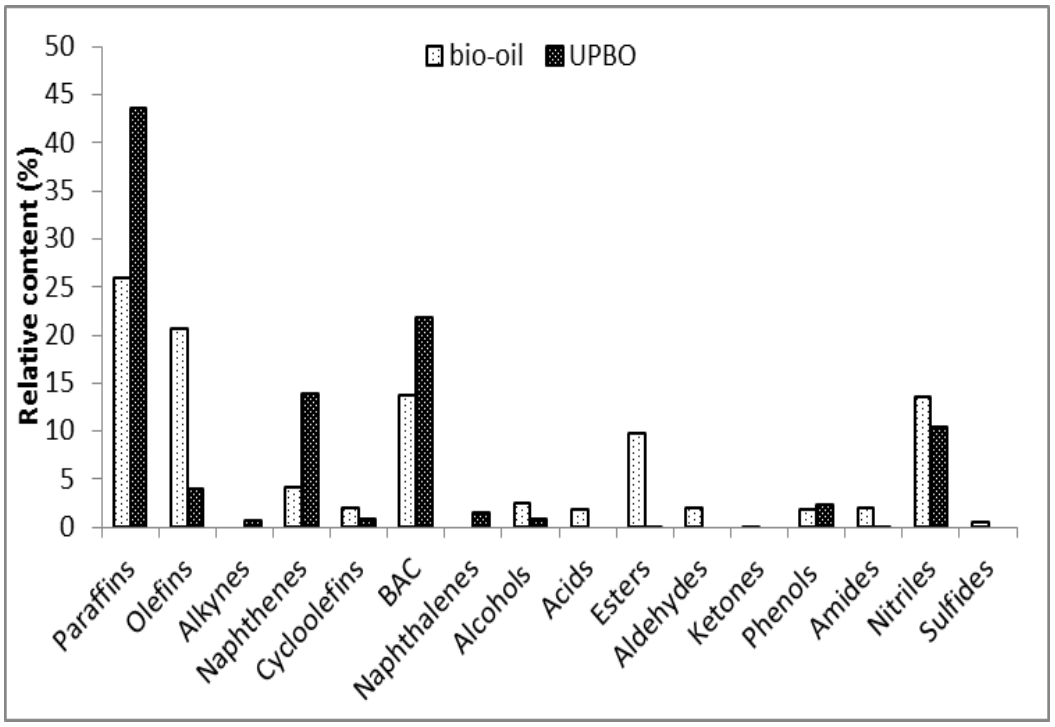

Figure 34. Comparison of chemical composition of algal bio-oil and upgraded bio-oil at 285^{0}C and 3.5 h.

Table 18 summarizes the major hydrocarbons detected in algal bio-oil and UPBO (285^{0}C, 3.5 h). Algal bio-oil originally contains about 26% paraffins, 20% olefins, 4% naphthenes and 2% cycloolefins. After HZSM-5 upgrading at 285^{0}C for 3.5 h, the upgraded bio-oil consisted of 44% paraffins, 3% olefins, 0.61% alkynes, 14% naphthenes and 0.71% cycloolefins. The selectivity of the HZSM-5 catalyst over C_6-C_{15} hydrocarbons was also observed as can be seen in Figure 35. Based on the figure, most of the paraffins and naphthenes produced were in the C_6-C_{15} range. The amount of olefins, on the other hand, significantly decreased, however, the remaining olefin compounds were also in the range of C_6-C_{15}.

Table 18. Hydrocarbon compounds in algal bio-oil and upgraded bio-oil at 285^{0}C and 3.5 h.

Compound	Relative Content (%)		Compound	Relative Content (%)	
	Bio-oil	UPBO (285ºC, 3.5 h)		Bio-oil	UPBO (285ºC, 3.5 h)
Paraffins			2-Undecene, (E)-	---	0.36
Propane, 2-nitro	---	0.6	2-Undecene, (Z)-	0.25	---
Propane, 2-methyl-2-nitro-	---	0.34	1-Dodecene	1.49	---
Propane, 2-bromo-2-methyl-	0.19	---	2-Dodecene, (Z)-	0.4	---
Heptane, 3-methyl-	---	0.24	1-Tridecene	3.83	0.86
Octane	2.43	5.14	3-Tetradecene, (Z)-	---	0.64
Heptane, 2,6-dimethyl-	---	0.56	5-Tetradecene, (E)-	0.35	---
Octane, 2-methyl-	---	0.36	7-Tetradecene	0.81	---
Octane, 3-methyl-	---	0.57	3-Hexadecene, (Z)-	0.2	---
Nonane	2.16	4.96	1-Pentadecene	0.81	---
Nonane, 3-methyl-	---	1.02	8-Heptadecene	1.04	---
Nonane, 2-methyl-	---	0.37	9-Octadecene, (E)-	0.95	---
Octane, 2,6-dimethyl-	---	1.14	3-Octadecene, (E)-	0.27	---
Decane	1.97	4.61	2-Hexadecene, 3,7,11,15-tetramethyl-	1.42	---
Heptane, 2,5,5-trimethyl-	0.19	---			
Nonane, 2,6-dimethyl-	---	0.34	***Alkynes***		
Undecane	2.13	4.3	3-Octyne, 2-methyl	---	0.61
Heptadecane, 2,6,10,15-tetramethyl-	---	0.74			
Tridecane	4.1	9.78	***Naphthenes***		
Undecane, 2,5-dimethyl-	0.98	---	Cyclopropane, trimethylmethylene-	---	0.3
Undecane, 2,6-dimethyl-	---	0.98	Cyclopentane, ethylidene-	0.38	---
Undecane, 3,8-dimethyl-	0.91	0.43	Cyclohexane, methyl-	---	1.09
Tetradecane	2.2	---	Cyclopentane, ethyl-	---	0.41
Tridecane, 4-methyl-	0.34	---	Cyclobutane, (1-methylethylidene)-	---	0.41
Octane, 2-cyclohexyl-	---	0.74	Cyclohexane, 1-bromo-4-methyl-	---	0.58
3,5-Dimethyldodecane	0.42	---	Cyclopentane, 1-ethyl-2-methyl-	---	1.04
Pentadecane	3.58	5.34	Cyclopropane, (2,2-dimethylpropylidene)-	---	0.7
Dodecane, 2,7,10-trimethyl-	1.14	---	Cyclopentane, 1-ethyl-2-methyl-, cis-	---	0.25
Hexadecane	0.67	0.32	Cyclopentane, propyl-	---	0.54
Heptadecane	0.62	---	Cyclopentane, 1-methyl-2-(2-propenyl)-, trans-	---	0.97
Pentadecane, 2,6,10-trimethyl-	0.32	---	Cyclohexane, 1,1,3-trimethyl-	---	0.27
Octadecane	0.21	---	Cyclopentane, 1-methyl-2-propyl-	---	0.74
Hexadecane, 2,6,10,14-tetramethyl-	1.38	---	Cyclohexane, 1-ethyl-2-methyl-, cis-	---	1
Eicosane	---	0.73	Cyclohexane, propyl-	---	0.75
			Cyclopropane, 1-heptyl-2-methyl-	2.3	0.65
Olefins			Cyclopentane, hexyl-	---	0.61
1-Octene	2.18	---	trans-1,2-diethyl cyclopentane	---	0.36
2-Octene, (E)-	0.38	0.16	Cyclopropane, 1-methyl-2-octyl-	0.85	---
2-Octene, (Z)-	0.16	---	Cyclohexane, pentyl-	---	0.45
4-Octene, (E)-	---	0.18	Cyclopentane, pentyl-	---	0.93
1-Heptene, 2,6-dimethyl-	0.29	---	Cyclohexane, 1-(cyclohexylmethyl)-2-methly-,cis	---	0.61
1-Nonene	2	---	Cyclohexane, undecyl-	---	0.9
2-Nonene	0.53	---	Cyclopentadecane	---	0.3
cis-2-Nonene	0.29	0.2	n-Tridecylcyclohexane	0.62	---
cis-4-Nonene	---	0.16			
6-Cyano-1-hexene	0.32	---	***Cycloolefins***		
2-Decene, (E)-	0.5	---	1-Ethylcyclopentene	---	0.31
2-Decene, (Z)-	---	0.46	Cyclohexene, 1-methyl-	0.35	0.4
5-Decene, (E)-	---	0.83	1,3,5,7-Cyclooctatetraene	1.66	---
1-Undecene	2.13	---			

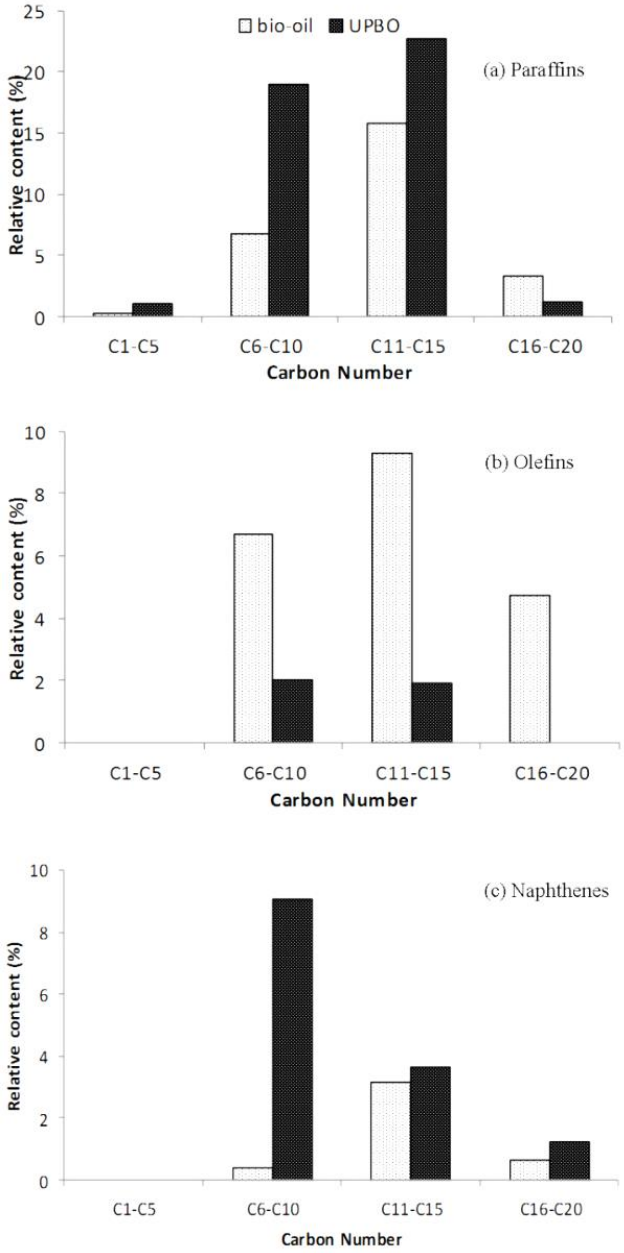

Figure 35. Selectivity of HZSM-5 based on carbon number.

Table 19 shows the major benzene and aromatic compounds (BAC) detected in algal bio-oil and in the upgraded product. BAC increased by about 60% from 14% of the original bio-oil to approximately 22% of UPBO. Most of the BAC compounds were still

present in UPBO at relatively higher values compared to the algal bio-oil. Initially, the algal bio-oil does not contain naphthalenes. However, after HZSM-5 upgrading at 285^0C for 3.5 h, some naphthalene compounds as shown in Table 19 were detected amounting to about 1.5%.

Table 19. Benzene and aromatic compounds in algal bio-oil and upgraded bio-oil at 285^0C and 3.5 h.

Compound	Relative Content (%)	
	Bio-oil	UPBO (285^oC, 3.5 h)
Pyrrole	1.05	---
Toluene	6.92	6.71
Ethylbenzene	1.95	3.03
Benzene, 1,3-dimethyl-	0.85	1.88
o-Xylene	---	2.18
Benzene, propyl-	0.44	1.01
Benzene, 1-ethyl-3-methyl-	0.28	1.73
Benzene, 1-ethyl-2-methyl-	0.29	---
1H-Pyrrole, 2-ethyl-4-methyl-	0.26	0.32
Benzene, 1,2,4-trimethyl-	0.51	1.01
Benzene, butyl-	0.49	0.71
Benzenepropanenitrile	0.56	---
Benzene, (1-methylpropyl)-	---	0.54
Benzene, 1-ethyl-2,3-dimethyl-	---	0.28
Indan, 1-methyl-	---	1.16
1H-Indene, 2,3-dihydro-4-methyl-	---	0.69
Benzeneacetic acid, 2-tetradecyl ester	---	0.49
Naphthalenes		
Naphthalene, decahydro-2-methyl-	---	0.32
Naphthalene	---	0.41
Naphthalene, 2-methyl-	---	0.46
Naphthalene, 1,8-dimethyl-	---	0.32

The oxygenated compounds present in algal bio-oil and UPBO are summarized in Table 20. The original bio-oil contains about 10% wt oxygen, which may be attributed to alcohols, acids, aldehydes, ketones, esters and phenols present. After upgrading at 285^0C for 3.5 h, however, the oxygen content decreased to about 3.4% wt (see Table 16), which can be attributed to the removal of acidic compounds, esters, aldehydes and ketones while minimal amount of alcohols and ketones were still detected in UPBO.

Table 20. Oxygenated compounds in algal bio-oil and upgraded bio-oil at 285^0C and 3.5 h.

Compound	Relative Content (%)		Compound	Relative Content (%)	
	Bio-oil	UPBO (285°C, 3.5 h)		Bio-oil	UPBO (285°C, 3.5 h)
Alcohols			***Esters***		
1-Octanol, 2-methyl-	0.57	---	Ethyl 9-hexadecenoate	0.44	---
1-Octanol, 2,7-dimethyl-	0.59	---	Hexadecanoic acid, ethyl ester	0.58	---
1-Octanol, 2-butyl-		0.56	11-Octadecenoic acid, methyl ester	0.84	---
2-Hexyl-1-octanol	0.17	---	Sulfurous acid, cyclohexylmethyl hexadecyl ester	---	0.18
1-Dodecanol, 3,7,11-trimethyl-	0.35	---			
3,7,11,15-Tetramethyl-2-hexadecen-1-ol	0.69	---	***Aldehydes***		
1-Decanol, 2-hexyl-	---	0.28	9-Octadecenal, (Z)-	1.88	---
Acids			***Ketones***		
9-Hexadecenoic acid	0.61	---	Ethanone, 1-(1H-pyrrol-2-yl)-	0.23	---
n-Hexadecanoic acid	1.2	---			
			Phenols		
Esters			Phenol, 2-methyl-	0.61	0.89
Methyl tetradecanoate	0.49	---	Phenol, 3-methyl-	1.19	1.04
9-Hexadecenoic acid, methyl ester, (Z)-	3.42	---	Phenol, 2-ethyl-	---	0.43
Hexadecanoic acid, methyl ester	3.86	---			

Table 21 compares the major nitrogenous and sulfides compounds present in the algal bio-oil and UPBO. The relative content of the amides and nitriles decreased significantly from approximately 2% to about 0.3% for amides and from 13.5% to

10.4% for nitriles after upgrading. The dimethyl disulfide originally present in the algal bio-oil (0.43%) was completely removed by HZSM-5 upgrading at 285^{0}C for 3.5 h.

Table 21. Nitrogenous compounds and sulfides in algal bio-oil and upgraded bio-oil at 285^{0}C and 3.5 h.

Compound	Relative Content (%)	
	Bio-oil	UPBO (285^{o}C, 3.5 h)
Tetradecanamide	---	0.21
Octadecanamide	0.81	---
N-Methyldodecanamide	0.46	0.12
Non-7-enoic acid, dimethylamide	0.16	---
N,N-Dimethyldodecanamide	0.59	---
Nitriles		
Butanenitrile, 3-methyl-	0.54	---
Pentanenitrile	0.45	0.66
Pentanenitrile, 4-methyl-	0.76	0.73
Hexanenitrile	0.55	1.16
Hexanenitrile, 3-methyl-	---	0.19
Heptanonitrile	1.55	1.38
Octanenitrile	0.78	1.33
Nonanenitrile	1.31	1.85
Tridecanenitrile	0.53	0.73
Hexadecanenitrile	5.28	2.26
Heptadecanenitrile	---	0.11
Oleanitrile	1.78	---
Sulfides		
Disulfide, dimethyl	0.43	---

5.3.3. Gas composition

The gas obtained after the reaction mainly consists of unreacted H_2, CO, CO_2 and hydrocarbon gases ranging from C_1 to C_3 as shown in Figure 36. As can be seen from the graph, CO_2 was produced in all treatments indicating potential decarboxylation of

carboxylic acids, which was initially present in the bio-oil. Production of CO, which may be attributed to the decarbonylation of carbonyl compounds such as aldehydes and ketones was also observed at higher temperatures (>285^{0}C). CH_4 production, on the other hand, tended to increase as temperature was increased. Similar trend was observed for C_2H_6 and C_3H_8, also which evolved at temperatures higher than 285^{0}C. Minor gaseous components detected include C_2H_4 and C_3H_6. The CO_2 in the gas product indicates potential deoxygenation reaction through decarboxylation [115]. The presence of C_1 to C_3 hydrocarbon gases and CO, on the other hand, indicates potential cracking and deoxygenation reactions [28, 115].

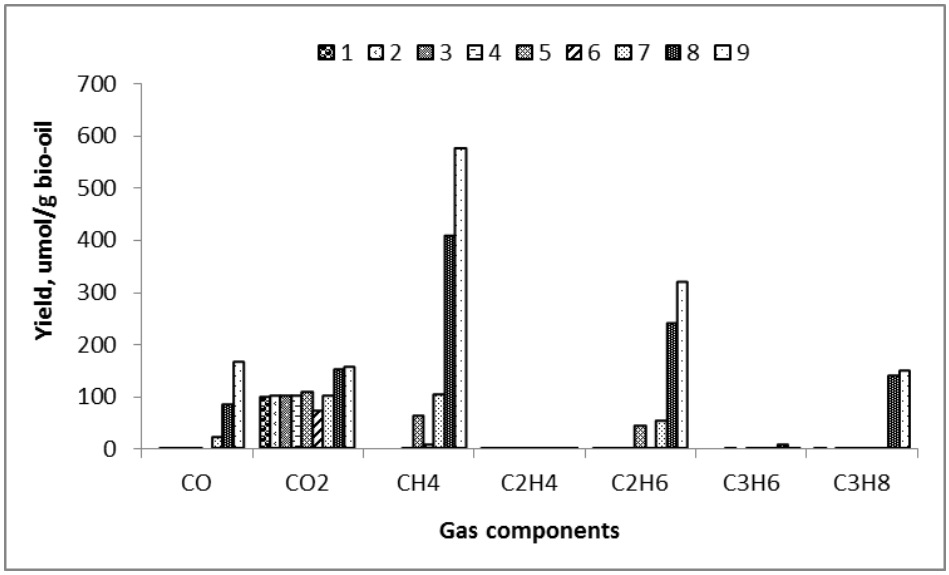

Figure 36. Composition of the gas obtained from various HZSM-5 upgrading conditions.

5.3.4. Mechanism of reactions

The upgrading of bio-oil is a complex process due to the presence of wide variety of hydrocarbons and oxygenated compounds. Hence, it is difficult to exactly identify

which family of compounds is contributing to the production of the observed products [115]. Nonetheless, the reaction mechanism for algal bio-oil upgrading using HZSM-5 as catalyst were deduced from the products formed and their compositions discussed in previous sections.

Chemical reactions over acid catalyst such as HZSM-5 may be attributed to thermal and thermo-catalytic effects [111, 116]. Thermal effects involve the separation of bio-oil into light and heavy organics and polymerization of unstable bio-oil components into char [111]. On the other hand, the major thermo-catalytic reactions includes deoxygenation, cracking, cyclization, aromatization, isomerization, and polymerization which result to coke, tar, gas water, and UPBO formation [116]. The thermo-catalytic reactions for oxygenated compounds in the bio-oil for HZSM-5 upgrading at 285^0C for 3.5 h were found to be consistent with the reaction mechanism proposed by Adjaye and Bakhshi (1995) for upgrading of model compounds for acid, ester, alcohol, phenol, aldehyde and ketone group over HZSM-5 catalyst [115]. Figure 37 shows the proposed reaction pathway for the conversion of bio-oil to an upgraded product using HZSM-5 catalyst.

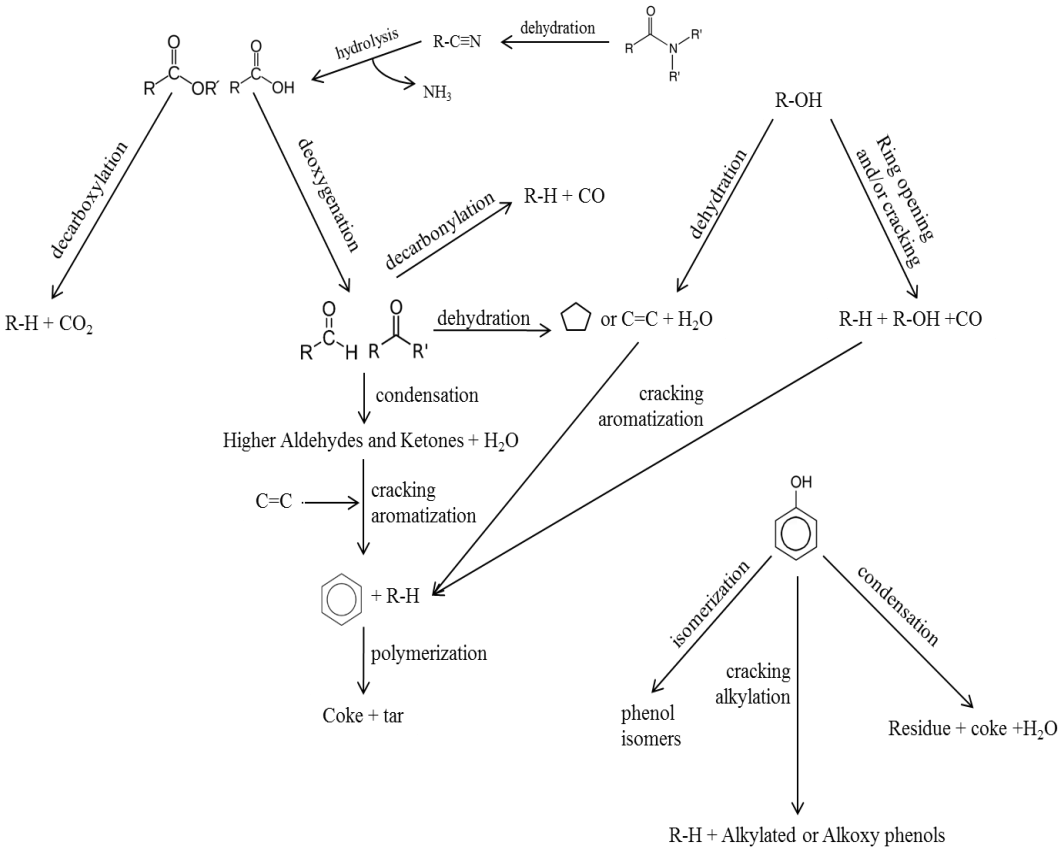

Figure 37. Proposed reaction mechanism for algal bio-oil upgrading using HZSM-5.

Acids and esters in the bio-oil may follow either one of two reaction pathways [115]. One reaction pathway may involve the decarboxylation of acids and ester derivatives through cracking to produce CO_2 and hydrocarbons. Another route could be the production of aqueous fraction of the liquid product, aromatic hydrocarbons, coke and tar by the successive deoxygenation, condensation, cracking, aromatization and polymerization reactions as illustrated in Figure 37. According to Adjaye and Bakhshi (1995), the deoxygenation of acids or esters produces long-chain aldehydes, ketones and water. Oxygen may also be eliminated from carboxylic groups mainly as water (by

dehydration) and CO_2 (by decarboxylation) over an acid catalyst such as HZSM-5. Water may also be produced from Aldol condensation reactions. The alkyl groups attached to the aldehyde or ketone may be removed from the main chain by cracking over the HZSM-5 catalyst. The olefins present promote aromatization reactions, which result in the initial formation of benzene followed by alkylation and isomerization to produce alkylated benzenes [115, 117]. Based on these reactions, the end products would include hydrocarbons, aromatic hydrocarbons and CO_2 while esters, acids and olefins may be consumed in the process. Based on the GC-MS analysis of UPBO, the majority of hydrocarbons produced from these reactions could be C_3-C_{16} paraffins. Coke and tar, on the other hand, may be formed by the polymerization of aromatic molecules. Naphthenes or cyclic alkanes, on the other hand, could have been formed from dehydration of alcohols over HZSM-5 catalyst. Carbon dioxide could be produced from decarbonylation of alcohols, aldehydes and ketones [115]. GC-MS analysis of UPBO also revealed that phenols were not very reactive over HZSM-5 catalyst, which is similar to that observed by Adjaye and Bakhshi (1995) [115]. However, isomerization and alkylation could have occurred but possibly not condensation since no reduction in phenols content was observed.

The reduction in nitrogenous compounds such as amides and nitriles, on the other hand, may be attributed to dehydration and hydrolysis reactions as illustrated in Figure 37. The amides present in the bio-oil could have been dehydrated to produce nitriles. Then, the moderate reduction in the nitriles present could be attributed to its hydrolysis over acidic HZSM-5 catalyst with minimal amount of water present in the system, which

could have limited the reaction. From this reaction, intermediate acid products may have been produced together with the evolution of NH_3 [28].

5.3.5. Degree of deoxygenation

The degree of deoxygenation (DOD) was estimated using Equation 5.1. Oxygen is the major heteroatom present in the bio-oil based on the ultimate analysis in Table 16 followed by nitrogen. Similar to the products yields, the response surface for DOD was also generated for various combinations of temperature and reaction time as shown in Figure 38. Based on the plot, temperature significantly affects the degree of deoxygenation of the algae bio-oil ($p=0.0092$). Maximum deoxygenation (66%) was achieved at 285^{0}C and 3.5 hours. DOD also tended to increase as temperature is increased. Based on the plot, at high temperatures, longer time also tended to result in higher degree of deoxygenation.

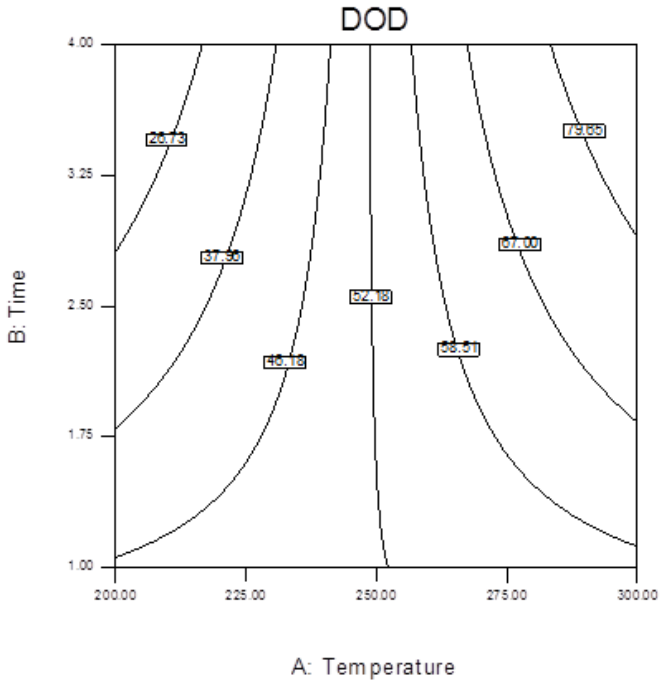

Figure 38. Degree of deoxygenation.

DOD was also plotted against UPBO yield as shown in Figure 39. The plot shows the negative correlation between UPBO and DOD. Based on the plot, lower DDO was achieved at higher UPBO yields while higher DOD was found in the region of low UPBO yield. This could be due to several reactions including decarbonylation and/or decarboxylation of the organic compounds present in algae bio-oil forming gaseous CO and CO_2. At high temperatures, more incondensable gases such as CO and CO_2 were produced resulting to lesser amounts of upgraded liquid product as discussed in Sections 5.3.1 and 5.3.3. Production of other by-products with oxygen-containing components also tends to decrease the amount of UPBO such as the formation of water (H_2O) producing the aqueous liquid layer. Hence, lower UPBO yields could be expected with

high DOD due to the conversion of algal bio-oil into oxygen-containing by-products. As can be seen from the plot, UPBOs obtained at low temperatures (No. 1-3) have high yields within the range of 78-86% wt but low degree of deoxygenation (8-30% wt); whereas, the UPBO obtained at 285^{0}C and 3.5 h has low yield (56% wt) but high DOD (66%).

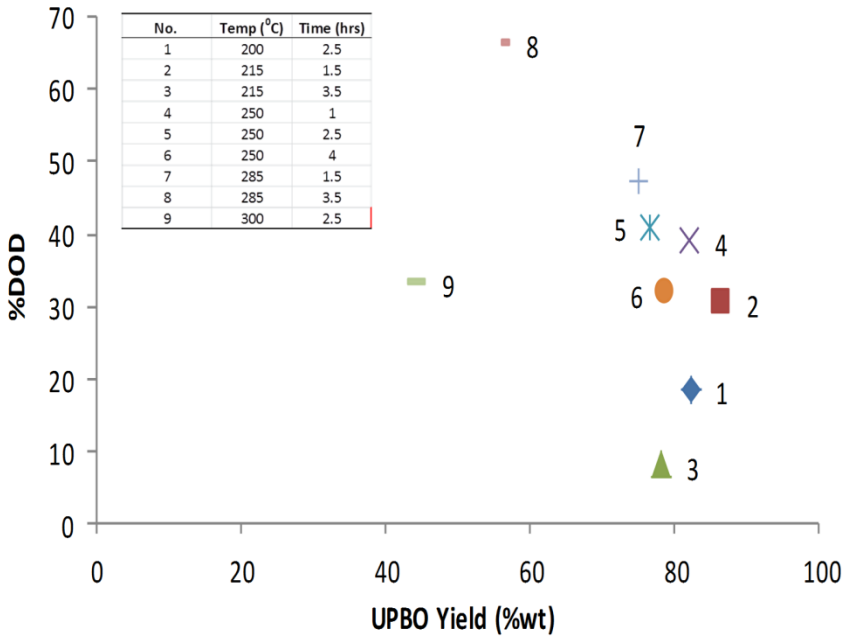

Figure 39. DOD versus UPBO yield.

5.3.6. Turnover frequency (TOF) and H_2 consumption

Turnover frequency (TOF) was used by Mahfud (2007) to express catalytic activity in terms of the amount of hydrogen consumed per gram of catalyst per time as shown in Equation 5.5 [118]. TOF can be used to approximate the catalytic activity of zeolites and reactions catalyzed by their protonic Brϕnsted acidic sites, and metal catalyst (i.e. Pt, Pd, Ni, Rh) [119]. Figure 40 shows the response surface for TOF (in

mmol H_2/g-hr) for the upgrading of bio-oil using HZSM-5 catalyst. The plot clearly shows that there is a significant increase in TOF as temperature was increased (p-value = 0.0021), which indicates that higher catalytic activity could be expected at higher temperatures. This observation is similar to the results obtained by Mahfud (2007) wherein the catalytic activity of Ruthenium increased to about 10 times after increasing the temperature from 45^0C to 60^0C based on TOF values. At 285^0C (3.5 h), the TOF was about 5.53 mmol H_2/g catalyst-hr. Hydrogen consumption (in Nl/kg bio-oil), on the other hand, was estimated using Equations 5.2 – 5.4. Several factors including temperature (p-value <0.0001), reaction time (p-value = 0.0005) and the interaction between temperature and time (p-value = 0.0006) affected H_2 consumption based on statistical analysis. Based on Figure 40, H_2 consumption increases with temperature and reaction time. The highest H_2 consumption recorded was about 20.44 Nl/kg bio-oil at 285^0C for 3.5 h.

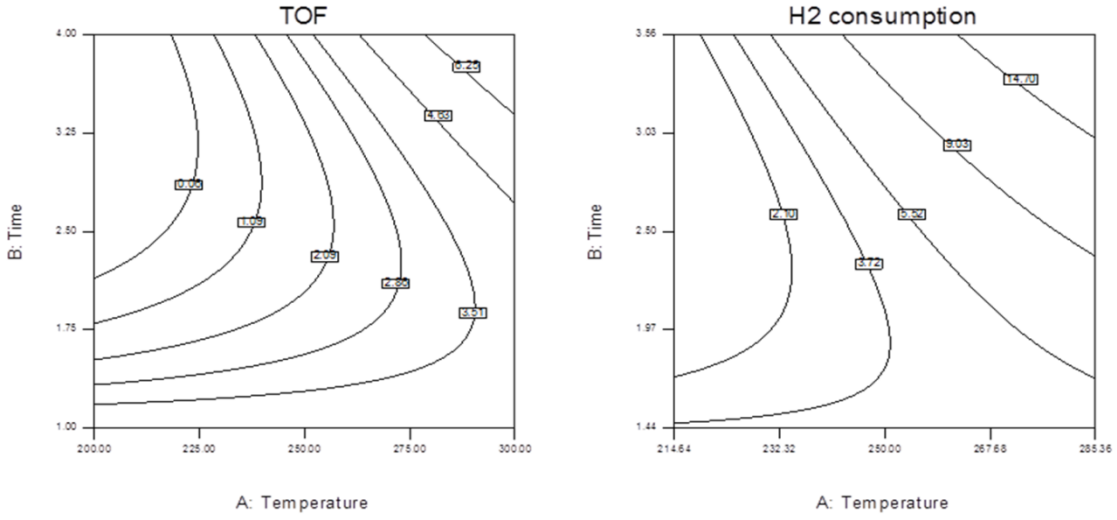

Figure 40. Turnover frequency and hydrogen consumption.

5.4. Conclusions

Upgrading over HZSM-5 catalyst of bio-oil from pyrolysis of *Nannochloropsis oculata* was done at various temperature and reaction time combinations following response surface method experimental design to determine the effects of these factors on products yields and upgraded bio-oil quality. Results showed that reaction temperature had significant effect on the upgraded product yield and quality. The best operating condition for HZSM-5 upgrading for *N. oculata* bio-oil was found to be 285^0C for 3.5 h. Catalytic treatment over HZSM-5 under this operating conditions can produce a more basic (pH 8.8) treated bio-oil with higher hydrocarbons content (86%), lower oxygenated compounds (3%) and lower nitrogenous components (11%). The heating value of the bio-oil was also improved consistent with the considerable increase in carbon and decrease in oxygen contents. Based on the van Krevelen diagram, the upgraded product at 285^0C for 3.5 h is almost similar to crude oil. Further processing or co-processing with crude oil may be explored to render the upgraded bio-oil components suitable as transport fuels. However, additional research to improve nitrogen reduction may be needed since the final nitrogen content was still higher than crude oil. The mechanism of reactions for bio-oil upgrading using HZSM-5 was also presented based on the products formed and composition of the upgraded bio-oil. In general, the results presented indicate that HZSM-5 can be an effective catalyst for algal bio-oil upgrading and this process may be more economical than treatment using noble metal catalysts (i.e. Pt, Pd, Ru).

6. OVERALL CONCLUSIONS AND RECOMMENDATIONS

This research primarily aimed to evaluate the technical feasibility of producing biofuels from pyrolysis of *Nannochloropsis oculata.* Also, physical and catalytic processes for the upgrading of the pyrolytic bio-oil produced were both explored in an attempt to improve the quality of the final products and render them as suitable replacement for crude oil or petroleum-derived transport fuels. Four studies were conducted to achieve the objectives of this research as presented below together with the major conclusions derived from the results obtained.

The first study dealt with the effects of temperature during pyrolysis of *N. oculata* in a pressurized fixed-bed batch-type reactor. Pyrolysis temperature was varied from 400 to 600^0C while pressure was maintained at 100 psi. Results indicated the following conclusions.

- The distribution of the products of pyrolysis greatly depends on temperature and the pyrolysis process can be manipulated to favor one of its three major products (i.e. char, bio-oil, gas). Char yield decreases to a certain extent as pyrolysis temperature is increased. Hence, peak production of char (52% wt) can be expected at lower temperatures (400^0C). Liquid product, which consist of aqueous and bio-oil fractions, is maximum (35% wt) at moderate temperatures (500^0C) then decreases due to secondary cracking reactions. Further increase in temperature to about 600^0C maximizes gas production to approximately 15% wt.

Higher amounts of hydrocarbon components can also be expected at higher temperatures.

- Bio-oil with high heating value (38 MJ/kg) due to its high carbon (76% wt) and hydrogen (11% wt) contents and low oxygen content (7% wt) can be produced from *N. oculata.* It also consists mainly of saturated (34.95%) and unsaturated (34.43%) aliphatics and aromatics (14.19%) ranging from C_8-C_{21}, which is similar to diesel fuel.
- Char and gaseous product can be used as alternative energy sources based on their heating values of about 27 MJ/kg and 27 MJ/m^3, respectively.
- Mass and energy conversion efficiencies were about 76% and 68%, respectively. Most of the mass and energy from the biomass were retained in the char.

The second study focused on the optimization of operating conditions, specifically temperature and pressure, to maximize the yield of liquid product from pyrolysis. Response surface analysis was used to determine the optimum condition. Temperature was varied from 400 to 600^{0}C while pressure was varied from 0 to 100 psig. The following conclusions were drawn from the results of this study.

- Char production only depends on temperature. Gas yield, on the other hand, is significantly affected by temperature and the interaction between temperature and pressure. Liquid yield is both significantly affected by temperature and pressure.
- Optimum operating conditions for liquid production are 540^{0}C and 0 psig. At this condition, liquid product yield was about 43% wt (20% wt aqueous;

23% wt bio-oil). Char and gas yields were approximately equal to 32 and 12% by wt, respectively.

- Bio-oil produced at optimum conditions has 72% carbon, 10% hydrogen, 8% nitrogen, 0.15% sulfur and 10% oxygen and has a heating value of about 36 MJ/kg.
- Compared to the results of the first study, bio-oil produced at higher yields has relatively lower heating value, carbon and hydrogen contents and higher oxygen content.
- The co-products, char (20 MJ/kg) and gas (21 MJ/m^3), produced at optimum condition also contain considerable amounts of energy.

The third study explored on the potential of physical upgrading of the bio-oil and aqueous liquid product (ALP) produced at optimum conditions by fractional distillation at atmospheric pressure. Results from distillation experiments lead to the following conclusions.

- Significant removal of moisture and improvement in heating values may result from separation of bio-oil components by fractional distillation. Most of the moisture from the bio-oil was separated in the first two fractions. Moreover, the heating values of the top layer of light fractions (BF1 and BF2) were higher than heavy fuel oil and FAME while that of middle and heavy fractions (BF3 - BF6) were higher than the original bio-oil.
- Most of the oxygenated compounds such as acids, ketones and phenols were separated in the middle fractions (BF3 and BF4).

- ALP contains considerable amount of organic compounds, which can be separated by fractional distillation. AF5, which was distilled at 150-180^{0}C, has a heating value of about 24 MJ/kg which is higher than wood-derived bio-oils.
- Complete separation can be achieved for high molecular weight olefins and naphthenes based on the separation factor.

Lastly, the fourth study assessed catalytic upgrading of the bio-oil produced at optimum condition using HZSM-5 as catalyst. Response surface methodology was used to evaluate the potential effects of temperature and reaction time on product yields and characteristics. Temperature was varied from 200 to 300^{0}C while reaction time was varied from 1 to 4 h. The following conclusions were derived from the results of this study.

- Reaction temperature greatly affected products yields. UPBO yield decreased with an increase in temperature due to conversion of the bio-oil into other products such as coke, tar, gas, char and aqueous product.
- Upgraded bio-oils at higher temperatures have lesser moisture contents and tend to be more basic. They also have higher carbon contents and lower nitrogen and oxygen contents which lead to higher heating values.
- The best operating condition for HZSM-5 upgrading for *N. oculata* is at 285^{0}C for 3.5 h based on van Krevelen diagram, compositional analysis and FTIR analysis.

- At 285^{0}C and 3.5 h, bio-oil with higher hydrocarbons content (86%), lower oxygenated compounds (3%) and lower nitrogenous components (11%) can be obtained.

Figure 41 summarizes the results of the pyrolysis and upgrading processes considered in this study to convert *Nannochloropsis oculata* to various products. Some general conclusions from the results of these studies are the following.

- High quality bio-oils can be produced from pyrolysis of *Nannochloropsis oculata* at moderate pressure (100 psi) and temperature (500^{0}C). However, the yield of bio-oil at this operating condition is lower (16.75% wt).
- High bio-oil yields (23.32% wt) can be obtained from pyrolysis at atmospheric pressure (0 psig) and moderate temperature (540^{0}C). However, the heating value of the bio-oil is lower due to lower carbon and hydrogen contents and higher oxygen content compared to that produced from pressurized pyrolysis.
- Significant increase in heating values and reduction in moisture content can be achieved by fractional distillation and HZSM-5 upgrading of the algal bio-oil. The distillates and upgraded bio-oil also has higher carbon and hydrogen contents and lower oxygen content. However, a secondary treatment to further reduce the oxygen and nitrogen content to acceptable levels may be necessary.
- The organic compounds from the aqueous liquid product can be recovered by fractional distillation at 150-180^{0}C. Significant amounts of esters, acids,

amides and lactams indicate that the distillate fraction from ALP may be used as fuel or feedstock for other industrial chemicals production.

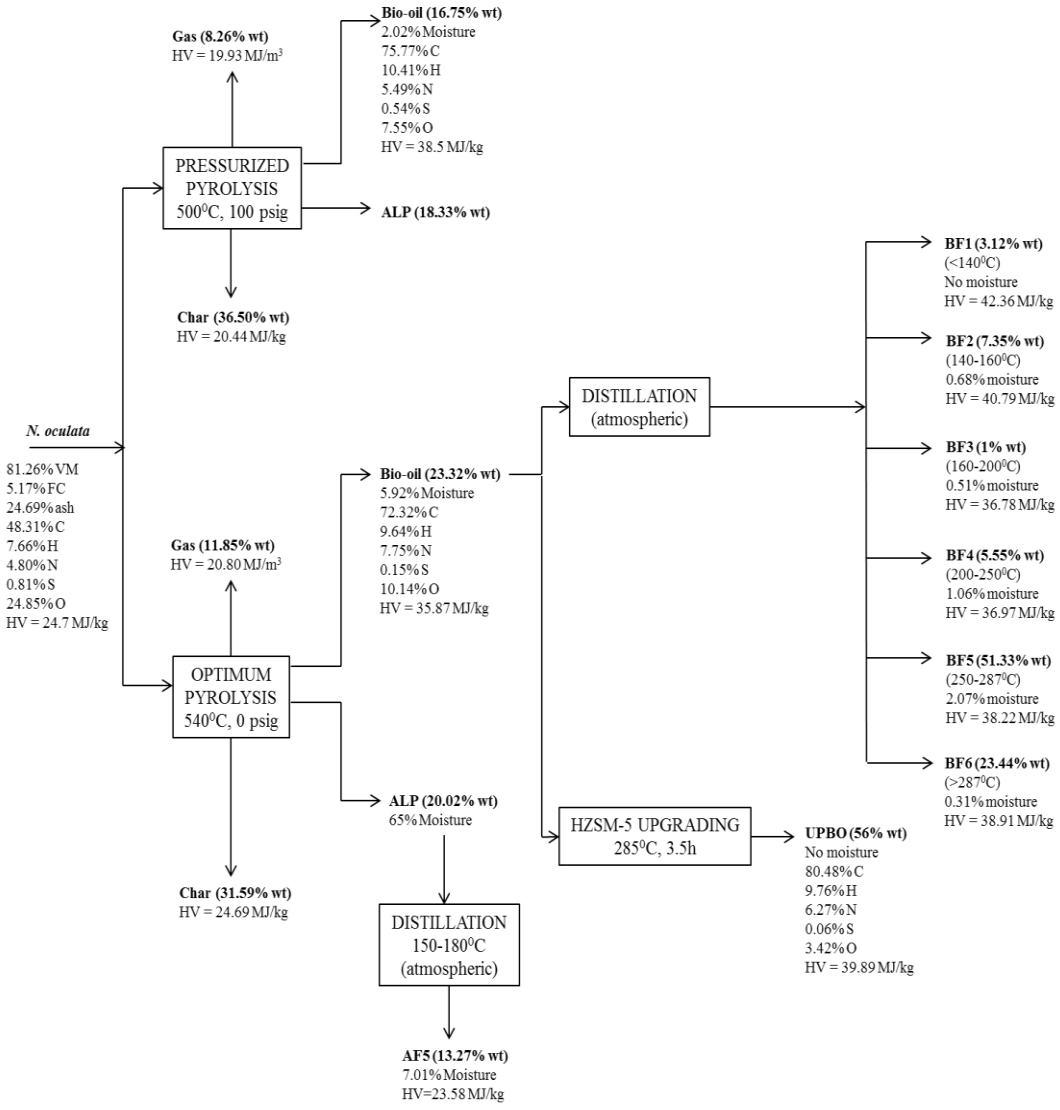

Figure 41. Summary of biofuels production from *Nannochloropsis oculata*.

Based on the conclusions drawn from the results of this research, further investigation on the following areas is recommended.

- In this research, the combination of temperature and pressure that maximizes bio-oil production (540^0C, 0 psig) was already established for batch pyrolysis of *N. oculata*. This operating condition may be tried in a continuous mode of operation to establish the applicability of batch results to a continuous process. Also, scale-up factors and kinetic parameters may also be explored for large-scale application of this process.
- Successive distillation and catalytic upgrading process may also be tried. Based on the distillation and upgrading studies, the light and middle distillates can be removed from the bio-oil prior to upgrading of the heavy distillates. Another option is to separate BF5 for upgrading while BF6, which mainly contains nitriles (80%), can be used as a feedstock for production of other valuable industrial chemicals.
- The ALP distillate obtained contains considerable amounts of acids (21%), esters (54%), amides (10%) and lactams (12%). Further separation of these components may be explored to establish procedures to produce value-added products and transport fuel components.
- The UPBO produced from HZSM-5 upgrading was found to have similar quality as crude oil based on the van Krevelen diagram. Co-processing of this product with crude oil may be explored to produce traditional transport fuels such as gasoline and diesel. Further processing (i.e. secondary catalytic treatment) or use of bi-functional catalyst (i.e. Ni-impregnated zeolite) may

also be an option to further remove the residual nitrogen and oxygen in UPBO to meet acceptable levels or refinery standards.

REFERENCES

[1] U.S. Energy Information Administration. Annual Energy Outlook 2013 with Projections to 2040. DOE/EIA-0383. (2013).
accessible online at www.eia.gov/forecasts/aeo

[2] L. James. Beyond Peak Oil and World Geopolitical Implications. Globalization. 7 (2008). accessible online at http://globalization.icaap.org/content/special/Leigh.html

[3] H. Terrell. The hydrocarbon blip. World Oil. 232 (2011).
accessible online at www.worldoil.com/May-2011-Whats-new-in-production.html

[4] P. Haldis. CIBC: Oil price to hit $150/bbl in 'Near Future'. Global Refining & Fuels Report. 12 (2008).
accessible online at http://www.hartenergy.com/Downstream/Newsletters/Global-Refining-And-Fuels-Report/

[5] L. Brennan, P. Owende. Biofuels from microalgae - A review of technologies for production, processing, and extractions of biofuels and co-products. Renewable and Sustainable Energy Reviews. 14 (2010) 557-77.

[6] L. Rodolfi, G.C. Zittelli, N. Bassi, G. Padovani, N. Biondi, G. Bonini, et al. Microalgae for oil: Strain selection, induction of lipid synthesis and outdoor mass cultivation in a low cost photobioreactor. Biotechnology & Bioengineering. 102 (2008) 100-12.

[7] S. Grierson, V. Strezov, G. Ellem, R. Mcgregor, J. Herbertson. Thermal characterisation of microalgae under slow pyrolysis conditions. Journal of Analytical and Applied Pyrolysis. 85 (2009) 118-23.

[8] X. Miao, Q. Wu, C. Yang. Fast Pyrolysis of Microalgae to Produce Renewable Fuels. Journal of Analytical and Applied Pyrolysis. 71 (2004) 855-63.

[9] P.J.l.B. Williams, L.M.L. Laurens. Microalgae as biodiesel and biomass feedstocks: Review and analysis of the biochemistry, bioenergetics and economics. Energy and Environmental Science. 3 (2009) 554-90.

[10] H.C. Greenwell, L.M.L. Laurens, R.J. Shields, R.W. Lovitt, K.J. Flynn. Placing microalgae on the biofuels priority list: a review of the technological challenges. Journal of the Royal Society 7(2010) 703-26.

[11] I.V. Babich, M. van der Hulst, L. Lefferts, J.A. Moulijn, P. O'Connor, K. Seshan. Catalytic pyrolysis of microalgae to high-quality liquid biofuels. Biomass & Bioenergy. 35 (2011) 3199-207.

[12] T. Bridgwater. Review: Biomass for energy. Journal of Science and Food Agriculture. 86 (2006) 1755-68.

[13] S. Xiu, A. Shahbazi. Bio-oil production and upgrading research: A review. Renewable and Sustainable Energy Reviews. 16 (2012) 4406-14.

[14] N. Mahinpey, P. Murugan, T. Mani, R. Raina. Analysis of Bio-oil, Biogas and Biochar from Pressurized Pyrolysis of Wheat Straw Using a Tubular Reactor. Energy & Fuels. 23 (2009) 2736-42.

[15] W.N.R.W. Isahak, M.W.M. Hisham, M.A. Yarmo, T.-Y.Y. Hin. A review on bio-oil production from biomass by using pyrolysis method Renewable and Sustainable Energy Reviews. 16 (2012) 5910-23.

[16] A. Marcilla, A. Gomez-Siurana, C. Gomis, E. Chapuli, M.C. Catala, F.J. Valdes. Characterization of microalgal species through TGA/FTIR analysis: Application to *nannochloropsis sp.* . Thermochimica Acta. 484 (2009) 41-7.

[17] D. Li, L. Chen, J. Zhao, X. Zhang, Q. Wang, H. Wang, et al. Evaluation of the pyrolytic and kinetic characteristics of Enteromorpha prolifera as a source of renewable biofuel from the Yellow Sea of China. Chemical Engineering Research and Design. 88 (2010) 647-52.

[18] W. Peng, Q. Wu, P. Tu. Pyrolytic characteristics of heterotrophic *Chlorella protothecoides* for renewable bio-fuel production. Journal of Applied Phycology. 13 (2001) 5-12.

[19] W. Peng, Q. Wu, P. Tu, N. Zhao. Pyrolytic characteristics of microalgae as renewable energy source determined by thermogravimetric analysis. Bioresource Technology. 80 (2001) 1-7.

[20] P. Pan, C. Hu, W. Yang, Y. Li, L. Dong, L. Zhu, et al. The direct pyrolysis and catalytic pyrolysis of *Nannochloropsis* sp. residue for renewable bio-oils. Bioresource Technology. 101 (2010) 4593-9.

[21] A. Teella, G.W. Huber, D.M. Ford. Separation of acetic acid from the aqueous fraction of fast pyrolysis bio-oils using nanofiltration and reverse osmosis membranes. Journal of Membrane Science. 378 (2011) 495-502.

[22] A.V. Bridgwater. Review of fast pyrolysis of biomass and product upgrading. Biomass & Bioenergy. 38 (2012) 68-94.

[23] G.W. Huber, S. Iborra, A. Corma. Synthesis of Transportation Fuels from Biomass: Chemistry, Catalysts, and Engineering Chemical Reviews. 106 (2006) 4044-98.

[24] Z. Qi, C. Jie, W. Tiejun, X. Ying. Review of biomass pyrolysis oil properties and upgrading research. Energy Conversion and Management. 48 (2007) 87-92.

[25] Y. Gu, Z. Guo, L. Zhu, G. Xu, S. Wang. Experimental research on catalytic esterification of bio-oil volatile fraction. Power & Energy Engineering Conference (APPEEC) 2010 Asia-Pacific2010. pp. 1-4.

[26] X. Junming, J. Jianchun, S. Yunjuan, L. Yanju. Bio-oil upgrading by means of ethyl ester production in reactive distillation to remove water and improve storage and fuel characteristics. Biomass & Bioenergy. 32 (2008) 1056-61.

[27] S. Thangalazhy-Gopakumar, S. Adhikari, R.B. Gupta. Catalytic pyrolysis of biomass over H+ZSM-5 under hydrogen pressure. Energy & Fuels. 26 (2012) 5300-6.

[28] Z. Li, P.E. Savage. Feedstocks for fuels and chemicals from algae: Treatment of crude bio-oil over HZSM-5. Algal Research. 2 (2013) 154-163.

[29] V.H. Smith, B.S.M. Sturm, F.J. deNoyelles, S.A. Billings. The ecology of algal biodiesel production. Trends in Ecology and Evolution. 25 (2009) 301-9.

[30] K. Tsukuhara, S. Sawayama. Liquid fuel production using microalgae. Journal of the Japan Petroleum Institute. 48 (2005) 251-9.

[31] A. Demirbas. Biomass resource facilities and biomass conversion processing for fuels and chemicals. Energy Conversion and Management. 42 (2001) 1357-78.

[32] A. Demirbas. Oily products from mosses and algae via pyrolysis. Energy Sources, Part A: Recovery, Utilization, and Environmental Effects. 28 (2006) 933-40.

[33] Z. Ji-lu. Bio-oil from fast pyrolysis of rice huskL Yields and related properties and improvement of the pyrolysis system. Jounal of Analytical and Applied Pyrolysis. 80 (2007) 30-5.

[34] A.E. Putun, E. Apaydin, E. Putun. Rice straw as a bio-oil source via pyrolysis and steam pyrolysis. Energy. 29 (2004) 2171-80.

[35] M. Asadullah, M.A. Rahman, M.M. Ali, M.S. Rahman, M.A. Motin, M.B. Sultan, et al. Production of bio-oil from fixed bed pyrolysis of bagasse. Fuel. 86 (2007) 2514-20.

[36] E. Salehi, J. Abedi, T. Harding. Bio-oil from Sawdust: Pyrolysis of Sawdust in a Fixed-Bed System. Energy & Fuels. 23 (2009) 3767-72.

[37] F. Karaosmanoglu, E. Tetik, E. Gollu. Biofuel production using slow pyrolysis of the straw and stalk of the rapeseed plant. Fuel Processing Technology. 59 (1999) 1-12.

[38] O. Ioannidou, A. Zabaniotou, E.V. Antonakou, K.M. Papazisi, A.A. Lappas, C. Athanassiou. Investigating the potential for energy, fuel materials and chemicals production from corn residues (cobs and stalks) by non-catalytic and catalytic pyrolysis in two reactor configurations. Renewable and Sustainable Energy Reviews. 13 (2009) 750-62.

[39] A.A. Boateng, D.E. Daugaard, N.M. Goldberg, K.B. Hicks. Bench-Scale Fluidized Bed Pyrolysis of Switchgrass for Bio-oil Production. Industrial & Engineering Chemical Research. 46 (2007) 1891-7.

[40] Z. Wang, W. Lin, W. Song, L. Du, Z. Li, J. Yao. Component fractionation of wood-tar by column chromatography with the packing material of silica gel. Chin Sci Bull. 56 (2011) 1434-41.

[41] J.-P. Cao, X.-Y. Zhao, K. Morishita, X.-Y. Wei, T. Takarada. Fractionation and identification of organic nitrogen species from bio-oil produced by fast pyrolysis of sewage sludge. Bioresource Technology. 101 (2010) 7648-52.

[42] F. Zeng, W. Liu, H. Jiang, H.-Q. Yu, R.J. Zeng, Q. Guo. Separation of phthalate esters from bio-oil derived from rice husk by a basification-acidification process and column chromatography. Bioresource Technology. 102 (2011) 1982-7.

[43] R. Lu, G.-P. Sheng, Y.-Y. Hu, P. Zheng, H. Jiang, Y. Tang, et al. Fractional characterization of a bio-oil derived from rice husk. Biomass & Bioenergy. 35 (2011) 671-8.

[44] C. Amen-Chen, H. Pakdel, C. Roy. Separation of phenols from eucalyptus wood tar. Biomass & Bioenergy. 13 (1997) 25-37.

[45] S. Wang, Y. Gu, Q. Liu, Y. Yao, Z. Guo, Z. Luo, et al. Separation of bio-oil by molecular distillation. Fuel Processing Technology. 90 (2009) 738-45.

[46] X. Guo, S. Wang, Z. Guo, Q. Liu, Z. Luo, K. Cen. Pyrolysis characteristics of bio-oil fractions separated by molecular distillation. Applied Energy. 87 (2010) 2892-8.

[47] X. Guo, S. Wang, Q. Wang, Z. Guo, Z. Luo. Properties of bio-oil from fast pyrolysis of rice husk. Biotechnology & Bioengineering. 19 (2011) 116-21.

[48] Z. Guo, S. Wang, Y. Gu, G. Xu, L. Xin, Z. Luo. Separation characteristics of biomass pyrolysis oil in molecular distillation. Separation and Purification Technology. 76 (2010) 52-7.

[49] R.H. Perry, D.W. Green. Perry's Chemical Engineers' Handbook. 6th ed. McGraw-Hill, Columbus, OH (1997).

[50] M.E. Boucher, A. Chaala, C. Roy. Bio-oils obtained by vacuum pyrolysis of softwood bark as a liquid fuel for gas turbines. Part I: Properties of bio-oil and its blends with methanol and a pyrolytic aqueous phase. Biomass & Bioenergy. 19 (2000) 337-50.

[51] X. Hu, R. Gunawan, D. Mourant, C. Lievens, X. Li, S. Zhang, et al. Acid-catalyzed reactions between methanol and the bio-oil from the fast pyrolysis of mallee bark. Fuel. 97 (2012) 512-22.

[52] X. Li, R. Gunawan, C. Lievens, Y. Wang, D. Mourant, S. Wang, et al. Simultaneous catalytic esterification of carboxylic acids and acetalisation of aldehydes in fast pyrolysis bio-oil from mallee biomass. Fuel. 90 (2011) 2530-7.

[53] J. Xu, J. Jiang, W. Dai, T. Zhang, Y. Xu. Bio-oil upgrading by means of ozone oxidation and esterification to remove water and to improve fuel characteristics. Energy Fuels. 25 (2011) 1798-801.

[54] Y. Xu, T. Wang, L. Ma, Q. Zhang, W. Liang. Upgrading of the liquid fuel from fast pyrolysis of biomass over MoNi/y-Al_2O_3 catalyst. Applied Energy. 87 (2010) 2886-91.

[55] Z. Tang, Q. Lu, Y. Zhang, X. Zhu, Q. Guo. One-step bio-oil upgrading through hydrotreatment, esterification and cracking. Industrial & Engineering Chemical Research. 48 (2009) 6923-9.

[56] A.G. Chakinala, J.K. Chinthaginjala, K. Seshan, W.P.M. van Swaaij, S.R.A. Kersten, D.W.F. Brilman. Catalyst screening for the hydrothermal gasification of aqueous phase of bio-oil Catalysis Today. 195 (2012) 83-92.

[57] M.V. Bykova, D.Y. Ermakov, V.V. Kaichev, O.A. Bulavchenko, A.A. Saraev, M.Y. Lebedev, et al. Ni-based sol-gel catalyst as promising systems for crude bio-oil upgrading: Guiacol hydrodeoxygenation study. Applied Catalysis B: Environmental. 113-114 (2012) 296-307.

[58] P. Duan, P.E. Savage. Catalytic hydrotreatment of crude algal bio-oil in supercritical water. Applied Catalysis B: Environmental. 104 (2011) 136-43.

[59] R. Gunawan, X. Li, D. Mourant, A. Larcher, H. Wu, C.-Z. Li. Insights in the esterification of mallee wood bio-oil using Amberlyst-70. Chemeca (2011) 1-8. accessible online at www.conference.net.au/chemeca2011/papers/070.pdf

[60] W. Vermeiren, J.-P. Gilson. Impact of zeolite on the petroleum and petchochemical industry. Topics in Catalysis. 52 (2009) 1131-61.

[61] E.F. Iliopoulou, S.D. Stefanidis, K.G. Kalogiannis, A. Delimitis, A.A. Lappas, K.S. Triantafyllidis. Catalytic upgrading of biomass pyrolysis vapors using transition metal-modified ZSM-5 zeolite. Applied Catalysis B: Environmental. 127 (2012) 281-90.

[62] J. Peng, P. Chen, H. Lou, X. Zheng. Catalytic upgrading of bio-oil by HZSM-5 in sub- and super-critical ethanol. Bioresource Technology. 100 (2009) 3415-8.

[63] H.J. Park, Y.-K. Park, J.-S. Kim, J.-K. Jeon, K.-S. Yoo, J.-H. Yim, et al. Bio-oil upgrading over Ga modified zeolites in a bubbling fluidized bed reactor. Studies in Surface Science and Catalysis. 159 (2006) 553-6.

[64] X. Zhu, R.G. Mallinson, D.E. Resasco. Role of transalkylation reactions in the conversion of anisole over HZSM-5. Applied Catalysis A: General. 379 (2010) 172-81.

[65] A. Carrero, G. Vicente, R. Rodriguez, M. Linares, G.L. del Peso. Hierarchical zeolites as catalyst for biodiesel production from Nannochloropsis microalgal oil. Catalysis Today. 167 (2011) 148-53.

[66] J.D. Adjaye, N.N. Bakhshi. Production of hydrocarbons by catalytic upgrading of a fast pyrolysis bio-oil. Part I: Conversion over various catalyst. Fuel Processing Technology. 45 (1995) 161-83.

[67] S. Czernik, A.V. Bridgwater. Overview of Applications of Biomass Fast Pyrolysis Oil. Energy Fuels. 18 (2004) 590-8.

[68] Q. Zhang, J. Chang, T.J. Wang, Y. Xu. Review of biomass pyrolysis oil properties and upgrading research. Energy Conversion and Management. 48 (2007) 87-92.

[69] A. Demirbas. Use of algae as biofuel sources. Energy Conversion and Management. 51 (2010) 2738-49.

[70] M.F. Demirbas. Biofuels from algae for sustainable development. Applied Energy. 88 (2011) 3473-80.

[71] K.M. Weyer, D.R. Bush, A. Darzins. Theoretical Maximum Algal Oil Production. Bioenergy Resource. 3 (2010) 204-13.

[72] U. Jena, K.C. Das, J.R. Kastner. Effect of operating conditions of thermochemical liquefaction on biocrude production from *Spirulina platensis*. Bioresource Technology. 102 (2011) 6221-9.

[73] A. Demirbas. Calculation of higher heating values of biomass fuels. Fuel. 76 (1997) 431-4.

[74] A.B. Ross, J.M. Jones, M.L. Kubacki, T. Bridgeman. Classification of macroalgae as fuel and its thermochemical behaviour. Bioresource Technology. 99 (2008) 6494-504.

[75] P.T. Martone, J.M. Estevez, F. Lu, K. Ruel, M.W. Denny, C. Somerville, et al. Discovery of Lignin in Seaweed Reveals Convergent Evolution of Cell-Wall Architecture. Current biology : CB. 19 (2009) 169-75.

[76] I. Sørensen, F.A. Pettolino, A. Bacic, J. Ralph, F. Lu, M.A. O'Neill, et al. The charophycean green algae provide insights into the early origins of plant cell walls. The Plant Journal. 68 (2011) 201-11.

[77] Y. Liang. Producing liquid transportation fuels from heterotrophic microalgae. Applied Energy. 104 (2013) 860-8.

[78] M.A. Carriquiry, X. Du, G.R. Timilsina. Second generation biofuels: Economics and policies. Energy Policy. 39 (2011) 4222-34.

[79] Y. Christi. Biodiesel from microalgae. Biotechnology Advances. 25 (2007) 294-306.

[80] B.B. Uzun, A.E. Pütün, E. Pütün. Composition of products obtained via fast pyrolysis of olive-oil residue: Effect of pyrolysis temperature. Journal of Analytical and Applied Pyrolysis. 79 (2007) 147-53.

[81] P. McKendry. Energy production from biomass (part 2): conversion technologies. Bioresource Technology. 83 (2002) 47-54.

[82] P. McKendry. Energy production from biomass (part 1): overview of biomass. Bioresource Technology. 83 (2002) 37-46.

[83] A.B. Ross, P. Biller, M.L. Kubacki, H. Li, A. Lea-Langton, J.M. Jones. Hydrothermal processing of microalgae using alkali & organic acids. Fuel. 89 (2010) 2234-43.

[84] R.K. Singh, K.P. Shadangi. Liquid fuel from castor seeds by pyrolysis. Fuel. 90 (2011) 2538-44.

[85] M. Ertaş, M. Hakkı Alma. Pyrolysis of laurel (Laurus nobilis L.) extraction residues in a fixed-bed reactor: Characterization of bio-oil and bio-char. Journal of Analytical and Applied Pyrolysis. 88 (2010) 22-9.

[86] E. Apaydin-Varol, E. Pütün, A.E. Pütün. Slow pyrolysis of pistachio shell. Fuel. 86 (2007) 1892-9.

[87] Z. Du, Y. Li, X. Wang, Y. Wan, Q. Chen, C. Wang, et al. Microwave-assisted pyrolysis of microalgae for biofuel production. Bioresource Technology. 102 (2011) 4890-6.

[88] S. Şensöz, D. Angın. Pyrolysis of safflower (Charthamus tinctorius L.) seed press cake in a fixed-bed reactor: Part 2. Structural characterization of pyrolysis bio-oils. Bioresource Technology. 99 (2008) 5498-504.

[89] X. Jiang, E. Naoko, Z. Zhong. Structure properties of pyrolytic lignin extracted from aged bio-oil. Chin Sci Bull. 56 (2011) 1417-21.

[90] L. Zhou, Z.M. Zong, S.R. Tang, Y. Zong, R.L. Xie, M.J. Ding, et al. FTIR and Mass Spectral Analyses of an Upgraded Bio-oil. Energy Sources, Part A: Recovery, Utilization, and Environmental Effects. 32 (2009) 370-5.

[91] I.V. Babich, M. van der Hulst, L. Lefferts, J.A. Moulijn, P. O'Connor, K. Seshan. Catalytic pyrolysis of microalgae to high-quality liquid bio-fuels. Biomass and Bioenergy. 35 (2011) 3199-207.

[92] D.C. Montgomery. Design and Analysis of Experiments. 5th ed. John Wiley & Sons, Inc., New York (2001).

[93] J. Akhtar, N.S. Amin. A review on operating parameters for optimum liquid oil yield in biomass pyrolysis. Renewable and Sustainable Energy Reviews. 16 (2012) 5101-9.

[94] W. Tsai, M. Lee, Y. Chang. Fast pyrolysis of rice husk: product yields and compositions. Bioresource Technology. 98 (2007) 22-8.

[95] L. Shen, D.-k. Zhang. Low-temperature pyrolysis of sewage sludge and putrescible garbage for fuel oil production. Fuel. 84 (2005) 809-15.

[96] K. Whitty, M. Kullberg, V. Sorvari, R. Backman, M. Hupa. Influence of pressure on pyrolysis of black liquor: 2. Char yields and component release. Bioresource Technology. 99 (2008) 671-9.

[97] F. Melligan, R. Auccaise, E.H. Novotny, J.J. Leahy, M.H.B. Hayes, W. Kwapinski. Pressurized pyrolysis of Miscanthus using a fixed bed reactor. Bioresource Technology. 102 (2011) 3466-70.

[98] M.S.H.K. Tushar, N. Mahinpey, P. Murugan, T. Mani. Analysis of gaseous and liquid products from pressurized pyrolysis of flax straw in a fixed bed reactor. Industrial & Engineering Chemical Research. 49 (2010) 4627-32.

[99] S.S. Tamhankar, J.T. Sears, C.-Y. Wen. Coal pyrolysis at high temperatures and pressures. Fuel. 63 (1984) 1230-5.

[100] R.N. Patel, S. Bandyopadhyay, A. Ganesh. Extraction of cardanol and phenol from bio-oils obtained through vacuum pyrolysis of biomass using supercritical fluid extraction. Energy. 36 (2011) 1535-42.

[101] G.W. Huber, R.D. Cortright, J.A. Dumesic. Renewable alkanes by aqueous-phase reforming of biomass-derived oxygenates. Angewandte Chemie International Edition. 116 (2004) 1575-7.

[102] R.D. Cortright, R.R. Davda, J.A. Dumesic. Hydrogen from catalytic reforming of biomass-derived hydrocarbons in liquid water. Nature. 418 (2002) 964-7.

[103] F.A. Agblevor, O. Mante, R. McClung, S.T. Oyama. Co-processing of standard gas oil and biocrude oil to hydrocarbon fuels. Biomass & Bioenergy. 45 (2012) 130-7.

[104] B.J. Xu, N. Lu. Experimental research on the bio oil derived from biomass pyrolysis liquefaction. Transactions of Chinese Society of Agricultural Engineers. 15 (1999) 177-81.

[105] A.P.I. (API). Alcohols and Ethers. in: P.N. 4261, (Ed.). 3rd ed, Washington, DC, 2001.

[106] C.S.M. Pereira, V.M.T.M. Silva, A.E. Rodrigues. Ethyl lactate as a solvent: Properties, applications and production processes - a review. Green Chemistry. 13 (2011) 2658-71.

[107] J.S. Bennett, K.L. Charles, M.R. Miner, C.F. Heuberger, E.J. Spina, M.F. Bartels, et al. Ethyl lactate as a tunable solvent for the synthesis of aryl aldimines. Green Chemistry. 11 (2009) 166-8.

[108] H.R. Schlten, P. Leinweber. Pyrolysis-field ionization mass spectrometry of agricultural soils and humic substances: effect of cropping systems and influence of the mineral matrix. Plant soil. 151 (1993) 77-90.

[109] M.C.C. Maguyon, S.C. Capareda. Evaluating the effects of temperature on pressurized pyrolysis of *Nannochloropsis oculata* based on products yields and characteristics. Energy Conversion and Management. 76 (2013) 764-773.

[110] Q. Zhang, T. Wang, C. Wu. Upgrading bio-oil by catalytic esterification. Proceedings of ISES Solar World Congress 2007: Solar Energy and Human Settlement (2007) 2372-2377.

[111] S. Vitolo, M. Seggiani, P. Frediani, G. Ambrosini, L. Politi. Catalytic upgrading of pyrolytic oils to fuel over different zeolites. Fuel. 78 (1999) 1147-59.

[112] Alcohols: A technical assessment of their application as motor fuels. API Publication No. 4261. July 1976.

[113] J. Tuttle, T. von Kuegelgen. Biodiesel Handling and Use Guidelines - third edition. National Renewable Energy Laboratory. (2004).

[114] Greenhouse Gases, Regulated Emissions, and Energy Use in Transportation (GREET) Model. Argonne National Laboratory.

[115] J.D. Adjaye, N.N. Bakhshi. Catalytic conversion of a biomass-derived oil to fuels and chemicals I: Model compound studies and reaction pathways. Biomass & Bioenergy. 8 (1995) 131-49.

[116] J.D. Adjaye, N.N. Bakhski. Production of hydrocarbons by catalytic upgrading of a fast pyrolysis bio-oil. Part II: Comparative catalyst performance and reaction pathways. Fuel Processing Technology. 45 (1995) 185-202.

[117] W. Haiyan, Z. Jing, C. Guojing, Z. Liang, W. Min, M. Jun. Reducing olefins content of FCC gasoline using a NANO-HZSM-5 catalyst. Petroleum Science and Technology. 26 (2008) 499-505.

[118] F.H. Mahfud. Exploratory studies on fast pyrolysis oil upgrading. Rijksuniversiteit Groningen, Jakarta, Indonesia, 2007. ISBN: 978-90-367-3236-9

[119] M. Boudart. Turnover rates in heterogeneous catalyst. Chemical Reviews. 95 (1995) 661-6.